CHEMICAL REVIEWS

Review

Cite This: Chem. Rev. XXXX, XXX, XXX−XXX

pubs.acs.org/CR

Selective Hydrogenation over Supported Metal Catalysts: From Nanoparticles to Single Atoms

Leilei Zhang,[†] Maoxiang Zhou,[†,‡] Aiqin Wang,*[,†] and Tao Zhang*[,†]

[†]State Key Laboratory of Catalysis, Dalian Institute of Chemical Physics, Chinese Academy of Sciences, Dalian 116023, China

[‡]University of Chinese Academy of Sciences, Beijing 100049, China

ABSTRACT: Selective catalytic hydrogenation has wide applications in both petrochemical and fine chemical industries, however, it remains challenging when two or multiple functional groups coexist in the substrate. To tackle this challenge, the "active site isolation" strategy has been proved effective, and various approaches to the site isolation have been developed. In this review, we have summarized these approaches, including adsorption/grafting of N/S-containing organic molecules on the metal surface, partial covering of active metal surface by metal oxides either via doping or through strong metal−support interaction, confinement of active metal nanoparticles in micro- or mesopores of the supports, formation of bimetallic alloys or intermetallics or core@shell structures with a relatively inert metal (IB and IIB) or nonmetal element (B, C, S, etc.), and construction of single-atom catalysts on reducible oxides or inert metals. Both advantages and disadvantages of each approach toward the site isolation have been discussed for three types of chemoselective hydrogenation reactions, including alkynes/dienes to monoenes, α,β-unsaturated aldehydes/ketones to the unsaturated alcohols, and substituted nitroarenes to the corresponding anilines. The key factors affecting the catalytic activity/selectivity, in particular, the geometric and electronic structure of the active sites, are discussed with the aim to extract fundamental principles for the development of efficient and selective catalysts in hydrogenation as well as other transformations.

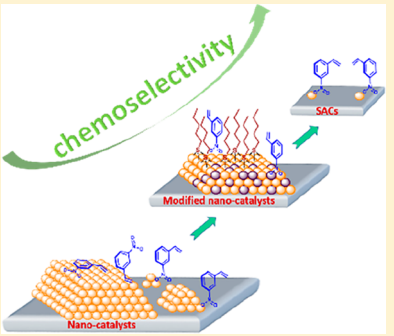

CONTENTS

1. INTRODUCTION

Hydrogenation is among the central themes of petrochemical, coal chemical, fine chemical, and environmental industries.[1−9] In the petrochemical industry, hydrodenitrogenation and hydrodesulfurization processes are widely employed to remove trace amounts of N/S elements in crude oil for downstream processing,[4,5] hydroreforming, and hydroisomerization are the main approaches to improving the octane value of the

Special Issue: Nanoparticles in Catalysis

Received: April 11, 2019

DOI: 10.1021/acs.chemrev.9b00230
Chem. Rev. XXXX, XXX, XXX−XXX

gasoline,[10,11] and selective hydrogenation is the direct route to eliminate the impurities of alkynes and dienes in ethylene, propylene, and butylene in the olefins industry for downstream polymerization.[12] In the coal chemical industry, hydrogenation of coal is regarded as the third generation of techniques for coal gasification.[1] On the other hand, in the synthesis of fine chemicals, various functional groups, such as −C≡C, −C═O, $-NO_2$, −C≡N, −COOH(R), and $-CONH_2$, are required to be selectively reduced by clean and cheap H_2 to their corresponding alkenes, alcohols, and amine products that are key intermediates for the fine chemical, polymer, agrochemical, and pharmaceutical industries.[2,7,13] It is estimated that 25% of chemical transformations include at least one hydrogenation step, and it is thus not surprised that the hydrogenation reaction is one of the most intensively investigated topics in catalysis.

The selective hydrogenation is the most dazzling jewel in the crown in hydrogenation transformations.[14] Chemoselective hydrogenation refers to when two or more functional groups coexist in one substrate, or different unsaturated substrates are present in the catalytic system, one of the functional groups (or substrate) is preferentially transformed while the others are left unsaturated. For example, in the hydrogenation reaction of acetylene in a large excess of ethylene, it is strictly demanded that acetylene is preferentially hydrogenated to ethylene whereas ethylene whether produced or fed is not further saturated to ethane.[12,15] In fine chemical industry, when the substrates bear multiple functional groups (e.g., 3-nitrostyrene), it is necessary to selectively reduce the target functional group while keeping the others intact for the synthesis of flavors, fragrances, agrochemicals, and pharmaceuticals, etc.[13] Therefore, the selective hydrogenation transformations are highly desirable both for bulk and fine chemical industries.

The key to the selective hydrogenation relies on the fabrication of efficient and selective catalysts.[16] Currently, two types of catalysts, namely homogeneous and heterogeneous catalysts, are explored for the target reactions. The homogeneous metal−ligand complexes are famous for their high selectivity thanks to the steric and electronic effects of ligands yet suffer from difficult separation and reuse as well as contamination of the products.[17] On the contrary, the heterogeneous catalysts are promising for practical applications in terms of catalyst separation and recovery.[3,18] Four types of heterogeneous catalysts have been developed for the selective hydrogenation reactions. The metal complexes immobilized on oxides or resins are the first generation of heterogeneous catalysts. Although they retain the merits of high selectivity, the loss of ligands and/or metals into solutions during the hydrogenation reactions is often inevitable due to the weak interaction with the support. The supported metal nanoparticles are then explored as the second-generation catalysts with the development of nanoscience (Figure 1a)[13] yet suffer from unsatisfactory chemoselectivity, mainly owing to the side reactions of overhydrogenation. However, if the nanocatalysts are properly modified by a second metal (such as Sn, Pb, Bi) or organic reagent (such as mercaptan, amines) (Figure 1b),[19,20] e.g., the Lindlar catalyst $Pd/CaCO_3$-Pb,[20−22] the chemoselectivity can be greatly improved. Unfortunately, the improvement in selectivity are usually at the expense of catalytic activity because a great portion of the surface atoms is shielded and thus inaccessible to the reactants. Therefore, it

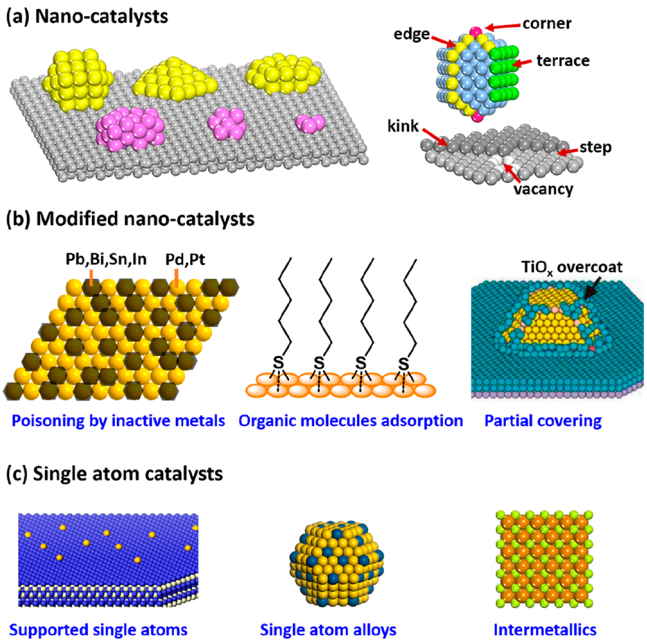

Figure 1. Illustration of supported nanocatalysts (a), modified nanocatalysts (b), and single-atom catalysts (c).

remains a challenge to achieve a high chemoselectivity without compromising the activity.

One prerequisite to the rational design of chemoselective catalysts is the understanding of the reaction mechanism that governs the chemoselectivity. So far, consensus has been reached that the selectivity, to a large degree, depends on the adsorption strength and configuration of the reactants/intermediates on the surface of catalysts, which in turn is determined by the electronic and geometric structures of the active sites.[23,24] For example, ethylene can have three different adsorption modes on Pd surface depending on the configuration of Pd atoms: ethylidyne mode on 3-fold sites, di-σ on 2-fold and π-bonded mode on isolated Pd single atom, and the adsorption strength decreases following the order of ethylidyne > di-σ > π-bonded.[23,25] In the semihydrogenation of acetylene, the weakest adsorption of ethylene, π-bonded mode, will favor its desorption from the surface and thus avoiding the overhydrogenation to ethane. Therefore, isolation of Pd as single atoms is required for attaining a high selectivity to ethylene. Similarly, when two or multiple functional groups coexist in the substrate and each of them can be adsorbed on the catalyst, there will be multiple adsorption patterns and consequently various products and poor chemoselectivity. Therefore, to achieve excellent chemoselectivity, it is highly desirable to allow only the target functional group to be adsorbed on the catalyst in a proper pattern. Correspondingly, the catalytic active sites should bear uniform geometric and electronic structure to avoid multiple adsorption patterns.

From this point of view, it is not surprising that homogeneous metal complexes can exhibit excellent selectivity because single-site active species with proper electronic structures allows for only one adsorption mode of the reactants. On the contrary, in the supported nanoparticles (Figure 1a), the heterogeneity in size/shape/composition is ubiquitous.[26,27] For example, a supported nanocatalyst usually has a broad spectrum of size distribution and the nanoparticles may expose different facets with different atomic structure.[26,28] For multicomponent nanoparticles, they may possess different

DOI: 10.1021/acs.chemrev.9b00230
Chem. Rev. XXXX, XXX, XXX−XXX

structure (core@shell, alloy, or cluster-in-cluster) and consequently distinct composition between surface and the bulk.[27,29,30] When focusing on one particle, the atom may locate on the terrace, kink, edge, corner sites, or at the metal−support interfaces and intimately interacted with the support,[31] and each of these sites bear different coordination environments and electronic structures. These various catalytic sites will lead to different adsorption modes of the reactants/intermediates and consequently poor selectivity in catalysis. As for the modified nanocatalysts by a second metal or surfactant (Figure 1b),[20] the enhanced chemoselectivity is ascribed to the improvement of homogeneity in the active sites. For example, when the corner/edge sites in the nanoparticles are covered/poisoned (concomitantly, the energy landscape is also tuned, e.g., the d-band center might be downshifted), the remaining atoms in the terraces are considered to be equally in catalysis. However, as stated above, these modulations are not fine enough, and atomically precise methodologies are urgently demanded.

Inspiration can be found in homogeneous and enzyme catalysts, where only one type of metal site exists, whose electronic and geometric structures are affected by the ligands.[17] Similarly, in nanocatalysts, the support can be regarded as the "macro ligands" of the nanoparticles, however, only those metal atoms in intimate proximity with the support whose electronic properties are directly modulated. Notably, these catalytic sites, frequently referred as interface sites, have demonstrated excellent activity and selectivity in various hydrogenation reactions.[32−36] Accordingly, if the nanoparticles are downsized to the lowest limit, i.e., the atomic dispersion, then each and every metal atom will directly interact with the heteroatoms in the support, and then the resultant catalysts will be a mimic of the homogeneous metal complexes. On this ground, a new generation of catalyst for the selective hydrogenation reactions: single-atom catalysts (SACs) were developed (Figure 1c).[37−39] Because of the ultimate dispersion of active metals and the homogeneous composition of the active species, SACs have demonstrated excellent catalytic activity and selectivity in various chemical/electrochemical/photochemical transformations,[40−44] including selective hydrogenation reactions. Moreover, they provide a good platform to investigate the structure−performance relationship in catalysis.

This review has summarized the advances in selective hydrogenation reactions of substrates with different functional groups, i.e., alkynes and dienes in excess alkenes, α,β-unsaturated aldehydes/ketones, and functionalized nitroarenes (mainly nitrostyrene) over supported metal catalysts in the past decade. As we mainly focus on metal catalysis, some hydrogenation-related processes such as hydrodenitrogenation, hydrodesulfurization, hydrodeoxygenation, hydroreforming, and hydroisomerization that require multifunctional catalysts (e.g., Brønsted acid sites for C−X (X = S, N, O, Cl, etc.) bond dissociation or isomerization, and metal sites for H_2 dissociation) have not been included, and the readers interested in those topics can refer to the related reviews.[4,5] And as transfer hydrogenation and asymmetric hydrogenation had been well described in several excellent reviews,[2,3,7,17] they were not included here, either. We summarize the catalytic performances of nanocatalysts, modified nanocatalysts, and SACs in the selective hydrogenation reactions with an attempt to reveal the key factors that influence the chemoselectivity and catalytic activity and to establish bridges between the three types of heterogeneous catalysts in terms of geometric and electronic structures of catalytically active sites. We hope that this collection will be a valuable reference source to chemists searching for effective and selective catalysts for hydrogenation reactions.

2. ADSORPTION OF SUBSTRATES ON SUPPORTED METAL NANOPARTICLES AND SINGLE ATOMS

Catalysis is an adsorption−transformation−desorption process of the reactant/intermediate/product on a catalyst,[45] where the active sites form intermediate "adduct" with the substrate, and thereby the activation energy of a transformation is lowered. According to DFT calculations and kinetic studies, various intermediates and reaction pathways probably exist in a catalytic cycle, of which the adsorption of the reactant on the active species is the initial step,[46,47] and it determines the following reaction pathways through which the substrate is converted to the product.[48]

The adsorption strength and manner of a substrate are dependent on the geometric and electronic structure of the active sites.[49] (1) The size of metal ensembles is an important factor. When continuous assemblies of metal atoms are present, the substrates tend to adsorb strongly on the 3-fold sites, followed by bridging and atop sites. A typical example is the adsorption of ethylene on Pd(111) surface,[23,25] where ethylene adsorbs strongly in the form of ethylidyne on 3-fold Pd sites, moderately with di-σ mode on bridging Pd sites, and weakly via π-mode on isolated Pd sites. (2) The topology of the metal assembles.[50,51] When the active metal is downsized to nanoparticles/clusters, their electronic structure also changes from continuous energy band of the bulk to discrete energy levels, thereby inducing strong electron energy quantization (Figure 2a). The quantum confinement effect

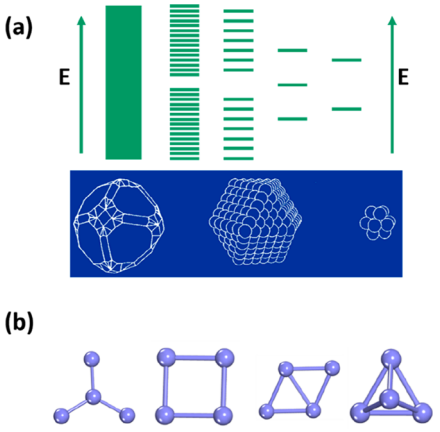

Figure 2. (a) Illustration of quantum effect, (b) Possible topological structures of M_4 clusters.

and discrete energy levels of the nanoparticles/clusters enable their isomerization (Figure 2b). (3) Coordination environment: Metal nanoparticles are not perfect spheres but irregular polyhedral composed of terrace, edge, corner, and kink as well as perimeters when loaded on support (Figure 1a).[31] The coordination number of atoms in these positions are quite different, which will result in different adsorption strength of the reactant. (4) Composition and structure:[52,53] In bi- or multimetallic nanoparticles, the interaction between each component not only change the assemblies of accessible metal atoms[29,30,54] but also modify the electronic structure

DOI: 10.1021/acs.chemrev.9b00230
Chem. Rev. XXXX, XXX, XXX−XXX

induced by charge transfer.[55] In addition, in core@shell structured nanoparticles, the difference in lattice spacing also leads to strain effect,[27,56] which alters the position of d band center of active metal and thus the adsorption behavior.

In selective hydrogenation reactions, it is desirable that the target functional group is preferentially adsorbed on the active sites. To avoid the multiple adsorption patterns, the catalyst should first have homogeneous geometric and electronic structure and on other hand bear unique redox or acidic/basic or electrophilic/nucleophilic property that lead the target functional group to be recognized.[57,58] Accordingly, the SACs are expected to provide superior selectivity to their nanoparticular counterparts in hydrogenation reactions.

3. ACTIVATION OF H_2

The adsorption and activation of H_2 constitutes another critical step in the hydrogenation reactions. The activation manner and the types of the H species (i.e., H^+, H^-) also have profound influence on the selectivity. For example, the hydrides on the surface of Pd nanoparticles can incorporate into the interstitial sites, forming subsurface hydride, which is known to be notorious for the selectivity.[59] And also when H_2 is heterolytically rather than homolytically cleaved, the produced H^+/H^- pairs prefer to reduce the polar bond rather than the nonpolar one.[60] Therefore, the common dissociation manner of H_2 will be briefly introduced in this section (Figure 3).

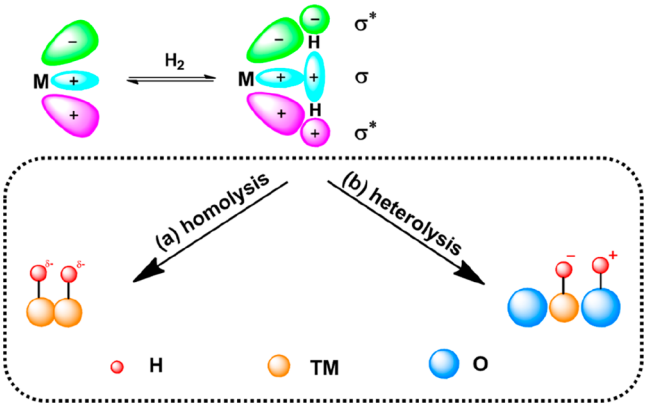

Figure 3. Homolytic and heterolytic dissociation of H_2. Adapted with permission from ref 64. Copyright 2007 The American Association for the Advancement of Science.

3.1. Homolytic Dissociation of H_2

H_2 can be easily dissociated on the VIII group metals, such as Pt, Pd, and Rh.[61−63] These metals have partially occupied d-orbitals, which can accept the σ electrons of H_2, and on the other hand, donate d-electrons to the σ^* antibonding orbital of H_2 (Figure 3). Consequently, the H−H bond is weakened and cleaved, forming two hydrides, that is, so-called homolytic dissociation of H_2.[64] This dissociation process resembles the oxidative addition of H_2 in homogeneous catalysis, where H_2 approaches the metal complexes and is transformed into two hydrides binding to the metal center, meanwhile, the oxidation state of the metal center is raised by two.[65] However, the oxidative addition of H_2 can take place on single metal atom in metal complexes because of the electron-donating effect of the ligands, whereas in metal nanoparticles, the homolysis of H_2 requires metal ensembles of more than one atom in the vicinity.[66] As the homolytic dissociation of H_2 requires the denotation of d-electrons of metal to H_2, therefore, a high electron density of the active sites is beneficial for the hydrogenation reaction. However, if the metal is poisoned by strong π-acceptors, e.g., CO and sulfur, the dissociation of H_2 will be greatly suppressed and consequently the catalyst is deactivated.

The hydride formed on the metal surface can penetrate into the interstitial sites of the metal, forming subsurface hydrides (H^{sub}).[67] The H^{sub} species can destabilize the surface adsorbed H^{ad} species and thus increase the reactivity of H^{ad}.[68] On the other hand, the H^{sub} can migrate back to the surface and increase the hydride coverage on the surface which impairs the chemoselectivity. Once the hydrides are formed, they can also migrate from the metal surface to the support, that is, so-called hydrogen "spillover" process.[69] Hydrogen spillover can only take place when the metal is supported on reducible oxides, graphitic carbonaceous materials, and nonreducible oxides with impurities or defects but not on perfect nonreducible oxides because of the lack of electron transfer path. As a result, the support can be partially reduced (i.e., creation of oxygen vacancies) and/or the remote substrates adsorbed on the support can be hydrogenated. When H_2O is present in the reaction system, the migration of hydrogen across the support can be accelerated, either through the proton transfer process in the form of hydronium ion species or by H_2O dissociation mechanism.[70] Accordingly, the catalytic activity can be greatly enhanced.

3.2. Heterolytic Dissociation of H_2

Apart from the homolytic dissociation, H_2 can also be activated through the heterolysis pathway. In this case, H_2 is cleaved to H^- and H^+ assisted by nucleophilic atoms or in strong electric field, which then binds to metal atom and proton acceptor (e.g., N atom), respectively.[71] Because no charge transfer occurs in this process, the valence state of the metal remains intact.

Heterolytic activation of hydrogen are well-known in homogeneous catalytic systems of enzymes, metal complexes (e.g., Shvo−Noyori catalysts), as well as frustrated Lewis pairs (FLPs).[72−75] However, recent reports have shown that in some heterogeneous catalysts, such as reducible metal oxides (e.g., CeO_2 and WO_3),[76] supported metal nanoparticles (e.g., Au/CeO_2),[77,78] and single-atom catalysts (e.g., Pd/TiO_2),[66,79,80] H_2 can also be heterolytically dissociated to H^+ and H^-. As aforementioned, on VIII group metal nanoparticles, a high electron density is required for the homolytic dissociation of H_2, however, at the metal−support interface sites, the metal atoms are generally electron-deficient and thus are more prone to cleave H_2 in a heterolytic manner. Typically, for supported Au nanocatalysts,[81] the fully occupied d-band of gold makes it difficult to accept the σ electrons of H_2, meanwhile, Au is unlikely to donate electron to σ^* antibonding orbital of H_2 because of the high electronegativity. Therefore, the heterolytic cleavage of H_2 is the preferred pathway. The similar case occurs for supported SACs, where hydrogen molecules can be favorably dissociated in a heterolytical manner because no continuous metal ensembles exist for H_2 homolysis. The heterolytic dissociation of hydrogen requires the participation of support or additive/promoter, where the electropositive d-block metal atom (M) serves as the hydride acceptor, while the electronegative heteroatom (X) from the support or promoter

DOI: 10.1021/acs.chemrev.9b00230
Chem. Rev. XXXX, XXX, XXX−XXX

as proton acceptor, resembling the homogeneous Shvo–Noyori catalysts and FLPs.[71]

The heterolysis of H_2 offers several advantages in the hydrogenation reactions. First, some polar group can be reduced in the outer sphere.[82] That is, the unsaturated group does not bind to the metal surface but the H^+/H^- pairs are transferred from the catalyst to the substrates.[71,83] Because of the noncompetitive adsorption of the substrate and H_2, there is enough room for the activation of H_2. Second, the H^+/H^- pairs kinetically prefer reducing the polar group, which will greatly enhance the chemoselectivity in the hydrogenation reactions.[60] Third, the activity of the catalysts can be finely tuned. When regarding the dissociation mechanism of H_2, one can rationally deduce that the high basicity (i.e., nucleophilicity) of X atom, or a significant polarization degree of M–X bond (i.e., strong electronic field) should promote the dissociation of H_2 and consequently accelerate the reaction rate.[83] For example, Beller and co-workers reported that the addition of NEt_3 promoted the hydrogenation of functionalized nitroarenes catalyzed by Co_3O_4@N-C.[84,85] In addition, the protons in H^+/H^- pairs are strong Brønsted acid in nature, and therefore the catalysts are expected to fulfill multiple functions in some reactions.[86,87]

4. SEMIHYDROGENATION OF ALKYNES

4.1. Gas-Phase Hydrogenation Reactions

Light olefins (ethylene, propylene, and butene) are key building blocks to produce plastics (e.g., polyethylene, PE) and other chemicals such as ethylbenzene, ethylene oxide, and ethylene dichloride.[12,88] Commercially, alkenes are manufactured by steam cracking of a broad range of hydrocarbon feedstocks (such as naphtha, gas oil, and condensates). Such-made olefins usually contain impurities of alkynes and dienes, e.g, the ethylene cut typically contains 0.5–3% of acetylene and the propylene cut 2–8% of propyne and propadiene.[89] These highly unsaturated compounds are poisonous to the Ziegler–Natta catalysts for the polymerization of olefins and thus need to be removed to <5 ppm level. Among various methods to eliminate alkynes, the semihydrogenation of alkynes (and diolefins) to alkenes has proved to be the most efficient one.[15] On the basis of the operation mode, there are front-end and back-end semihydrogenation. In the front-end process, reactors are situated prior to the removal of C_1 cuts, and a large excess of H_2 is present in the feed gas. In this case, the selective hydrogenation of alkynes becomes more challenging because of the high H_2/alkyne ratio and possible danger of thermal runaway. On the contrary, the back-end process is more popular, where a stoichiometric amount of hydrogen is present (H_2/alkyne = 1.5–2) in the feed gas.

The semihydrogenation of alkynes generally follows Horiuti–Polanyi mechanism,[90] where H_2 is first adsorbed and dissociated on the catalyst, and then the alkyne is adsorbed and two hydrides are added to the unsaturated bond in a successive manner. Apart from the desired hydrogenation of alkynes to alkenes, there are three side reactions (Figure 4): the overhydrogenation of alkenes (including those in the feedgas) to alkanes, the C–C coupling (oligomerization) of the alkynes and intermediates to higher hydrocarbons (called green oil), and the cracking of alkyne/intermediates to form coke.[15] These side reactions not only lead to the waste of the alkene feedstock, the oligomerization and coking also cause serious operation problems such as shortened cycles due to

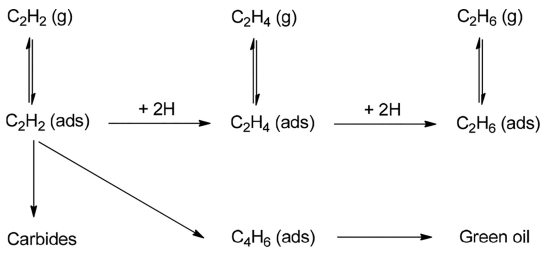

Figure 4. Reaction network for acetylene hydrogenation. Adapted with permission from ref 15. Copyright 2015 Springer Nature.

catalyst deterioration, the need for regeneration, and plugging of piping.[89] Therefore, there is urgent demand in industry for the development of catalysts that can efficiently suppress these side reactions in the semihydrogenation of alkynes.

Various catalysts have been explored for the selective hydrogenation of alkynes, of which Pd based catalysts have attracted the most intensive attention because of their high intrinsic activity (TOF = 0.2–1.0 s^{-1}).[15] Unfortunately, the selectivity to alkenes over unmodified Pd catalysts was quite low because of the severe side reactions of overhydrogenation and oligomerzation.[91] It is believed that the side reactions are caused by the strong adsorption of the unsaturated reactants/intermediates on the coordinatively unsaturated edge and/or corner sites on the Pd nanoparticles. Accordingly, strategies to selective poisoning/covering these sites by CO,[92] sulfur,[93] or second metal (Au, Ag, Cu, Zn, Ga)[94−98] have been developed to improve the selectivity of Pd catalysts. For example, the industrially employed catalyst is bimetallic Ag–Pd/Al_2O_3, and the feedgas usually contains a low concentration of CO. Even though, the selectivity to ethylene at full conversion of acetylene remains to be enhanced yet. For example, in the partial hydrogenation of acetylene under back-end conditions, 45% ethylene, 28.8% ethane, and 26.2% green oil were obtained at full conversion.[99] In addition, the increased selectivity is often accompanied by the decrease of Pd utilization efficiency due to the covering/poisoning. Therefore, for the rational design of both active and selective catalysts, it will be helpful to understand how the structure of the catalysts influences their performance in the semihydrogenation reactions.

Ensemble effect is the primary factor to determine the selectivity in the semihydrogenation of alkynes. Depending on the assemblies of Pd atoms, ethylene has three adsorption modes: ethylidyne mode on 3-fold Pd sites, di-σ-mode on bridged Pd dimers, and π-bonded mode on isolated Pd single atoms (Figure 5), and adsorption strength decreases in the order of ethylidyne > di-σ > π-bonded.[23,25] For the ethylidyne and di-σ-modes, the energy required for desorption is larger than that for hydrogenation, therefore, the hydrogenation pathway is preferred to desorption, leading to low selectivity to ethylene. On the contrary, when ethylene is adsorbed through

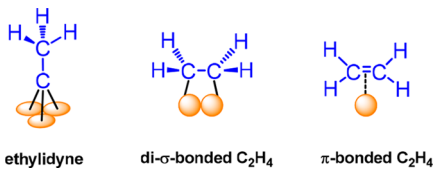

Figure 5. Adsorption patterns of ethylene on Pd catalysts with different geometric structures.

DOI: 10.1021/acs.chemrev.9b00230
Chem. Rev. XXXX, XXX, XXX–XXX

π-bonded mode, the energy barrier for desorption is lower than that for hydrogenation and ethylene will desorb from the catalyst surface without further hydrogenation, thus leading to high selectivity to ethylene (Figure 6).[95,100] Therefore,

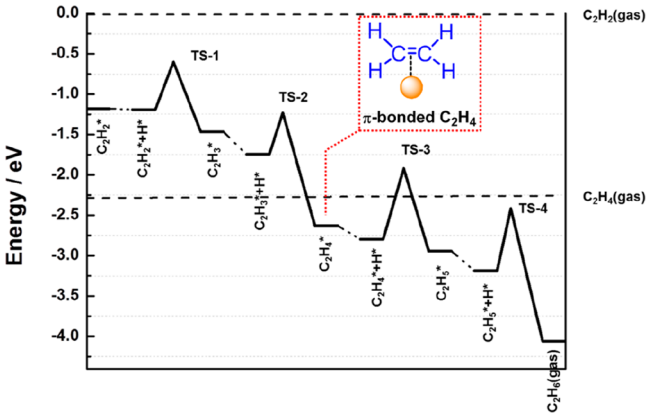

Figure 6. Activation energy profile of each fundamental steps in the hydrogenation of acetylene catalyzed by Pd single atoms. Reproduced with permssion from ref 95. Copyright 2016 American Chemical Society.

reduction of ensembles of Pd will weaken the adsorption strength of the alkenes and consequently increase the chemoselectivity, that is, the so-called "active site isolation concept".[94,101] Actually, for the aforementioned approaches, such as selective poisoning by CO or sulfur and forming alloys/intermetallics with a second metal, the selectivity improvement arose from the isolation of the active sites.[95,101] A more promising method for the "active site isolation" is to construct single-atom catalysts, which can also maximize the efficiency for metal utilization.[79,102,103] In addition to suppress the overhydrogenation, the "active site isolation concept" is also able to suppress the structure sensitive side reactions of oligomerization and coking, as the C−C coupling of the reactant/intermediates requires at least four continuous Pd sites,[104] and coking generally occurs on extensive terrace sites where the reactant/intermediates are strongly adsorbed.

Another important factor to affect the selectivity is the subsurface structure of the Pd catalysts. For example, when H_2 is dissociated on the surface Pd atoms, the hydride can migrate into the subsurface region (the few layers below the surface) and occupy the interstitial sites, forming β-hydride or β-H species (Figure 7).[59,67,68,105] During the hydrogenation reaction, the subsurface hydride can diffuse back to the surface and lead to high concentration (coverage) of surface hydride, which is detrimental to the selective hydrogenation. However, when the interstitial sites are occupied by other atoms (e.g., C atoms from fragments of hydrocarbons), the formation of subsurface hydride and their diffusion can be suppressed, and the selectivity to ethylene can be improved to a great degree (Figure 7).[59,105−108] Because both of subsurface hydride and carbide can be formed during the hydrogenation reaction, which species dominate is dependent on the reaction conditions (such as temperature, H_2/alkyne ratios) as well as the nature of the metal. Generally, high H_2/alkyne ratios (or high H_2 pressure) promotes the formation of hydride and the high ability of the metal (e.g., Ni) to cleave C−C bond facilitates the occupancy of interstitial sites by carbon. Although the subsurface carbides can restrain the deep

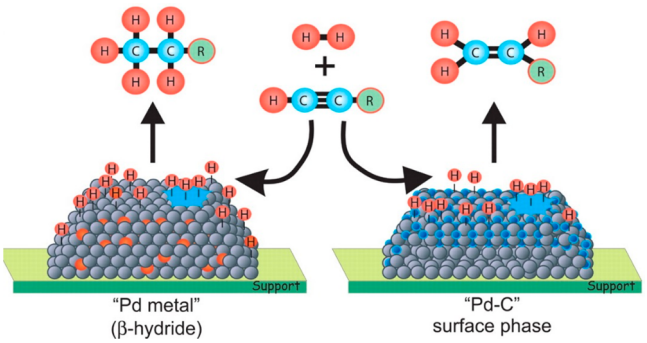

Figure 7. Schematic representation of hydrides and carbides over Pd nanoparticles and their impact on the selectivity in hydrogenation reactions of acetylenes. Adapted with permission from ref 59. Copyright 2008 The American Association for the Advancement of Science.

hydrogenation to some degree, their extensive formation is usually accompanied by coking and deactivation of the catalysts. Therefore, a delicate balance between subsurface carbide and hydride is required for the selective and stable catalysts. The "active site isolation" strategy, in principle, is able to suppress the formation of subsurface carbide and hydride because of the limited atomic layers.[109] It should be noted that the electronic structure of the catalysts is usually modified concomitantly with the geometric structure. For example, with the expansion of lattice of Pd, the d-band downshifts,[21] which weakens the adsorption of alkenes. Meanwhile, the electron transfer from the second metal to Pd in alloys/intermetallics makes Pd sites negatively charged,[98] which promotes the dissociation of H_2 in an oxidative addition manner.

On the basis of the "active site isolation" strategy, various Pd-based catalysts have been developed for the selective hydrogenation of alkynes to alkenes. In addition to Pd, other metal catalysts, such as Au, Rh, and Ni, as well as metal oxides catalysts were also reported. A summary of the catalytic performances of different catalysts is listed in Table 1. Although operation conditions (feed gas composition, space velocity, temperature, pressure) and metal content may vary greatly, one can still see that Pd-Zn/ZnO catalyst with isolated Pd sites appears the most promising one, affording 90% ethylene selectivity at 94% acetylene conversion under mild reaction conditions (80 °C, 0.1 MPa H_2) in the presence of excess ethylene.

4.1.1. Pd Based Catalysts. *4.1.1.1. Selective Poisoning/Covering.* In industry, CO is usually chosen as a selectivity modulator in the semihydrogenation of alkynes, and their promotional role is ascribed to thermodynamic factor. DFT calculations reveal that when CO molecules are adsorbed, they form a densely packed monolayer on the surface of Pd and thus reduce the size of accessible Pd ensembles.[92] In this way, not only the adsorption of the unsaturated reactants/intermediates and H_2 is weakened, but also the diffusion of the carbon containing species to form oligomers is limited. Consequently, the selectivity to alkenes is significantly enhanced. On the other hand, CO may also react with the unsaturated intermediates to form green oil.

López investigated the influence of CO in the feedgas on the selectivity of 1 wt %Pd/Al_2O_3 catalysts.[141] In the semihydrogenation of acetylene (70 °C, H_2/C_2H_2 = 5, SV = 16800 $cm^3\ h^{-1}\ g^{-1}$), 85% ethane, and 15% oligomers were obtained

DOI: 10.1021/acs.chemrev.9b00230
Chem. Rev. XXXX, XXX, XXX−XXX

Table 1. Catalysts for the Gas-Phase Selective Hydrogenation of Alkynes

catalysts	feedgas composition	SV ($ml \cdot g_{cat}^{-1} \cdot h^{-1}$)	T (°C)	P (MPa)	conv (%)	selectivity (%)	ref
Rh_2/MgO	C_4H_6/H_2 = 2/98		40	0.1	97	99	110
$Pd_4S/CNFs$	C_4H_6/H_2 = 1/5		150	0.1	99	100	112
$Pd_4S/CNFs$	$C_2H_2/C_2H_4/H_2$ = 1/9/1.8	6×10^4	250	0.1	100	95	113
$Pd_4S/CNFs$	alkyne/C_3H_6/C_3H_8 = 1.5/10/1.75[a]	5.8×10^5	200	1.8	100	85	93
$Pd_4S/CNFs$	$C_2H_2/C_2H_4/H_2$ = 1/9/1.2	2.16×10^6	250	1.8	46.6	96	93
Ti−Pd/PHSNs	$C_2H_2/C_2H_4/H_2$ = 1/99/2	7200	45	0.1	70	69	114
Pd−La/SiO_2	$C_2H_2/C_2H_4/H_2$ = 1/99/2		60	0.1	45	80	115
Pd@C/CNT	$C_2H_2/C_2H_4/H_2$ = 0.5/20/3	6×10^4	150	0.1	93	70	116
$Pt_{0.1}Cu_{14}/Al_2O_3$	$C_4H_6/C_3H_6/H_2$ = 2/20/16	12000	160	0.1	100	95	117
$AuPd_{0.01}/SiO_2$	$C_2H_2/C_2H_4/H_2$ = 1/20/20	6×10^4	160	0.1	86	56.4	97
$AgPd_{0.01}/SiO_2$	$C_2H_2/C_2H_4/H_2$ = 1/20/20	6×10^4	160	0.1	93	80	96
$CuPd_{0.006}/SiO_2$	$C_2H_2/C_2H_4/H_2$ = 1/20/20	6×10^4	160	0.1	100	85	98
Pd−0.41Cu(SR)	$C_2H_2/C_2H_4/H_2$ = 0.95/99.05/1.9		60	0.1	80	60	118
Pd−0.7Ag(I)	$C_2H_2/C_2H_4/H_2$ = 0.95/99.05/1.9		60	0.1	65	80	119
Pd_2Ag_3/TiO_2	$C_2H_2/C_2H_4/H_2$ = 0.73/52.6/1.46	7.2×10^4	60	0.1	57.4	90.3	120
Pd_2Ga	$C_2H_2/C_2H_4/H_2$ = 0.5/50/5	1.8×10^5	200	0.1	94	74	144
nano-PdGa@Al_2O_3	$C_2H_2/C_2H_4/H_2$ = 0.5/50/5	24000	200	0.1	81	82	122
$Pd_2Ga/MgO/MgGa_2O_4$	$C_2H_2/C_2H_4/H_2$ = 0.5/50/5		200	0.1	98	70	123
PdGa	$C_2H_2/C_2H_4/H_2$ = 0.5/50/5	36000	200	0.1	78	78	144
Pd_3Ga_7	$C_2H_2/C_2H_4/H_2$ = 0.5/50/5	18000	200	0.1	81	82	144
Pd_2Ga/CNT	$C_2H_2/C_2H_4/H_2$ = 0.5/50/5	7.5×10^6	200	0.1	90	58.1	124
Pd−Zn/ZnO	$C_2H_2/C_2H_4/H_2$ = 2/40/20	1.8×10^5	80	0.1	94	90	95
Pd−Zn/ZnO	$C_2H_2/C_2H_4/H_2$ = 2/40/20	5.4×10^5	110	0.1	79	97	95
PdZn-1.2@ZIF-8C	$C_2H_2/C_2H_4/H_2$ = 0.65/50/5	48000	120	0.1	85	80	125
$PdIn/MgAl_2O_4$	$C_2H_2/C_2H_4/H_2$ = 0.5/50/5	2.88×10^5	90	0.1	96	92	126
Pd_1/graphene	$C_4H_6/C_3H_6/H_2$ = 1.9/70/4.7	33000	50	0.1	98	100	102
Pd_1/C_3N_4	$C_2H_2/C_2H_4/H_2$ = 0.5/25/1	30000	110	0.1	80	92	148
Pd_1/ND@G	$C_2H_2/C_2H_4/H_2$ = 1/20/10	60000	180	0.1	100	90	103
Pd_1/ZnO	$C_2H_2/C_2H_4/H_2$ = 2/40/20	36000	80	0.1	80	94	132
$Pd/Ni(OH)_2$	$C_2H_2/C_2H_4/H_2$ = 0.65/50/5	24000	100	0.1	80	80	133
DP Au/Al_2O_3	$C_4H_6/C_3H_6/H_2$ = 0.3/30/20	20000	170	0.1	100	100	127
DP Au/Pd(90)	$C_4H_6/C_3H_6/H_2$ = 0.3/30/20	20000	120	0.1	100	100	128
Au/SiO_2	$C_2H_2/C_2H_4/H_2$ = 0.8/83.2/16	92000	175	0.1	94	47	129
Au-Ag/SiO_2	$C_2H_2/C_2H_4/H_2$ = 0.8/83.2/16	92000	200	0.1	98	30	130
Au/CNT-i	C_4H_6/H_2 = 0.6/42.2	81000	150	0.1	80.4	100	131
Au/ZrO_2	C_4H_6/H_2 = 2.15/97.85	8100	120	0.1	87	100	156
IRMOF-3-SI-Au	C_4H_6/H_2 = 2/98		130	0.1	97	90	157
Cu-Al HT-C873-R573	C_3H_4/H_2 = 1/3	16800	250	0.1	100	82	134
$Cu_{2.75}Ni_{0.25}Fe$	C_3H_4/H_2 = 2.5/7.5	16800	250	0.1	100	97	89
$AgNi_{0.125}/SiO_2$	$C_2H_2/C_2H_4/H_2$ = 1/20/20	60000	160	0.1	90.4	31.4	135
$Al_{13}Fe_4$	$C_2H_2/C_2H_4/H_2$ = 0.5/50/5	90000	200	0.1	80	82	136
Ni_6In/SiO_2	C_2H_2/H_2 = 1/5	36000	180	0.1	63	100	137
CeO_2	C_3H_4/H_2 = 1/30		250	0.1	96	91	138
CeO_2	C_2H_2/H_2 = 1/30		250	0.1	86	81	138
In_2O_3	C_2H_2/H_2 = 1/30		350	0.1	100	85	139
$CrO_x/(110)\gamma$-Al_2O_3	C_2H_2/C_2H_4 = 0.475/9.25	21660	140	0.1	100	98.5	140

[a]Methyl acetylene/propadiene/propene/propane = 0.85/0.65/10/1.75, H_2/(methyl acetylene + propadiene) = 1.2.

when CO was absent. However, the addition of trace amount of CO ($CO/H_2 < 0.002$) remarkably decreased the selectivity of ethane meanwhile increased the ethene and oligomers. A further increase of CO concentration ($CO/H_2 = 0.04$) led to the total inhibition of overhydrogenation, and the selectivity to ethene increased to 30%. However, at $CO/H_2 > 0.1$, the catalyst was severely deactivated by the formation of oligomers and the selectivity to ethene decreased. Noteworthy, the products distribution over Pd-CO (i.e., Pd catalyst in the presence of CO) was quite similar to that on Cu based catalyst,[92] implying that CO might greatly decrease the hydride coverage on the Pd surface and thus suppress the deep hydrogenation reaction. The transformation of nonselective catalysts into selective ones by CO poisoning could be extended to other metals. Gates and co-workers prepared Rh_2 and Rh_3 clusters supported on MgO or zeolite HY, respectively.[110,111] These clusters showed excellent activity for the hydrogenation of butadiene, yet the selectivity was quite low. However, when the catalysts were treated by pulse of CO, the Rh_2 dimers could be highly selective for the reaction (40 °C, 2% butadiene in H_2), e.g., 99% selectivity to butene was achieved at 97% conversion. On the contrary, the Rh_3 trimers redispersed as single site $Rh(CO)_2$ on HY, which was totally inactive because of the deep poison of CO. The

DOI: 10.1021/acs.chemrev.9b00230
Chem. Rev. XXXX, XXX, XXX−XXX

alkenes hydrogenation did not begin until the butadiene was completely consumed, suggesting that the preferential adsorption of butadiene led to the high selectivity.

Sulfur, a well-known poisoner for metal catalysts, was also employed to improve the selectivity of Pd catalysts in the semihydrogenation of alkynes. Anderson and co-workers modified Pd/TiO_2 catalysts through adsorption of diphenyl sulfide followed by H_2 reduction at 50 or 120 °C.[142] The as-modified catalyst was active for acetylene hydrogenation but totally inactive for ethylene hydrogenation (Figure 8a). It was suggested that the sulfide modification met the geometric requirement for the hydrogenation of C_2H_2 but not for C_2H_4.

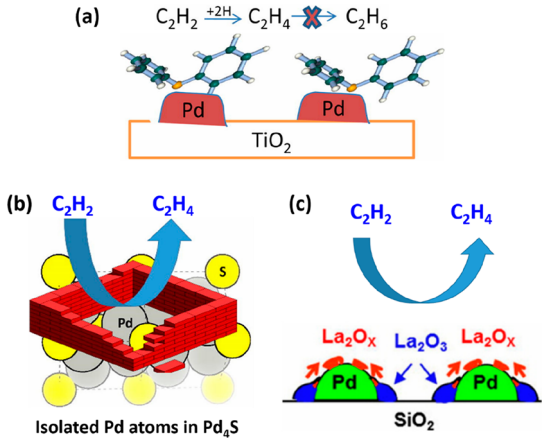

Figure 8. Illustration of (a) Pd/TiO_2 catalyst poisoned by diphenyl sulfide, (b) "Pd site isolation" in Pd_4S catalyst, and (c) La-Pd/SiO_2 catalysts covered by La_2O_x induced by high temperature reduction for selective hydrogenation of acetylene. (a) Adapted with permission from ref 142. Copyright 2011 Elsevier. (b) Adapted with permission from ref 93. Copyright 2017 Elsevier. (c) Adapted with permission from ref 115. Copyright 2014 Elsevier.

Carbon nanofibers (CNFs) supported Pd_4S nanoparticles were evaluated in the semihydrogenation of butadiene.[112,113] Under reaction conditions of 150 °C and butadiene/H_2 = 1/5, 100% selectivity to butene could be obtained at 99% conversion over Pd_4S/CNFs, whereas butane was the only product over unmodified Pd/CNFs. Similarly, in the hydrogenation of acetylene in excess ethylene ($C_2H_2/C_2H_4/H_2$ = 1/9/1.2−1.8, 250 °C, SV = 60000 h^{-1}, 0.1 MPa), 95% selectivity to ethylene at full conversion of acetylene could be obtained.[113] Even at the higher pressure condition which was required for industrial application, the selectivity to ethylene could still reach as high as 96−97% at 46.6% conversion.[93] Notably, negligible oligomers were produced although the H_2/C_2H_2 ratio was quite low. Similarly, in the hydrogenation of mixed C_3 feeds (methyl acetylene/propadiene/propene/propane = 0.85/0.65/10/1.75, H_2/(methyl acetylene + propadiene) = 1.2−1.8, 200 °C, SV = 5.8 × 10^5 h^{-1}), 83−85% selectivity could be achieved at full conversion of alkyne and diene. Characterization by in situ high energy X-ray diffraction revealed that the Pd and S formed solid solution where S atoms occupy the substitutional sites of Pd. Consequently, the continuous Pd ensembles were well separated, which was believed to account for the high selectivity (Figure 8b). In spite of superior selectivity to monoenes and negligible formation of oligomers, the Pd_4S catalyst required much higher temperature (200−250 °C) to achieve high conversion than that for commercial PdAg catalysts (60−80 °C), which compromised its efficiency.

The support can also effectively poison/cover Pd nanoparticles for isolation of Pd sites, especially when reducible oxides, such as TiO_2 and ZnO, are used as supports and reduced at high temperatures. Wen and co-workers modified the porous hollow SiO_2 supported Pd catalysts with TiO_2 through impregnation with tetrabutyl titanate.[114] In the semihydrogenation of acetylene under tail-end conditions ($C_2H_2/C_2H_4/H_2$ = 1/99/2, 40−60 °C), the selectivity to ethylene was increased from 52% to 65% when Pd nanoparticles were properly decorated by TiO_2. However, severe covering of Pd induced by high temperature reduction or at high Ti/Pd ratios led to significant decrease of the catalytic activity. Kim and co-workers also modified the Pd/SiO_2 catalyst with La/Ti/Nb by impregnation method.[115] In the hydrogenation of acetylene (60 °C, H_2/C_2H_2 = 2), the addition of La (La/Pd = 1) greatly improved the selectivity to ethylene, especially when the catalysts were reduced at high temperature (500 °C) (Figure 8c). When both of La and Ti (Ti/Pd = 0.2) were added in a sequential manner, the selectivity was further enhanced. Similar phenomenon was observed when Nb was used as promoter. XPS combined with H_2 chemisorption and ethylene−TPD experiments showed that strong metal−support interactions occurred upon high temperature reduction. The partial covering of Pd nanoparticles by La_2O_3 as well as the charge transfer to Pd greatly reduced the adsorption of ethylene as well as the coverage of surface hydrides and thus led to high selectivity.

Besides reducible metal oxide, carbon materials can also modulate the catalytic performance by covering or encapsulating Pd nanoparticles. Su and co-workers reported a core−shell structured Pd@C/CNTs catalyst by pyrolysis of ionic liquid coated Pd/CNTs at 700 °C under inert atmosphere.[116] HRTEM images showed that the Pd nanoparticles were coated by graphitic carbon with 1−4 layers (thickness <1.5 nm). In the hydrogenation of acetylene ($C_2H_2/C_2H_4/H_2$ = 0.5/20/3, SV = 6 × 10^4 h^{-1}, 150 °C), 70% selectivity to ethylene was obtained at 93% conversion, and the selectivity to oligomers was below 10%. By contrast, the selectivity to ethylene was extremely low (−400%) and a great portion of green oil was produced over uncoated Pd/CNTs. The carbon shell outside Pd nanoparticles might reduce the accessible Pd ensembles, which weaken the adsorption of ethylene and thus enhancing the ethylene selectivity. Meanwhile, modification of electronic property of Pd by carbon may also contribute to the selectivity increase,[91] although to a minor degree. In addition, the possible contribution of subsurface carbide to the selectivity was not discussed in those reports. One major concern is that the selectivity increase is at the cost of activity. For example, the reaction temperature to achieve >90% conversion was 150 °C for Pd@C/CNTs, whereas it was 30 °C for Pd/CNTs.

4.1.2.2. Pd Based Alloys/Intermetallics. Although the selective poisoning/covering approach could greatly suppress the side reactions of overhydrogenation, the atom utilization efficiency was significantly lowered due to covering of the surface metal atoms. Therefore, researchers resorted to alternative route to achieve the "active site isolation" strategy, namely, construction of alloys/intermetallics.[96−98,117] The intermetallics (also called intermetallic compounds, intermetallic alloys) is a type of metallic alloy that forms a solid-state compound exhibiting defined stoichiometry and long-range-ordered crystal structure (Figure 9). Taken Pd as an example,

DOI: 10.1021/acs.chemrev.9b00230
Chem. Rev. XXXX, XXX, XXX−XXX

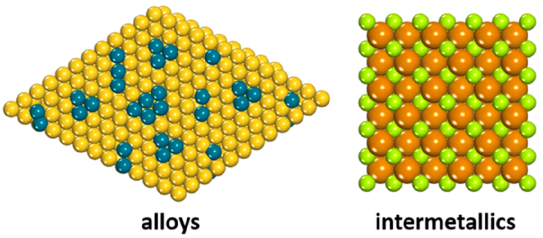

Figure 9. Illustration of bimetallic alloys (left) and intermetallics (right).

Pd can form alloys with various metals such as Au, Ag, Cu, and intermetallics with others (Zn, Ga, In, etc.). In these alloys/intermetallics, the continuous Pd ensembles can be separated or even totally isolated (i.e., single atom alloys, SAAs) depending on the composition of the materials. Consequently, the selectivity to alkenes in the hydrogenation of alkynes can be improved to a large extent.

As a proof of the SAA concept, Sykes and co-workers studied the selective hydrogenation of 1,3-butadiene on Pt/Cu(111) model surface where Pt dispersed as single atoms.[117] H_2-TPD experiments showed that H_2 was readily dissociated on Pt/Cu(111) surface and the H atoms could migrate to Cu sites. In the presence of H atom, the adsorption of butadiene only produced butene, whereas in the absence of adsorbed H atoms, butadiene desorbed readily without decomposition or self-hydrogenation. These results suggested Pt−Cu SAA catalyst should be efficient and selective for the selective hydrogenation of alkynes. Accordingly, the authors prepared Al_2O_3 supported PtCu bimetallic nanoparticles, where the Pt/Cu ratios were kept at low level to ensure the isolation of Pt atoms. As expected, $Pt_{0.1}Cu_{14}/Al_2O_3$ exhibited promising catalytic performances in the hydrogenation of butadiene in excess propene. Under reaction conditions of 120−160 °C, 1,3-butadiene/propylene/H_2 = 2/20/16, SV = 12000 h^{-1}, >95% selectivity to butene could be obtained at full conversion of butadiene, and only 0.5−1.2% propylene was hydrogenated. In addition, the catalytic activity and selectivity could be well maintained during 46 h of time-on-stream test.

On the basis of extensive works on bimetallic catalysts,[30] Zhang and co-workers prepared SiO_2 supported Pd-based SAAs with a second metal (M = Au, Ag, Cu) by either two-step reduction (for Au−Pd) or coimpregnation method (for Cu−Pd and Ag−Pd).[96−98] In the hydrogenation of acetylene in excess ethylene ($C_2H_2/C_2H_4/H_2$ = 1/20/20, SV = 60000 h^{-1}), the addition of the IB group metal to Pd greatly enhanced the selectivity to ethylene, although the catalytic activity was lower than Pd/SiO_2. For example, 56.4% selectivity could be obtained at 86% conversion of acetylene over $AuPd_{0.01}/SiO_2$ at reaction temperature of 160 °C.[97] $AgPd_{0.01}/SiO_2$ showed much better catalytic performance than $AuPd_{0.01}/SiO_2$, and 80% selectivity to ethylene was achieved at an acetylene conversion of 93%.[96] Impressively, the catalytic activity and selectivity were further enhanced on $CuPd_{0.006}/SiO_2$, and 85% selectivity was obtained at full conversion of acetylene.[98] Microcalorimetry studies showed that both the initial adsorption heat and uptake of C_2H_4 over Pd/SiO_2 were significantly decreased over the Pd SAA catalysts than the pure Pd/SiO_2, indicating the adsorption of C_2H_4 was greatly weakened on isolated Pd sites. On the other hand, despite the initial adsorption heat of H_2 on the $CuPd_{0.006}/SiO_2$ SAA catalyst was lower than that on Pd/SiO_2, it was higher than that on Cu/SiO_2, implying the capability for dissociation of H_2 of $CuPd_{0.006}/SiO_2$ was enhanced when compared with Cu/SiO_2. Taken together, the weakened adsorption of C_2H_4 and the enhanced H_2 dissociation ability of the Pd centered SAA catalysts led to both of the high selectivity to ethylene and high catalytic activity. As for the trend of catalytic performances of $CuPd_{0.006}/SiO_2$ > $AgPd_{0.01}/SiO_2$ > $AuPd_{0.01}/SiO_2$ (Figure 10a), the higher selectivity was ascribed to the higher electron

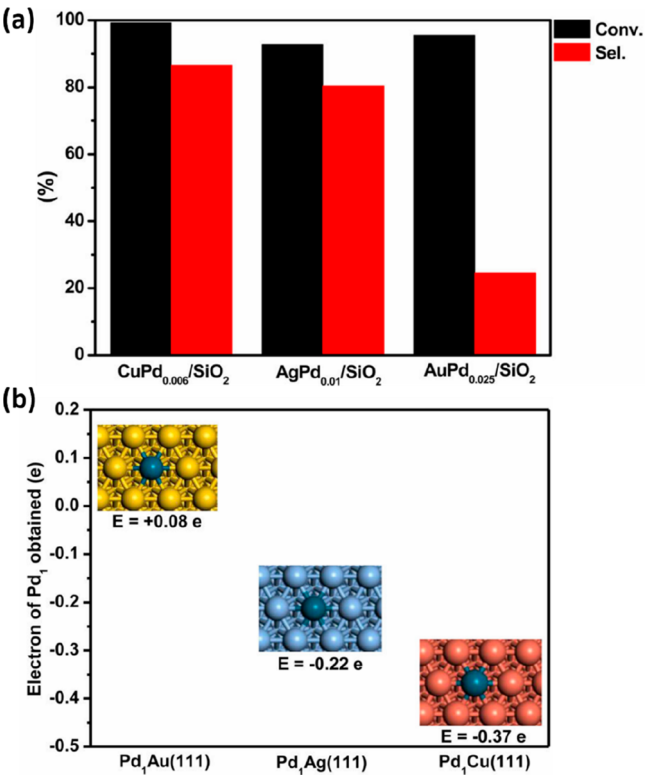

Figure 10. (a) Catalytic performance of SiO_2 supported Cu−Pd, Ag−Pd, and Au−Pd SAA catalysts in the hydrogenation of acetylene; (b) DFT calculation results of electron states of isolated Pd atoms on alloying into Au(111), Ag(111), and Cu(111) surfaces. Adapted with permission from ref 98. Copyright 2017 American Chemical Society.

density of Pd in $CuPd_{0.006}/SiO_2$ catalyst, which would repel the nucleophilic C═C bond and facilitate their desorption (Figure 10b). The enhanced activity was owing to the easier spillover of hydride on Cu than on Au. However, during the 24 h run stability test, gradual decrease of the catalytic activity was observed over these Pd-based SAA catalysts. The underlying reason needs to be addressed further by operando characterizations. Similar results were also obtained by Bachiller-Baeza and co-workers, who discovered that the incorporation of Cu into Pd supported on graphite greatly improved the selectivity in the partial hydrogenation of 1,3-butadiene.[143]

The preparation methods had profound impact on the surface composition and structure of Pd based bimetallic catalysts and consequently on the catalytic performances. For example, Moon and co-workers reported that a large proportion of Cu or Ag was deposited on the Al_2O_3 support when the catalyst was prepared by impregnation method. By contrast, selective deposition of Cu and Ag on the surface of Pd could be achieved by surface redox method and thus led to more effective isolation of the continuous Pd ensembles.[118,119] In the selective hydrogenation of acetylene (0.95% acetylene in

DOI: 10.1021/acs.chemrev.9b00230
Chem. Rev. XXXX, XXX, XXX−XXX

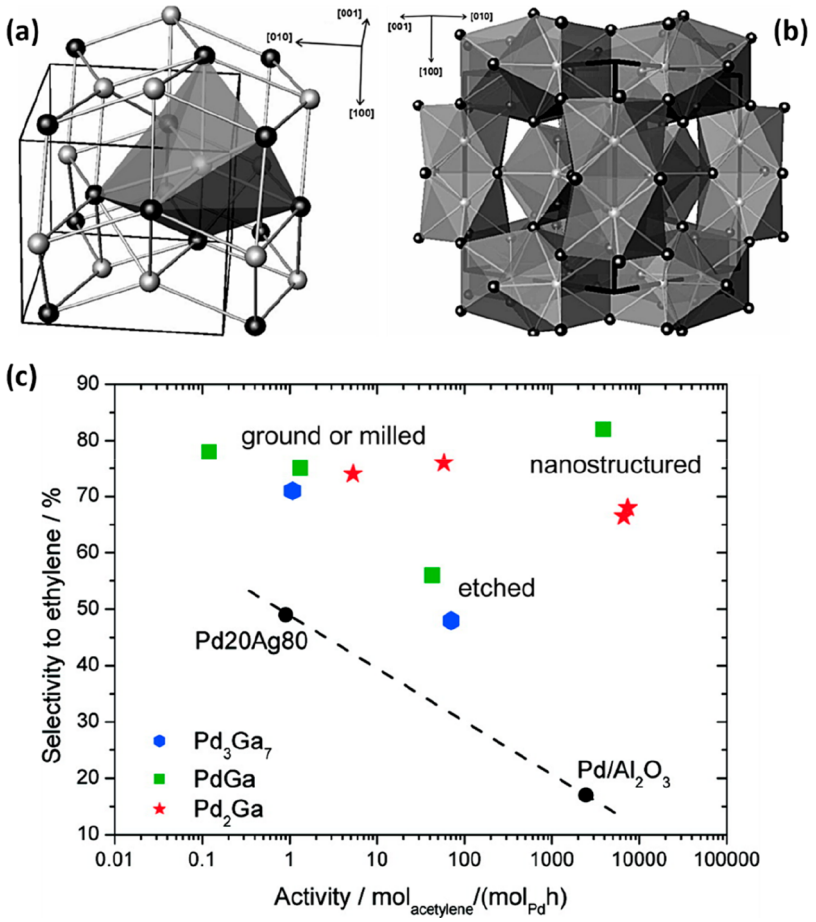

Figure 11. Illustration of the crystal structure of PdGa (a) and Pd_3Ga_7 (b) intermetallics. In PdGa, each Pd atom (white spheres) is surrounded by seven Ga atoms (black spheres), while in Pd_3Ga_7, each Pd atom (white spheres) is surrounded by eight Ga atoms (black spheres). (c) Catalytic performances of different Pd−Ga intermetallics in the acetylene hydrogenation (dashed line is a guide to the eye). (a,b) Adapted with permission from ref 94. Copyright 2008 Elsevier. (c) Adapted with permission from ref 121. Copyright 2010 American Chemical Society.

ethylene), the selectivity to ethylene was higher over Pd−Cu(Ag) catalysts made by surface redox method. A photoreduction method was also employed to prepare Ag−Pd/TiO_2 catalysts.[120] TiO_2 is a well-known semiconductor, which generates electrons upon irradiation by UV light and can reduce metal ions bearing large oxidation potential, such as Pd(II) and Ag(I). In the hydrogenation reactions (60 °C, $C_2H_2/C_2H_4/H_2$= 0.73/52.6/1.46, SV = 72000 mL g^{-1} h^{-1}), 90.3% selectivity to ethylene was achieved at 57.4% conversion of acetylene over Pd_2Ag_3/TiO_2, whereas the selectivity was −183% on Pd/TiO_2. Notably, at the same Ag/Pd ratios, the catalyst prepared by photoreduction method was much more selective than that prepared by impregnation method, demonstrating the more selective deposition of Ag on the surface of Pd by the photoreduction method.

As aforementioned, in bi/multimetallic alloys, different atoms are randomly distributed on the lattice positions (Figure 9), and the compositions are varied from one particle to another, which leads to insufficient isolation of active metal ensembles. In addition, the surface segregation and deconstruction might occur in alloy catalysts during the reactions, which will further degrade the isolation effect. On the contrary, in intermetallics, the active metal atoms are exclusively surrounded by the second metal atoms at proper compositions. Moreover, the (covalent) interaction between each component leads to high thermal stability and structural integrity under reaction conditions, both of which make intermetallics be more promising candidates for the selective hydrogenation catalysts.

Armbrüster and co-workers investigated the catalytic performances of Pd−Ga intermetallics for the partial hydrogenation of alkynes.[94,121−123,144,145] In their initial work, they prepared series of Pd−Ga intermetallics (Pd_3Ga_7, PdGa, Pd_2Ga) by melting corresponding amounts of elemental Pd and Ga under inert atmosphere (Figure 11a,b).[94,121] These materials gave ∼80% selectivity to ethylene in the semihydrogenation of acetylene (Figure 11 c) under reaction conditions of 200 °C, $C_2H_2/C_2H_4/H_2$ = 0.5/50/5, SV = 1.8−2.4 × 10^4 mL g^{-1} h^{-1}. In situ characterizations revealed that no hydride formation, phase transition, or decomposition occurred during the hydrogenation reaction, implying the high stability of the catalysts. However, due to the extremely low surface area of these samples, their intrinsic activity was quite low. Effects to increase the surface area by partially dissolution of Ga using ammonia solution failed because of the deconstruction.[145] Subsequently, the authors synthesized supported nanoparticulate GaPd intermetallics either by using Mg−Pd−Ga hydrotalcite as precursor[121,123] or by colloid method.[122] Notably, when the size was decreased to nanometer scale, the catalytic activity of these supported PdGa intermetallics was enhanced by 4−5 orders of magnitude, while the selectivity to alkenes was well maintained at 70−80%. For example, the activity of the $Pd_2Ga/MgO/MgGa_2O_4$ catalyst

DOI: 10.1021/acs.chemrev.9b00230
Chem. Rev. XXXX, XXX, XXX−XXX

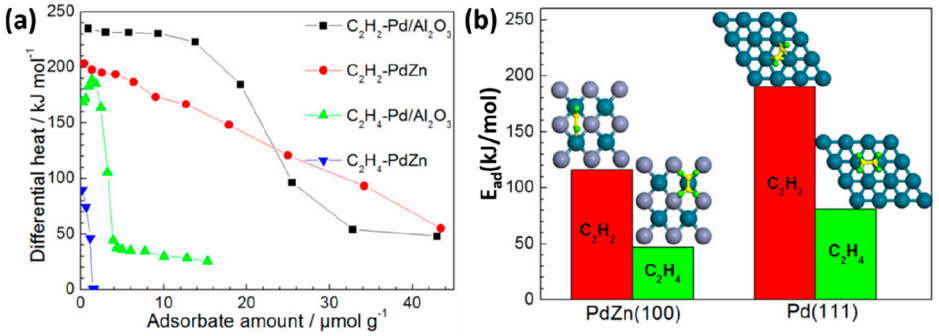

Figure 12. Microcalorimetry of acetylene or ethylene adsorption on PdZn and Pd/Al_2O_3 catalysts (a) and DFT modeling of acetylene and ethylene adsorption on PdZn(100) or Pd(111) surfaces (b). Adapted with permission from ref 95. Copyright 2016 American Chemical Society.

was enhanced by a factor of more than 5700 compared to a bulk Pd_2Ga sample.[123] And in the case of Al_2O_3 supported $GaPd_2$ and GaPd nanoparticles, the catalytic activity was increased by a factor of 1300 and 35000, respectively.[122]

Su and co-workers also investigated the catalytic performances of Pd−Ga intermetallics in the semihydrogenation of acetylene.[124] CNTs supported Pd_2Ga nanoparticles were prepared via impregnation method. In the hydrogenation of acetylene (200 °C, $C_2H_2/C_2H_4/H_2$= 0.5/50/5, SV= 7.5 × 10^6 mL g^{-1} h^{-1}), a moderate selectivity of 58.1% to ethylene was obtained at 90% conversion of acetylene. However, the selectivity of Pd_2Ga/CNTs was much inferior to that of $Pd_2Ga/MgO/MgGa_2O_4$ as well as $GaPd_2/Al_2O_3$ (70−80%),[122,123] which might arise from the inhomogeneous composition between nanoparticles prepared by impregnation method. It seems that in Ga-rich PdGa intermetallics (such as Pd_1Ga_1 and Pd_3Ga_7, Figure 11), the Pd atom is well isolated by surrounding Ga atoms. While in Pd-rich ones, continuous Pd ensembles (e.g., Pd_3 trimer) might still exist.[146] Although DFT calculations and scanning tunneling microscopy images showed that ethylene can be adsorbed on these Pd_3 trimers via weak π-binding mode,[146] experimental results, by contrast, demonstrated that the Pd_3 entities in Pd_3In intermetallics were indeed detrimental to the selectivity.[126]

Compared with PdGa, PdZn intermetallics were more active and selective for acetylene hydrogenation. Zhang, Wang, and co-workers prepared PdZn/ZnO catalysts by impregnation method.[95] In the hydrogenation reactions under conditions of 60 °C, $C_2H_2/C_2H_4/H_2$ = 2/40/20, SV = 5.4 × 10^5 h^{-1}, 90% selectivity to ethylene was achieved at full conversion of acetylene, which was unprecedented as the ethylene would be reduced when the alkynes were totally consumed over most of the catalysts reported. Impressively, the PdZn intermetallic catalysts showed excellent catalytic activity, e.g., a TOF value as high as 5.6 s^{-1} was obtained at steady state, which was, although lower than that of the benchmark Pd/Al_2O_3, yet much higher than most of the catalysts reported in the literatures (usually TOF = 0.2−1.0 s^{-1}). In addition, the high catalytic performance could be well maintained during 20 h time-on-stream test, whereas the catalytic activity gradually decreased over Pd/Al_2O_3. Microcalorimetry tests revealed that the initial adsorption heat of C_2H_4 on PdZn catalysts (90 kJ/mol) was much lower than that on Pd/Al_2O_3 (169 kJ/mol) (Figure 12a), indicating the weak adsorption of C_2H_4 on the isolated Pd sites was responsible for the high selectivity. On the contrary, the adsorption heat of C_2H_2 was only slightly decreased from 235 kJ/mol on Pd/Al_2O_3 to 203 kJ/mol over Pd single atoms. DFT calculations revealed that C_2H_4 can only be adsorbed via a weak π-bond mode on Zn−Pd−Zn ensembles, however, C_2H_2 can be adsorbed through a moderate σ-mode (Figure 12b), in good agreement with microcalorimetry measurement results. The distinct adsorption modes between C_2H_2 and C_2H_4 might arise from their subtle differences in electronic density and bond length. On the other hand, DFT calculations also implied that the PdZn ensembles might provide sites for the coupling of acetylene to form oligomers, which was detrimental to both the selectivity and stability. In this respect, the fabrication of supported Pd single atoms without Pd−M (M refer to the second metal) ensembles (e.g., supported Pd single atoms) might be helpful to achieve 100% selectivity to alkenes in the partial hydrogenation of alkynes.

Traditionally, intermetallics are prepared via high-temperature melting method, which led to particles with large size and low catalytic activity, and therefore the synthesis of small-sized nanoparticles is desirable to improve the atom utilization efficiency. On this ground, Zhou and co-workers employed MOFs, a kind of materials with abundant pores and large surface areas, to fabricate sub-2 nm PdZn intermetallic nanoparticles.[125] The support was prepared by pyrolysis of ZIF-8, a kind of Zn-containing MOFs material, at 650 °C under Ar atmosphere, by which the MOF was transformed into N-doped carbon where Zn ions were coordinated to N atoms. Pd was then loaded by impregnation method, followed by H_2 reduction at 400 °C. By changing the loading, PdZn nanoparticles with different sizes from 1.2 to 10 nm could be obtained. In the hydrogenation reaction of acetylene under conditions of $C_2H_2/C_2H_4/H_2$ = 0.65/50/5, SV = 4.8 × 10^4 h^{-1}, the small sized nanoparticles not only showed much higher specific activity but also higher selectivity to ethylene. For example, 80% selectivity could be obtained over PdZn-1.2 nm, whereas 50% over PdZn-10 nm. DFT calculations revealed that over small PdZn nanoparticles, the barrier for desorption of ethylene was much lower than that for hydrogenation and thus led to higher selectivity. On the contrary, the energies required for desorption and hydrogenation were similar on the bigger ones. This conclusion is questionable, however, because if Pd is well isolated by Zn in PdZn intermetallics, the selectivity, rather than the catalytic activity should not be depended on the size of particles. The deterioration of selectivity with increase of the size of PdZn nanoparticles in this work probably arose from the presence of continuous Pd ensembles in bigger PdZn nanoparticles. Because the loading of Pd in PdZn-10 nm was 12.2-fold higher than that in PdZn-1.2 nm, PdZn intermetallic might be incompletely formed in PdZn-10 nm when no extra Zn source was added, as evidenced

DOI: 10.1021/acs.chemrev.9b00230
Chem. Rev. XXXX, XXX, XXX−XXX

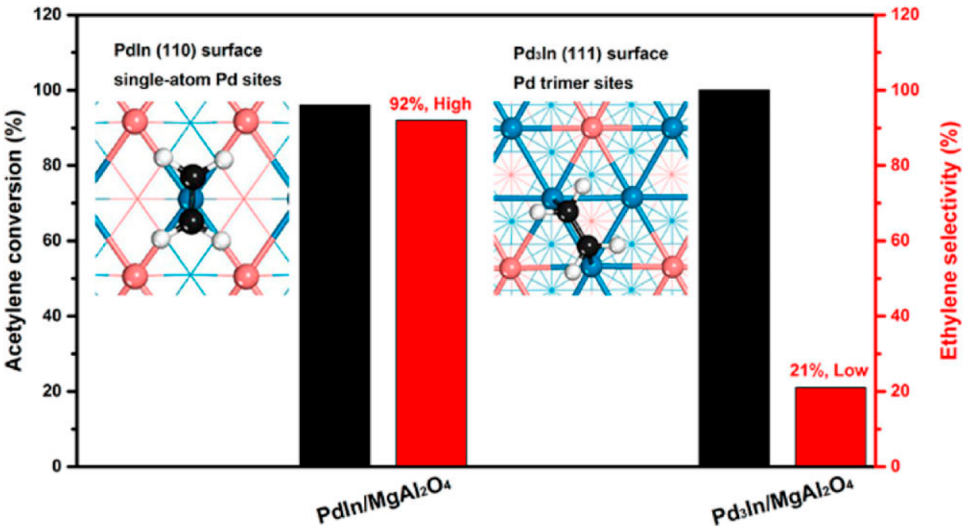

Figure 13. Geometric structure of PdIn(110) and $Pd_3In(111)$ surface and their catalytic performance in the hydrogenation of acetylene. Adapted with permission from ref 126. Copyright 2017 American Chemical Society.

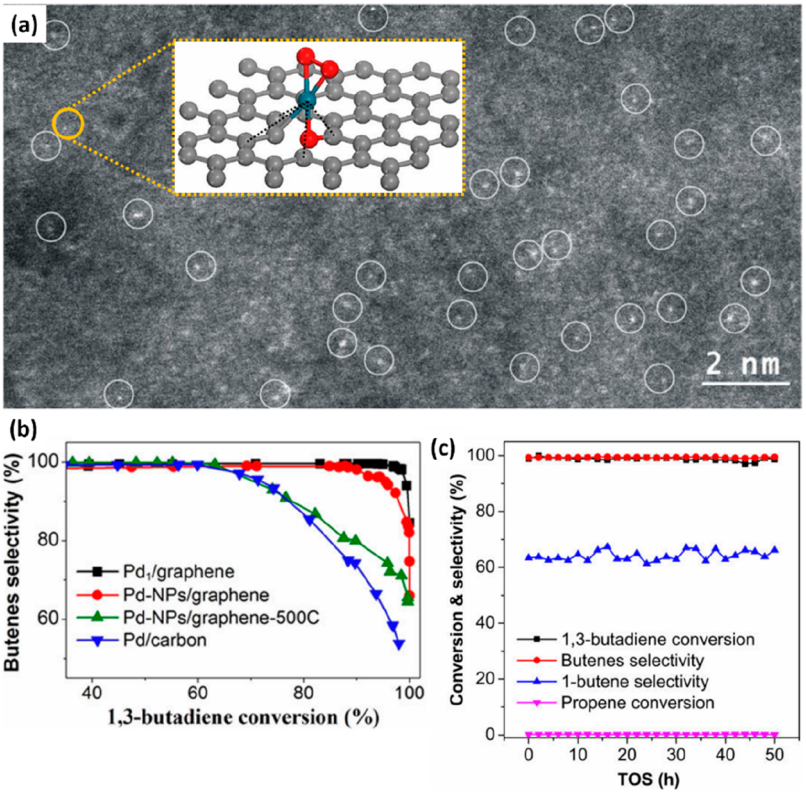

Figure 14. (a) HAADF-STEM images of Pd_1/graphene; (b) butenes selectivity as a function of conversion over different Pd catalysts; (c) durability test on Pd_1/graphene in the presence of 70% propene. Adapted with permission from ref 102. Copyright 2015 American Chemical Society.

by the gradual upshift of the peak with an increase of the Pd loading in R-space in XAFS spectra.

Apart from PdGa and PdZn, Pd−In intermetallic compounds were also investigated in the semihydrogenation of acetylene in excess ethylene.[126] DFT calculations revealed that in Pd_3In intermetallics, which mainly expose the (111) surface and Pd exists as trimers, the energy barrier for ethylene hydrogenation and desorption was comparable (Figure 13). On the contrary, in PdIn intermetallics, where each Pd atom was isolated by four In atoms, the energy barrier for ethylene desorption was much lower than that for hydrogenation, suggesting PdIn should achieve high chemoselectivity to ethylene in the semihydrogenation of acetylene. As expected, under reaction conditions of $C_2H_2/C_2H_4/H_2 = 0.5/50/5$, SV = 2.88×10^5 h^{-1}, 92% selectivity to ethylene was obtained at 96% conversion of acetylene over $PdIn/MgAl_2O_4$, whereas 21% selectivity at full conversion over $Pd_3In/MgAl_2O_4$. In addition, DFT calculation revealed that the catalysis of PdIn intermetallics was dependent on the plane exposed, with PdIn(110) surface more selective than PdIn(111) due to the

DOI: 10.1021/acs.chemrev.9b00230
Chem. Rev. XXXX, XXX, XXX−XXX

complete isolation of Pd in the former case. Similar plane-dependent catalysis was also found in PdGa and PdZn intermetallics/alloys.[146,147] Experimentally, efforts need to be put toward the exposure of (110) surface by changing the morphology of the intermetallic nanoparticles.

4.1.2.3. Supported Single-Atom Catalysts. The construction of alloys/intermetallics greatly improved the atom utilization efficiency compared with the selective poisoning approach. However, the prepared alloys/intermetallics are either bulk materials (e.g., PdGa intermetallics made by melting method) or nanoparticles with sizes larger than 2 nm, where a great portion of active metal atoms are still buried in the inner part of the alloy/intermetallic particles. On this ground, the supported SACs where each and every active metal atoms are exposed have been fabricated for the selective hydrogenation of alkynes.

Pd single atoms supported on g-C_3N_4 or graphene were studied for the hydrogenation of alkynes.[79,102,148] Lu and co-workers prepared Pd_1/Graphene through ALD method (Figure 14a).[102] Under reaction conditions of 50 °C, butadiene/propene/H_2 = 1.9/70/4.7, SV = 3.3 × 10^4 mL g_{cat}^{-1}·h^{-1}, 100% selectivity to butenes was achieved at 98% conversion of butadiene (Figure 14b), of which 71% was the more valuable 1-butene, and the proportion of propylene hydrogenation was always below 0.1%. The high activity and selectivity could be well maintained during a 100 h time-on-stream stability test (Figure 14c). DFT calculation revealed that butadiene adsorbed on the Pd single atoms in the mono-π-bond rather than the di-π-bond manner,[149] which not only prevented the overhydrogenation of butene but also efficiently suppressed the C−C coupling reaction as well as the cracking of hydrocarbons because these reactions need continuous Pd ensembles. It is noted that suitably spaced and homogeneously composed functional groups on the graphene were the prerequisite for the successful preparation of single-atom Pd catalysts. Pd single atoms could only be obtained when the phenolic group mainly existed on the graphene after annealing at 1050 °C, whereas mixtures of Pd single atoms and nanoparticles were formed when various oxygen-containing groups coexisted with high density.

Similarly, Pd_1/g-C_3N_4 was also fabricated by ALD technique and exhibited promising selectivity in the semihydrogenation of acetylene.[148] For example, when the conversion was higher than 80%, the selectivity over Pd nanoparticles decreased abruptly to 35% at a conversion of 99%, however, the selectivity was still higher than 83% on the Pd_1/g-C_3N_4 catalyst. In addition, the Pd single atoms showed higher stability than their particulate counterparts. During a 100 h durability test, the conversion decreased from 87% to 35%, and the selectivity reduced from 95% to 87% on the Pd nanoparticles accompanied by the formation of noticeable amount of green oil. On the contrary, the conversion was only slightly declined from 54% to 46%, and the selectivity dropped slightly from 96% to 92% on Pd_1/g-C_3N_4 catalyst. The deactivation of the single-atom catalyst, based on HAADF-STEM images, was attributed to the sintering of a small portion of Pd single atoms to Pd nanoparticle. The ALD technique proves to be efficient for the preparation of well-defined single-atom catalysts, however, the method demands for expensive equipment and metal precursors and difficult to be scaled up, and therefore it is highly desirable to develop facile and low-cost synthetic methods for supported single-atom catalysts.

Nanodiamond−graphene supported Pd single atoms (denoted as Pd_1/ND@G) were prepared by deposition−precipitation method, and gave >90% selectivity at 100% conversion of acetylene under reaction conditions of 180 °C, $C_2H_2/C_2H_4/H_2$= 1/20/10, SV = 60000 m Lg^{-1} h^{-1}.[103] XAFS characterizations revealed that Pd atoms bonded strongly to three C atoms in the defects of graphene, which were responsible for the good durability. However, the TOF value of Pd_1/ND@G was calculated to be 0.064 s^{-1} (180 °C), which was orders of magnitude lower than that of PdZn/ZnO (5.6 s^{-1}, 60 °C)[95] and Pd_4S/CNFs (27 s^{-1}, 200 °C).[93] The low catalytic activity, according to DFT calculations, might be ascribed to the low mobility of atoms (e.g., C atoms) coordinating to Pd atoms in nonreducible materials, which made the activation of H_2 and subsequent spillover of hydride difficult to occur.[69]

Besides carbonaceous materials, metal oxide supported Pd single atoms were also effective catalysts for the hydrogenation of alkynes. ZnO supported Pd single-atom catalyst 0.01 wt % Pd/ZnO was obtained by reducing the catalyst precursor at lower temperatures (100 °C).[132] In the hydrogenation of acetylene in excess ethylene (80 °C, $C_2H_2/C_2H_4/H_2$ = 2/40/20, SV = 3.6 × 10^4 h^{-1}), the selectivity to ethylene could reach as high as 98% at a conversion of 80%, even better than the PdZn/ZnO intermetallic catalyst.[95] $Ni(OH)_2$ supported Pd single-atom catalysts also showed high selectivity in the partial hydrogenation of acetylene.[133] Under reaction conditions of 100 °C, $C_2H_2/C_2H_4/H_2$ = 0.65/50/5, SV = 24000 mL g^{-1} h^{-1}), 80% selectivity to ethylene could be achieved at 80% conversion. However, further increasing the conversion led to decrease of the selectivity. In a 12 h stability test, the selectivity gradually decreased to 70%, indicating possible surface reconstruction of the catalysts under reaction conditions, which might be caused by reduction of the support. Interestingly, the hydroxyl groups on the support significantly influenced the catalytic activity in the hydrogenation reaction, as catalysts with deficient hydroxyl groups on the support exhibited inferior activity. The reason might be related to the dissociation of H_2, the rate-determining step of the reaction. It was reported that over single atom catalysts, H_2 generally underwent heterolytic dissociation into H^+/H^- pairs at the M−O (M = Pd, Pt, etc.) interface,[66] of which H^- bonds to metal atoms, whereas H^+ coordinates to O atom. The presence of proton on the O atom could greatly reduce the barrier for hydride spillover, thus the reaction rate could be accelerated to a large degree.

4.1.2. Au Based Catalysts. The selective hydrogenation of alkynes on Au based catalysts is generally ascribed to the thermodynamic factor. DFT calculations revealed that on Au catalysts, only the triple bonds can be adsorbed and activated, whereas the C═C bond is too weakly adsorbed to be activated. Therefore, the preferential adsorption of C≡C bond resulted in the selective hydrogenation of alkynes even in the presence of excess alkenes.[150] In addition, it is difficult for Au to cleave H_2.[151,152] As a consequence, quite low hydride coverage on the Au surface also contributed to the suppression of the overhydrogenation side-reactions.

Louris and co-workers studied series of supported Au catalysts in the semihydrogenation of 1,3-butadiene. Under reaction conditions of T > 170 °C, butadiene/propene/H_2 = 0.3/30/20, GHSV = 20000 h^{-1}, the selectivity to butene was up to 100% at full conversion of butadiene.[127] Neither the size of gold nanoparticles (2−5 nm) nor the nature of the support

DOI: 10.1021/acs.chemrev.9b00230
Chem. Rev. XXXX, XXX, XXX−XXX

had influences on the activity. On the contrary, the chemical state of Au had a remarkable influence, that is, only metallic Au gave the best catalytic activity, whereas positively or negatively charged Au species were less active. To improve the catalytic activity, the authors subsequently added trace of Pd to Au catalysts. As expected, the catalytic activity of the Au−Pd alloys was enhanced by 1 order of magnitude, while the selectivity could be maintained at a high level.[128] DRIFTS measurements of adsorbed CO revealed that the Pd atoms were surrounded by Au atoms, i.e., Au alloyed Pd single atoms were formed. The isolated Pd atoms did not alter the adsorption behavior of the unsaturated reactants, however, greatly enhanced the ability of the catalyst to dissociate H_2[153] and thus improved the catalytic activity.

Mou and co-workers investigated the catalytic performances of Au/SiO_2 for the partial hydrogenation of acetylene under conditions close to current industrial operations ($C_2H_2/C_2H_4/H_2$ = 0.80/16.0/83.2, SV = 92000 mL h^{-1} g^{-1}), and obtained 94% conversion and 50−70% selectivity to ethylene.[129] Similarly, the metallic Au nanoparticles were also found to be more active than those slightly negatively or positively charged gold species, in good agreement with the work of Louris' groups.[127] Given the concerted catalysis in Au based bimetallic catalysts, the authors also prepared $Au-Ag/SiO_2$ catalysts for the selective hydrogenation of acetylene.[130] Under tail-end operation condition, the bimetallic $Au-Ag/SiO_2$ catalyst showed superior activity and selectivity to Au/SiO_2.

CNTs supported Au NPs were also evaluated in the partial hydrogenation of butadiene.[131] The CNTs were pretreated either by boiling in concentrated acid (CNTs-o), or by NH_3 at 600 °C after the acid treatment (CNT-i). In the hydrogenation of butadiene (150 °C, butadiene/H_2/N_2 = 0.6/42.2/57.2, SV = 81000 mL h^{-1} g^{-1}), 100% selectivity to butene was achieved at 80.4% conversion over Au/CNT-i, and no overhydrogenation products were detected. The Au/CNT-i was 1 order of magnitude more active than Au/CNT-o and was among the most active Au catalysts reported in literatures. Kinetic studies as well as H_2-TPD experiments showed that the NH_3 treatment greatly enhanced the ability of the catalyst to dissociate H_2, which was responsible for the high catalytic activity of Au/CNT-i. It might be that the NH_3 treatment resulted in the doping of N in CNTs, which together with Au nanoparticles formed Frustrated Lewis pairs and promoted the dissociation of H_2 via the heterolysis manner.[81]

With the development of SACs,[37,38] supported Au SACs were investigated for the selective hydrogenations. As mentioned before, Au NPs generally showed far inferior catalytic activity to Pd based catalysts because of their low ability to dissociate H_2.[128] However, when gold existed as isolated cation Au^{3+}, they showed comparable catalytic activity to Pd catalysts.[154−157] Xu and co-workers earlier reported series of Au/ZrO_2 catalysts for the hydrogenation of butadiene.[154,156] It was found that the catalytic activity had remarkable correlation with the Au^{3+}/Au^0 ratio in the samples. The catalysts containing exclusively Au^{3+} species showed the highest activity (TOF = 0.41 s^{-1}). With the decrease of Au^{3+}/Au^0 ratio, the catalytic activity gradually decreased, and was reduced by 14-fold (TOF = 0.03 s^{-1}) when metallic Au nanoparticles were exclusively present. Moreover, upon that the metallic Au nanoparticles were leached by KCN solution, the treated sample where cationic Au^{3+} were exclusively present (0.08 wt %) showed much higher catalytic activity (TOF = 0.42 s^{-1}) than the untreated one. These results suggested that metallic Au nanoparticles were just spectators in catalysis, whereas the cationic Au^{3+} were the true active species. It is noteworthy that the chemical state of Au also affected the selectivity of the catalysts.[156] Over Au^{3+}/ZrO_2, the butadiene was hydrogenated to butene with 100% selectivity at higher conversions (80−90%) of butadiene, and among the butenes products, 60% was the more valuable 1-butene. However, when metallic Au nanoparticles were present, not only the overhydrogenation product butane was detected but also the proportion of 1-butene decreased, implying different catalytic mechanism of Au^{3+} and Au^0 species for the reaction. It is well-known that in homogeneous catalysis, Au(III), fulfilling the dual role of soft, carbophilic Lewis acid and transition metal, is able to activate both C−C multiple bonds and hydrogen and catalyze the hydrogenation reaction of alkenes.[158,159] Therefore, the ZrO_2 supported isolated Au^{3+} can be regarded as mimics of homogeneous Au(III) complexes, where the cationic Au^{3+} activates both the triple bond and hydrogen, while the ZrO_2 serves as ligands of Au(III). However, it is unknown whether Au(III) supported on other oxides would be effective for the hydrogenation reaction. Therefore, the role of the ZrO_2 support the activation manner of H_2 and butadiene, and the nature of the active site (i.e., whether Au(III) single atom or the $Au-ZrO_2$ interface site) deserves further investigations.

To answer these questions, Liu and co-workers investigated the Au/ZrO_2 in the hydrogenation of butadiene by DFT calculations.[155] The results showed that the cation Au^{3+} detected by Xu[154] via ex situ XPS and H_2 titration technique was unstable during the hydrogenation reaction, and could be reduced to Au(I) species where Au atom bonds to one OH group and one lattice O atom in the ZrO_2 support. The H_2 molecule is dissociated on the Au−O bond in a heterolysis manner, where the proton binds to the lattice O atom and the hydride on Au atoms.[77] When the nucleophilic butadiene molecule approaches, the proton on the lattice O was first added to the double bond followed by the hydride on Au atom, and then the butene molecule was desorbed as a result of the large exothermicity of the hydrogenation. The deep hydrogenation of the butene was prohibited because of its competitively unfavorable adsorption when compared with butadiene. It is also emphasized that the ZrO_2 behaved more than the support of Au but also participated in the activation of H_2. In other words, it is the Au−O−Zr interface that acts as the true active species in the catalysis.

Corma's group also found that isolated Au(III) was much more active and selective than metallic Au nanoparticles in the selective hydrogenation of butadiene.[157] They prepared MOFs supported single site Au(III) catalysts IRMOF-3−SI−Au, where Au(III) cations were coordinated to the Schiff base groups in the support. In the semihydrogenation reaction, a selectivity of 97% to butene was achieved over IRMOF-3−SI−Au whereas 92% on Au/TiO_2 containing metallic Au nanoparticles. In addition, IRMOF-3−SI−Au (TOF = 540 h^{-1}) was 1 order of magnitude more active than the latter (TOF = 50.4 h^{-1}). It was considered that the Au(III) has the same d^8 electronic structure as Pd(II), which rendered them similar to catalytic performances of Pd(II) species in hydrogenation reactions.[170] In homogeneous catalysis, both homogeneous Au(I) and Au(III) catalysts were reported to be highly active for the hydrogenation reactions.[158−160] However, in the above-mentioned supported Au SACs, whether Au(I) or Au(III) is the true active species might depend on the

DOI: 10.1021/acs.chemrev.9b00230
Chem. Rev. XXXX, XXX, XXX−XXX

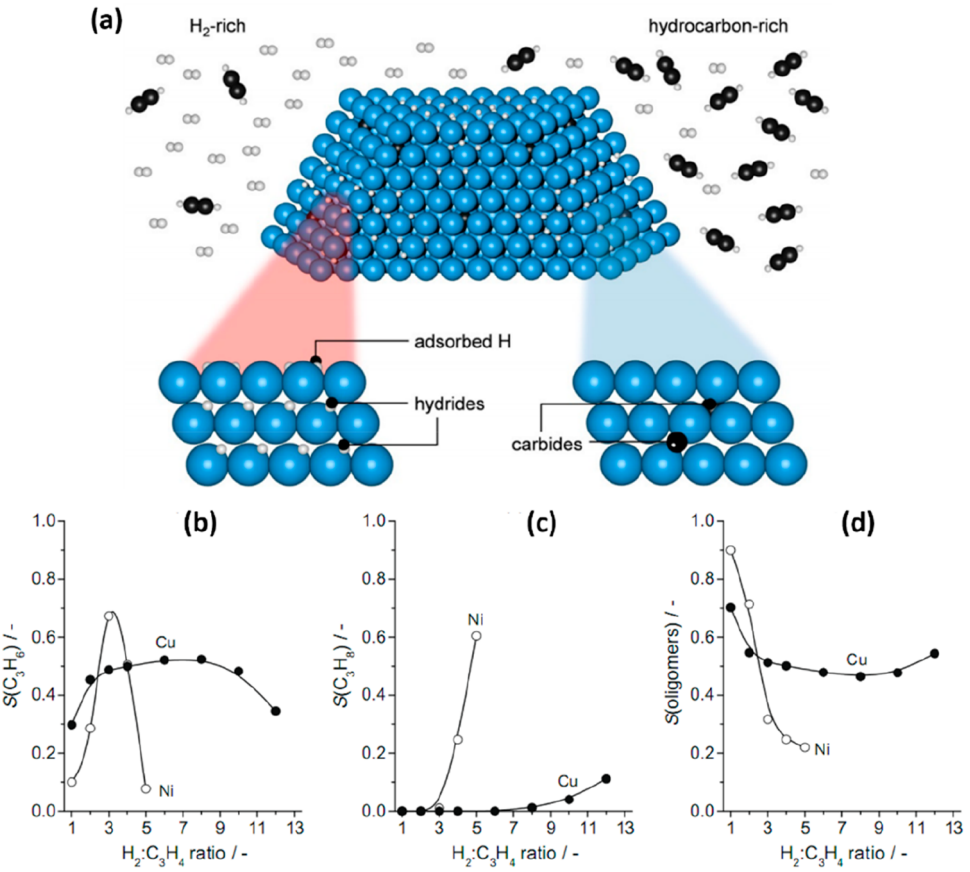

Figure 15. (a) Illustration of the formation of hydrides and carbides under H_2-rich and C_3H_4-rich conditions, respectively. Selectivity to C_3H_6 (b), C_3H_8 (c), and oligomers (d) vs the H_2:C_3H_4 ratio over copper (●) and nickel (○) catalysts in the hydrogenation of C_3H_4. (a) Adapted with permission from ref 16. Copyright 2015 John Wiley and Sons. (b−d) Adapted with permission from ref 134. Copyright 2010 Elsevier.

coordination environment (e.g., nature of the support) and the reaction conditions.

Taken together, the supported Au SACs are indeed much more efficient catalysts than the NPs counterparts for the hydrogenation reactions and might adopt different activation mechanism of the reactants from supported Au nanocatalysts. For example, Au SACs are more like Lewis acid for the activation of H_2 rather than a transition metal,[155] which, together with the heteroatom in the ligand/support, form Lewis acid−base pairs and activate H_2 in the heterolysis manner, thereby their ability to activate H_2 is greatly improved.

4.1.3. Nonprecious Metal Catalysts. Concerns on the scarcity and high cost of noble metals have driven the search for nonprecious alternatives for the chemoselective hydrogenation of alkynes.

Pérez-Ramírez and co-workers investigated Cu−Al and Ni−Al catalysts that were prepared by calcination and reduction of their hydrotalcite precursors for the semihydrogenation of propyne.[134] For Cu−Al catalysts, the selectivity was strongly dependent on the reaction temperature. When $T \geq 200$ °C (C_3H_4:H_2:He = 2.5:7.5:90 and SV = 16800), full conversion of propyne could be obtained, with up to 80% selectivity to propylene, 20% selectivity to oligomers, and trace of propane. When the temperature decreased, the selectivity to propylene decreased at the expense of oligomers, e.g., the green oil could account for 80−90% when $T \leq 150$ °C. On the contrary, the H_2/C_3H_4 ratio in the feedstock had no appreciable effect on the selectivity; in a broad H_2/C_3H_4 ratio window of 2−10, the selectivity to propylene could maintain at a moderate level (45−50%). However, the Ni−Al catalyst behaved quite differently from the Cu−Al catalysts. For the Ni−Al catalysts, the H_2/C_3H_4 ratio rather than the reaction temperature determined the selectivity (Figure 15a). The best selectivity to propylene (∼70%) was obtained only when $H_2/C_3H_4 = 3$. A large proportion of oligomers were produced at $H_2/C_3H_4 < 3$, whereas the deep hydrogenation products dominated at $H_2/C_3H_4 > 3$ (Figure 15b−d). The different behaviors of the two catalysts were ascribed to their distinct intrinsic properties. Ni is well-known to dissociate H_2 readily even at low temperatures. Meanwhile, Ni can catalyze the cracking of C−C bond to form carbides.[161] Whether the hydrides or carbides dominated on the surface/subsurface of Ni was dependent on the H_2/C_3H_4 ratios. At low H_2/C_3H_4 ratios, subsurface carbides formed and the overhydrogenation reaction was suppressed. At high H_2/C_3H_4 ratios, however, hydride was predominant on the surface and saturated alkane became the main product. On the contrary, Cu had low ability to dissociate H_2, and thereby required a higher temperature (e.g., >200 °C) to overcome the barrier for cleaving H_2, consequently, the semihydrogenation rather than the C−C coupling of alkyne was the preferred reaction pathway.

Considering that Cu based catalysts have merits of high selectivity to alkenes in a broad window of H_2/alkyne ratios, and the only side reaction of oligomerization arises from the low ability to dissociate H_2, Pérez-Ramírez's group tried to ameliorate the selectivity of Cu catalysts via addition of Ni.[89] Ternary Cu−Ni−Fe catalysts were then prepared with the coprecipitation method and evaluated in the semihydrogena-

DOI: 10.1021/acs.chemrev.9b00230
Chem. Rev. XXXX, XXX, XXX−XXX

tion reactions of acetylene and propyne. Fe was chosen as the structure modifier to promote the dispersion of Cu and Ni and prohibit their segregation. As expected, the addition of trace Ni boosted the selectivity to propylene from 70% on Cu_3Fe catalysts to 97% over $Cu_{2.75}Ni_{0.25}Fe$ under reaction condition of $C_3H_4/H_2/He$ = 2.5/7.5/90, T = 250 °C, SV= 16 800 cm^3 g^{-1} h^{-1}, and P = 1 bar. In addition, the catalytic activity was greatly enhanced. Even under low reaction temperatures of 150 °C, full conversion of propyne was achieved on $Cu_{2.75}Ni_{0.25}Fe$, whereas the Cu_3Fe deactivated rapidly under the same conditions. The improvement was ascribed to the facile dissociation of H_2 on Ni sites, which increased the coverage of hydride on Cu sites and thus suppressed the oligomerization. On the other hand, the trace amount of Ni might exist as tiny assemblies, which did not change the adsorption behavior of propylene. Noteworthy, the $Cu_{2.75}Ni_{0.25}Fe$ inherited the merits of high tolerance to H_2/alkynes ratios, and the selectivity to propylene was always >90% in a broad H_2/alkynes range of 2−6. By contrast, the industrial Pd catalysts can only be selective in a narrow range of 1−2. The high tolerance to H_2/alkynes is highly desirable for the front-end hydrogenation because the catalysts can accommodate the possible fluctuations in the feed coming from the steam cracker. Similar catalytic performance was obtained in the semihydrogenation of acetylene (250 °C, $C_2H_2/C_2H_4/H_2$ = 1/5.4/3); 80% selectivity to ethylene was achieved at full conversion of acetylene, and <10% ethane and <10% oligomers were produced owing to the less steric hindrance of C_2 for C−C coupling and overhydrogenation reaction when compared with C_3. The only drawback of the catalysts is the higher operating temperature (250 °C) compared with Pd based catalysts (<100 °C). However, the higher chemoselectivity and lower price of the $Cu_{2.75}Ni_{0.25}Fe$ might offset their low catalytic activity.

Ni, when forming alloys/intermetallics with another metal, can also be a promising catalyst for the selective hydrogenation reaction. Studt and co-workers predicted that NiZn alloys can serve as alternatives for the commercial AgPd catalysts in the hydrogenation reaction of acetylene based on the consideration that the stabilities of alkenes and alkynes on the catalysts, rather than the activation energies for further transformation, are the dominant parameters governing the catalytic selectivity.[100] Accordingly, they prepared $MgAl_2O_4$ spinel supported NiZn alloys, which as expected demonstrated higher selectivity to ethylene than the state-of-the-art AgPd catalysts at high acetylene conversion level.[162] On the basis of their work on Pd based SAA catalysts,[96−98] Zhang and co-workers also prepared nonprecious Ni−Ag SAA catalysts for the partial hydrogenation of acetylene.[135] Under reaction conditions of $C_2H_2/C_2H_4/H_2$ = 1/20/20, SV = 60000 h^{-1}, full conversion of acetylene could be obtained over Ni/SiO_2, yet the selectivity was rather poor (−1100%), whereas Ag/SiO_2 was totally inactive for the reaction. The bimetallic $AgNi/SiO_2$ catalysts showed obvious synergistic effect in the catalysis, e.g., 31.4% selectivity to ethylene could be achieved at 90.4% conversion over $AgNi_{0.125}/SiO_2$. Furthermore, the addition of Ag to Ni effectively suppressed the side reaction of methanation. The separation of continuous Ni ensembles by Ag was believed to be responsible for the high selectivity.

Inspired by the great success of Pd based intermetallics for the selective hydrogenation of alkynes,[95,121,122,126] Armbrüster and co-workers fabricated $Al_{13}Fe_4$ intermetallics by melting of cleaned pieces of Fe and Al under inert atmosphere.[136] In the semihydrogenation of alkyne under reaction condition of 200 °C, $C_2H_2/C_2H_4/H_2$ = 0.5/50/5, high selectivity of 81−84% to ethylene was achieved at high acetylene conversion level (80%). The only byproduct was C_4 compound formed by C−C coupling reaction, and higher hydrocarbons were not detected. In addition, the high catalytic performance of $Al_{13}Fe_4$ catalyst was well preserved during the 160 h time-on-stream test, with negligible amounts of coke being detected on the spent catalysts by Raman and TPO measurements. Therefore, the $Al_{13}Fe_4$ catalyst showed great potential for practical application, as the selectivity was only slightly lower than that of industrial benchmark catalyst (selectivity = 90%), however, the price is much more attractive. Control experiments revealed that either unsupported Fe powders, or 4 wt % Fe/Al_2O_3, was totally inactive for the reaction even after high temperature reduction, thus precluding the possible contribution of bulk Fe or Fe nanoparticles to the catalysis. In situ XPS and XRD measurements showed that surface hydride and carbide were not formed on the catalysts, demonstrating the high structural stability of the Fe−Al intermetallics. DFT calculations suggested that in $Al_{13}Fe_4$, Fe was isolated by Al, which is similar to Pd_2Ga intermetallics where Pd was isolated with Ga atoms.[94,121,123] The absence of continuous Fe sites greatly decreased the adsorption strength of the unsaturated reactants and thus avoided side reactions of deep hydrogenation, cracking of C−C as well as the severe C−C coupling that typically occurred on bulk and nanoparticles of Fe (e.g., the Fischer−Tropsch synthesis). The intermetallics of $Al_{13}Co_4$ showed similar catalytic performances to $Al_{13}Fe_4$, suggesting construction of intermetallics is a powerful approach to the efficient catalysts for selective hydrogenation reactions.

Although construction of alloys/intermetallics with a second metal is effective strategies to improve the selectivity of Pd or Ni based catalysts, the choice of the second metal deserves careful consideration. For example, in the Ni−In bimetallic catalysts for the semihydrogenation of acetylene, the In ingredient played a role of "double edged sword".[137] At low In/Ni ratios, In could separate the continuous Ni ensembles and therefore increase the selectivity to ethylene and suppress the formation of oligomers. However, with an increase of In/Ni ratios, decrease of both the selectivity and durability was observed. NH_3−TPD experimental results showed that with an increase of In/Ni ratios, the acidity of the catalyst became strong. The In_2O_3 ingredient, which is Lewis acid intrinsically, catalyzes the polymerization of acetylene/ethylene to form green oil and coke at high In contents and therefore impairs the selectivity to ethylene and aggravates the deactivation of the catalyst.

CeO_2, a well-known promoter, stabilizer, or cocatalyst for reactions such as oxidation, water−gas shift, and combustion of alkanes, can efficiently catalyze the partial hydrogenation of alkynes solely. Pérez-Ramírez and co-workers reported that under reaction conditions of 250 °C, H_2/alkyne = 30, 0.1 MPa, high selectivity of 91% (81%) to propylene (ethylene) was obtained at 96% (86%) propylene (acetylene) conversion.[138] The only byproduct was green oil (<10%), and no deep hydrogenation products were detected. In terms of the selectivity, CeO_2 was superior to most of the transition metal catalysts developed so far for the target reaction, thus showing great potential for industrial application. ICP-OES examination showed that no transition metal (such as Pd, Ni, Pt, Au) contained in CeO_2, and when the metal was added on purpose (e.g., 0.05 wt % Pd), the selectivity was decreased dramatically, therefore precluding the possible contribution of transition

DOI: 10.1021/acs.chemrev.9b00230
Chem. Rev. XXXX, XXX, XXX−XXX

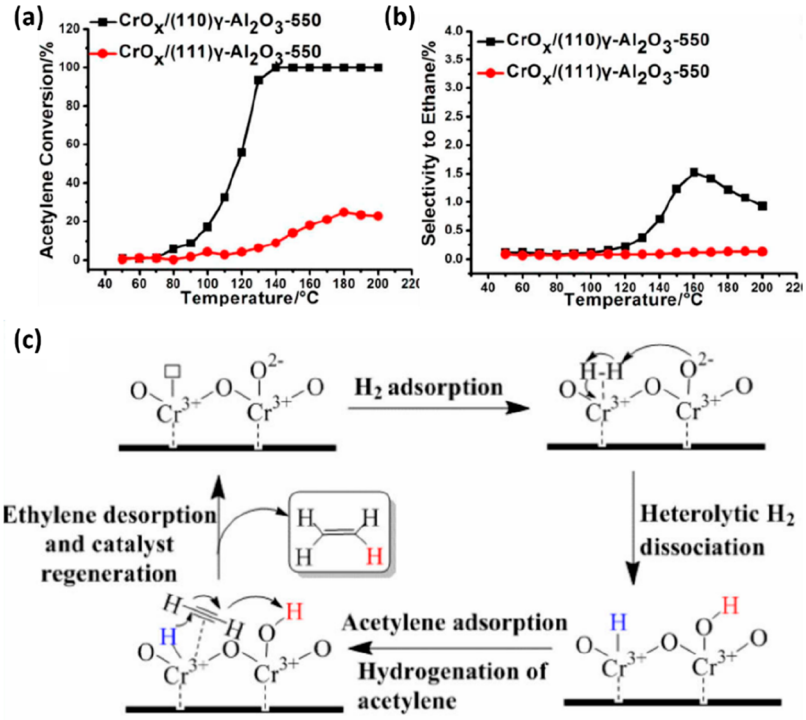

Figure 16. (a) Acetylene conversion and (b) selectivity to ethane in the hydrogenation reactions on $CrO_x/(110)\gamma$-Al_2O_3 and $CrO_x/(111)\gamma$-Al_2O_3 catalysts; (c) proposed mechanism of the hydrogenation of acetylene. Adapted with permission from ref 140. Copyright 2017 American Chemical Society.

metals to the catalysis. The catalytic performances were largely dependent on the reduction degree of CeO_2. When the reaction was conducted at higher temperature (e.g., above 300 °C where CeO_2 began to be reduced), or CeO_2 was prereduced by H_2, both of the activity and selectivity decreased remarkably, suggesting the oxygen vacancies were detrimental to the reaction. Reaction mechanism investigation through FTIR measurements and DFT calculations showed that H_2 was cleaved on immobile surface oxygen atoms forming two OH groups, while the alkyne was adsorbed on Ce atom. The isolation of Ce atom by four oxygen atoms prevented the C−C coupling and overhydrogenation side reactions. Nevertheless, Datye and co-workers proposed different catalytic mechanism of CeO_2 for the semihydrogenation reaction.[76] They prepared CeO_2 doped with single Ni atoms, which showed much higher catalytic activity in the hydrogenation reaction of acetylene when compared with nondoped CeO_2. On the basis of DFT calculations, they believed that the Ce and O atoms surrounding an oxygen vacancy formed frustrated Lewis pairs (FLPs), which was responsible for the dissociation of H_2 in a heterolytic manner. The formed O−H and Ce−H species then efficiently hydrogenated acetylene molecule to generate ethylene. The Ni single atoms did not directly take part in the hydrogenation reaction but assisted to create oxygen vacancies under H_2 atmosphere.

Partially reduced In_2O_3 was also found as an efficient catalyst for the semihydrogenation of acetylene.[139] Under reaction conditions of 350 °C, H_2/C_2H_2 = 30, 0.1 MPa, 85% selectivity to ethylene could be achieved at full conversion of acetylene, and the selectivity to ethane was below 5%. It was noted that high H_2/C_2H_2 ratio was prerequisite for the high selectivity, as a great proportion of green oil was produced at low H_2/C_2H_2 ratio. Even in the presence of excess ethylene, the high selectivity could be well preserved, and there was no noticeable deterioration of the catalytic performance during 100 h stability test. DFT calculations revealed that the In_3O_5 ensembles surrounding the oxygen vacancies were the active sites for the hydrogenation reaction.

Ding and co-workers reported that $(110)\gamma$-Al_2O_3 supported CrO_x catalyst was selective for the acetylene hydrogenation.[140] Under conditions of 140 °C, C_2H_2/C_2H_4 = 0.475/9.25, SV = 21660 h^{-1}, 98.5% selectivity could be achieved at full conversion (Figure 16a,b). The crystal facets of γ-Al_2O_3 had profound effect on the catalytic activity. When CrO_x was loaded on a (110) facet, full conversion could be obtained, while 20−40% on a (111) facet. It was believed that CrO_x supported on low-energy (110) facets was more reducible than that on high-energy (111) surface, which was responsible for the high catalytic performance. A heterolysis mechanism of H_2 on the $CrO_x/(110)\gamma$-Al_2O_3 was proposed, producing hydride bonded to unsaturated Cr(III) cation and proton on lattice oxygen anion, which species then hydrogenated the acetylene in a sequential manner (Figure 16c).

4.2. Catalysts for Liquid-Phase Semihydrogenation Reactions

The liquid-phase semihydrogenation of acetylenic compounds is important transformations for the industrial production of *cis*-alkenes, key building blocks for drugs, vitamins, fragrances, and agrochemicals.[12,20,163] Traditionally, these hydrogenation reactions were conducted in semibatch reactors using Lindlar catalysts (5 wt %Pd/$CaCO_3$ modified by lead and sometimes quinoline).[20,22,261] The toxic nature of the catalyst as well as the extremely low atom utilization efficiency of Pd (e.g., usually $^1/_{10}$ of Pd atoms were available for the hydrogenation reaction) has motivated researchers to develop more efficient alternatives for the target reactions. Indeed, the "active site isolation" strategy proved also effective for the liquid-phase hydro-

DOI: 10.1021/acs.chemrev.9b00230
Chem. Rev. XXXX, XXX, XXX−XXX

Table 2. Catalysts for the Liquid-Phase Hydrogenation of Alkynes

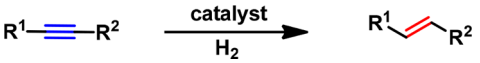

substrate	catalyst	T (°C)	P (MPa)	conv (%)	selectivity (%)	ref
phenylacetylene	Ag/SiO_2	100	10	30	100	177
phenylacetylene	Au/TiO_2	100	10	30	96	177
phenylacetylene	$Au@CeO_2$	25	3	99	99	178
phenylacetylene	$Au@CeO_2$/HT	120	3	99	>99	179
diphenylacetylene	Pd−Pb NCs	25	0.1	96	96	21
1-decyne	Pd−Pb NCs	25	0.1	100	99.4	21
18-carbon polyunsaturated fatty acids	Pd/Al_2O_3-thiolate	30	0.6	>70	80−90	164
2-methyl-3-butyn-2-ol	Pd_3S/C_3N_4	30	0.1		100	166
1-phenyl-1-propyne	$Pd@MPSO/SiO_2$	30	0.1	99	98	165
phenylacetylene	$SiO_2@CuFe_2O_4$-Pd		0.1	98	98	168
phenylacetylene	Pd/Cu_2O	30	0.1	99	98	169
phenylacetylene	Pd/N,O-carbon	25	0.1	99	97	180
phenylacetylene	$Pd@mpg\text{-}C_3N_4$	30	0.1	100	94	181
3-hexyn-1-ol	$Pd\text{-}^{int}B/C$	30	0.3		98	167
1-octyne	Pd@Ag/HAP	25	0.1	99	99	170
phenylacetylene	$Pd@Ag@CeO_2$-1.5	40	1.5	98	99	171
H_2/1-pentyne=4	Pd/ZnO	100	0.1	41	87	172
phenylacetylene	$Pd_5Au_5/ZnTi$	45	0.1	100	92.5	173
1-hexyne	$PdAu\text{-}SAA/SiO_2$	25	0.5	100	85	174
phenylacetylene	$Pd_{0.18}Cu_{15}/Al_2O_3$	25	0.69	90	94	175
1-hexyne	$[Pd]mpg\text{-}C_3N_4$	70	0.5		90	79
1-hexyne	AgTCM-mpg-CN	30	1		100	176

genation of alkynes, such as selective poisoning with thiolate,[164,165] incorporation of p-block atoms into interstitial sites of Pd,[166,167] bimetallic and core@shell structure,[168−175] and construction of single-atom catalysts.[79,176] Because the mechanism is similar for both gas-phase and liquid-phase hydrogenations, more details are not repeated here. A summary of the catalysts developed so far for the liquid-phase selective hydrogenation of alkynes is presented in Table 2. In comparison with the gas-phase hydrogenations, liquid-phase reactions proceed usually at milder conditions (low temperature and H_2 pressure), which allows for the more extensive use of organic modifiers to the Pd catalysts.

4.3. Summary

In summary, the semihydrogenation of alkynes and dienes to alkenes is of great significance in both academia and industry. On the basis of the theoretical understanding of the adsorption behaviors of alkyne/alkene and H_2 on metal surfaces, many strategies have been developed toward highly efficient and selective catalysts, such as incorporation of interstitial atoms into the lattice of Pd (e.g., $Pd\text{-}^{int}B$),[167] selective poisoning surface sites by CO or sulfur (e.g., Pd_4S),[93,112,166] and utilization of metal oxides (e.g., CeO_2, In_2O_3).[138−140] Among others, the "active site isolation" strategy is proved to be the most effective, by which all of the side reactions requiring continuous metal ensembles (overhydrogenation, oligomerization, and C−C cracking) can be effectively suppressed.[94,101] The ultimate isolation of the metal ensembles is single atom dispersion, and accordingly, various single-atom catalysts, including those anchored on the support or alloyed with a second metal, have been fabricated and shown promising activity and far superior selectivity to their nanoparticulate counterparts in the semihydrogenation reactions, either in gas phase or liquid phase.[79,96−98,102,117,126,148,155,174,176] Impressively, for some metals with low ability to dissociate H_2 in their bulk or nanoparticulate form, their catalytic activity was boosted when dispersed as single atoms (e.g., Au_1/ZrO_2, Ag_1/C_3N_4).[154,155,176] In addition, owing to the suppression of coking and oligomerization, the durability of SACs was greatly improved, thus showing great potential for practical applications. However, before their industrial application to replace the current industrial catalysts, some issues should be addressed.

First, the catalytic activity of SACs should be further enhanced. In the gas-phase semihydrogenation reactions of alkynes, although a great many SACs have been developed, of which only a few showed competitive catalytic activity with benchmark Pd/Al_2O_3 catalysts, e.g., the PdZn/ZnO catalyst developed by Zhang, Wang, and co-workers, gave comparable TOF (5.3 s^{-1}) value to Pd/Al_2O_3.[95] However, for most of the others, the intrinsic activity was quite low (<0.1 s^{-1}),[102,148] and also high reaction temperature (>100 °C) was required.[103] It is generally accepted that the dissociation of H_2 is the rate-determining step in the semihydrogenation reactions, therefore, the low intrinsic activity of SACs may arise from the high H_2 dissociation barrier on metal single atoms. That is, H_2 readily dissociates on Pd nanoparticles following a homolysis mechanism, whereas on single atoms H_2 cleaves in a heterolysis way. The energy barrier for heterolytic dissociation and/or spillover might be higher, which leads to low coverage of H species on the surface. It was reported that the heterolysis of H_2 was favored when the M−X bond (M = active metal atom, e.g., Pd; X = heteroatoms coordinated to Pd, e.g., O) was strongly polarized or if the X atom was highly nucleophilic.[83] In addition, the spillover of H species in oxide supported SACs is accelerated with the assistance of the second metal (in SAAs) or hydroxide group on the support (in supported SACs). Therefore, rational selection of the second metal and/or support, together with careful characterizations of the catalysts by in situ or operando techniques would be

DOI: 10.1021/acs.chemrev.9b00230
Chem. Rev. XXXX, XXX, XXX−XXX

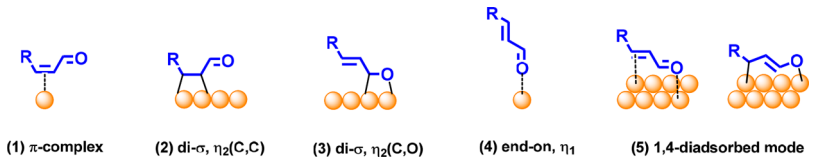

Figure 17. Adsorption patterns of α,β-unsaturated aldehydes on metal nanoparticles and single atoms. Adapted with permission from ref 47. Copyright 1995 Elsevier.

helpful for the development of more efficient SACs for the semihydrogenation of alkynes.

Second, when constructing SAAs/intermetallics, much attention should be paid to the type of the second metal and the composition/structure of the catalysts. It was reported that the second metal not only isolated the active metal but also participated into the reaction in some cases. For example, some metals such as In and Ga, when existing as partially reduced metal oxides, could serve as Lewis acid and catalyze side reactions of oligomerization and coking;[94,123,137,144] Zhang and co-workers also reported that in PdZn/ZnO catalysts, the Pd−Zn ensemble might act as the active sites for the coupling of alkynes to form oligomers.[95] In addition, it is not in any intermetallics that the active metal (e.g., Pd) is totally isolated, instead in some intermetallics (e.g., Pd_3In), continuous Pd sites still exist resulting in inferior selectivity.[126] Even if Pd exists exclusively as single atoms in the intermetallics, the catalytic performance might also be influenced by the strain and electronic effect induced by the structure of the catalysts, e.g., core−shell structure.[182]

Third, most of the lab studies were conducted under low pressure (0.1 MPa) and/or noncompetitive conditions (i.e., alkenes were absent in the feedgas). However, industrially, a large excess of alkene is present in the feedstocks and the hydrogenation is conducted under moderate pressures (1.5−3.5 MPa). Generally, it is more challenging to achieve high chemoselectivity under competitive and high pressure operation conditions. Therefore, to develop selective catalysts for industrial applications, the catalysts need to be evaluated under mimic industrial operating conditions.

Fourth, in the liquid-phase semihydrogenation of acetylenic compounds, much emphasis should be placed on the regioselectivity and stereoselectivity of the catalysts. In the hydrogenation of acetylenic compounds, series of stereoisomers (e.g., *cis*- and *trans*-alkenes) and regioisomers could be produced simultaneously, of which the *cis*-alkenes are more desirable in fragrances and agrochemicals industries. Therefore, the isomerization side reactions of *cis*-alkenes should be effectively suppressed. Some approaches, such as subtle modification of the electronic structure of the catalyst, rational selection of the support, can suppress the β-elimination step which causes isomerization of olefins.

5. CHEMOSELECTIVE HYDROGENATION OF α,β-UNSATURATED ALDEHYDES/KETONES OVER SUPPORTED METAL NANOPARTICLES AND SINGLE ATOMS

α,β-Unsaturated aldehydes/ketones represent another group of challenging substrates for chemoselective hydrogenation reactions, where both C═O and C═C groups coexist in one molecule.[183,184] The desired products are α,β-unsaturated alcohols resulted from the preferential hydrogenation of C═O bond, which are widely employed in the manufacture of perfumes, flavorings, and pharmaceuticals. However, the C═C is more sensitive and prone to reduce based on both thermodynamic (the bond energy is 715 kJ/mol for C═O and 615 kJ/mol for C═C) and kinetic considerations. Therefore, the selective hydrogenation of the C═O bond while leaving the C═C group intact in α,β-unsaturated aldehydes/ketones remains a great challenge. Industrially, metal hydrides (e.g., $NaBH_4$) or Cu−Cr based catalysts are employed in this transformation, which, however, suffered from environmental issues.[184] From the technical and economic point of view, the chemoselective hydrogenation of α,β-unsaturated aldehydes/ketones over supported metal catalysts is a mild, efficient, and straightforward approach.

α,β-Unsaturated aldehydes/ketones can be adsorbed on the catalysts via different patterns depending on the type of the active metals and the size of the metal ensembles (Figure 17).[47,185,186] For example, on an extensive Pt(111) surface, either C═C or C═O bonds can be adsorbed via di-σ or π mode, respectively. The C═O bond can also be solely adsorbed via the end-on mode. In addition, because C═C and C═O groups are conjugated in one molecule, they can be coadsorbed adopting the 1,4-di-σ modes. Among these adsorption patterns, the C═C di-σ mode and the 1,4-di-σ mode both lead to the saturation of C═C group, while the C═O η_2(C,O) mode is prone to result in the decarbonylation side reaction.[52,187] The end-on mode, however, can facilitate the preferential hydrogenation of C═O bond and yield the desired products.

As mentioned in section 4, the hydrogenation of the C═C bond occurs on continuous metal ensembles where the C═C bond is adsorbed via strong ethylidyne or di-σ mode (Figure 5), while the decarbonylation reaction also demands for continuous or at least bridging metals sites.[52,187] Therefore, efficient separation or total isolation of the metal ensembles (i.e., the "active site isolation" approach) should be effective to inhibit the side reactions of overhydrogenation and decarbonylation. On the other hand, in the target C═O group, the C end is positively charged, while the O end is electron-rich, and thus positively charged centers in the catalysts (such as Brønsted acid and Lewis acid) can promote the polarization and activation of C═O bond.[188] Accordingly, various strategies, such as selective poisoning,[189−191] fabrication of alloys,[192,193] confinement of nanoparticles into porous materials,[194,195] and employment of reducible metal oxides as support,[196−198] have been developed with the aim of preferential adsorption of the carbonyl group via the η_1(O) manner and simultaneously hindering the C═C bond to approach the metal surface. A summary of the catalysts developed so far for the selective hydrogenation of α,β-unsaturated aldehydes/ketones is presented in Table 3.

5.1. Selective Poisoning by Organic Modifiers

Selective poisoning by thiol or amine molecules is a common and efficient strategy to reduce the metal ensembles and modify the electronic structures of supported nanoparticles, by

DOI: 10.1021/acs.chemrev.9b00230
Chem. Rev. XXXX, XXX, XXX−XXX

Table 3. Catalysts for the Selective Hydrogenation of α,β-Unsaturated Aldehydes/Ketones

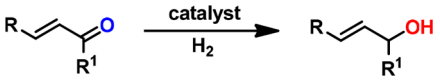

substrates	catalysts	T (°C)	P (bar)	conv (%)	selectivity (%)	ref
cinnamaldehyde	Pt_3Co-amines	25	1.5	100	95	189
citral	Ru/AlO(OH)-ethylenediamine	70	20	100	81[a]	190
furfural	Pd/Al_2O_3-thiol	190	1		70	199
cinnamaldehyde	Pt/Al_2O_3-thiol	50	40		95	200
benzalacetone	$Au_{25}(SC_2H_4Ph)_{18}/Fe_2O_3$	0	1	43	100	191
nitrobenzaldehyde	$Au_{99}(SPh)_{42}/CeO_2$	80	20		100	201
cinnamaldehyde	Au-SPOs	60	40	>95	>99	202
cinnamaldehyde	Pt/n-Al_2O_3−aspartic acid	30	10	99	91	203
crotonaldehyde	PtSn@SiO_2			41.1	66.7	204
cinnamaldehyde	Pt/Al_2O_3@SiO_2	27	30		>85[a]	205
furfural	$Fe(NiFe)O_4$−SiO_2	90	20	94.3	∼100	206
citral	Ag@CeO_2	150	15	99	96	194
citral	Au@CeO_2/HT	120	30	99	99	179
cinnamaldehyde	Pt@UIO-66	80	40	98.7	91.7	207
cinnamaldehyde	Pt/MIL-100@MIL-100	25	1	95	96	195
cinnamaldehyde	MIL-101@Pt@MIL-101	25	30	98.5	99.8	208
crotonaldehyde	Au@ZIF-8	80	5	13	93	209
furfural	Pt/CeO_2@UIO-66-NH_2	80	10	99.3	>99	210
crotonaldehyde	Au−In/SBA-15	120	20	94	75	192
crotonaldehyde	Ag−In/SBA-15	140	20	99	87	193
crotonaldehyde	Au−Ag/SBA-15	120	30		72.3	211
cinnamaldehyde	Au−Ir/TiO_2	100	20		83.4	212
cinnamaldehyde	Pt−Co/RGO	40	20	94.6	89.5	213
cinnamaldehyde	Pt/CoAl-MMO	70	20	93.1	75.9	214
cinnamaldehyde	PtCo/MgCoAl-LDH	80	20		99[a]	215
citral	PtSn/$MgAl_2O_4$			35	65	216
citral	PtFe/C	70	1		90−95	217
citral	PtSn/C	70	1		98	217
cinnamaldehyde	Pt−Sn nanowires	25	1	∼10	87	218
cinnamaldehyde	Pt-FeO_x/SiO_2	150	10		95[a]	219
cinnamaldehyde	Pt/Fe_3O_4	30	5	94.2	92.2	220
cinnamaldehyde	RuFe/Al_2O_3	130	20	96.2	96.7	221
cinnamaldehyde	Ni−Co	100	50	63	62	222
cinnamaldehyde	Co−Al	150	1	50	60	223
furfural	Ni−In	180	30	100	>99	224
cinnamaldehyde	Au/$Zn_{0.7}Fe_{0.3}O_x$	140	10	75.4	88.5	196
crotonaldehyde	Pt/ZnO	30	40	40	90	225
citral	Cu/ZnAl	80	10	100	75	226
cinnamaldehyde	Pt/ZnO-Cr	110	70	100	96	227
cinnamaldehyde	Cu_1Cr/SBA-15	150	1	11	50	228
ketoisophorone	Pt/OMS-2	110	10	70	91	229
cinnamaldehyde	Pt/OMS-2	110	10	96	80	229
5-hydroxymethyl-2-furaldehyde	$Ru(OH)_x/ZrO_2$	120	15	100	>99	197
furfural	Cu−Cr−Zn−Zr	170	20	96	100	230
crotonaldehyde	Au/CeO_2	100	10	88	87	231
cinnamaldehyde	Cu/CeO_2	100	10	30	72	232
cinnamaldehyde	Pt/CeO_2−ZrO_2	60	10	95	94	233
citral	Ru/GaOOH	120	13	55.3	96.8	234
citral	3 wt %Pt/60C-40TiO_2	90	8.3	100	>90	235
furfural	Ru/TiO_2−C	40	40	100	97	236
crotonaldehyde	Ir/Mo_2C	100	20	80	>99	198
cinnamaldehyde	Ir/MoO_x	100	20	>99	93	237
furfural	Ir/MoO_x	100	20	98	99	237
furfural	Pt/g-C_3N_4	100	50	>99	>99	238
furfural	Pt/C−N	100	10	99	99	239
furfural	Co@CPNs	180	30	99	99	240
cinnamaldehyde	Pt_3Fe/CNT	60	20	98.1	95.9	241
cinnamaldehyde	Pt/CNS	60	10	87.5	90.5	242

DOI: 10.1021/acs.chemrev.9b00230
Chem. Rev. XXXX, XXX, XXX−XXX

Table 3. continued

substrates	catalysts	T (°C)	P (bar)	conv (%)	selectivity (%)	ref
cinnamaldehyde	Pt/rGO	40	20	89.6	69.6	243
acrolein	Pd_1Ag_{800}/SiO_2	200	5		31	244
furfural	$Pt_{0.05}$^Au/SiO_2	150	10	10	99	245
furfural	Ni−N−C	140	14	99	98	246

[a]Yield of the product.

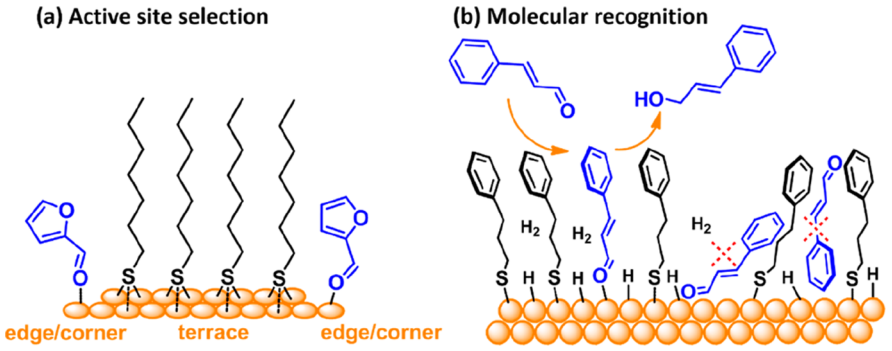

Figure 18. Illustration of approaches for tuning the selectivity of nanocatalysts in hydrogenation of α,β-unsaturated aldehydes using organic modifiers. (a) active site selection; (b) molecular recognition. Adapted with permission from ref 19. Copyright 2014 American Chemical Society.

which the chemoselectivity can be greatly improved in hydrogenation reactions.

Amines capped Pt_3Co nanoparticles were studied in the hydrogenation of α,β-unsaturated aldehydes.[189] A selectivity as high as 95% to cinnamyl alcohol was obtained at full conversion in the hydrogenation of cinnamaldehyde at 25 °C under 0.15 MPa H_2. Moreover, the selectivity was well preserved even when the reaction time was prolonged. DFT calculations demonstrated that the amines could prevent the adsorption of cinnamaldehyde in a "lying-down" mode, thereby the C═C was less likely to be saturated. The promotional role of amines was related to the length of alkyl chain, i.e., the longer, the better, indicating there must be van der Waals interactions between the tail of modifier and the substrates, which also assisted the "end-on" adsorption of the reactant on the catalyst. Li's group also discovered that the employment of ethylenediamine as an additive to Ru/AlO(OH) catalyst improved the chemoselectivity to unsaturated alcohol in the hydrogenation reaction of citral.[190]

Similarly, thiol molecules were good modifiers of nanocatalysts for the hydrogenation of α,β-unsaturated aldehydes.[19,199,200] Specifically, the modifiers fulfilled two tasks in the catalysis. First, the active site selection (Figure 18a). When the thiols were exposed to metal surfaces, they tended to occupy the terrace sites forming densely packed monolayers, whereby the continuous metal sites were covered and the noncontinuous corner/edge sites are left uncovered. This "active site isolation" effect was demonstrated by CO-adsorption FTIR measurements.[199] Because of the reduced assemblies of accessible metal atoms, the adsorption modes of the reactant were limited, and consequently the selectivity was improved. For example, in the hydrogenation of furfural in fixed-bed reactor at 190 °C and 0.1 MPa H_2, the selectivity to furfural alcohol was below 5% over Pd/Al_2O_3 catalyst owing to the side reactions of decarbonylation and hydrogenation of C═C bond resulting from the lying-down adsorption mode. However, over octadecanethiol modified Pd/Al_2O_3, furfural could only be adsorbed via the $\eta_1(O)$ pattern and the selectivity was increased to above 70%. Second, recognition of specially structured reactants (Figure 18b). For α,β-unsaturated aldehydes containing long alkane/alkene chains, as the alkane/alkene chains are flexible and thus the C═C group can reach the metal surface, the "active site selection" route is not effective enough to achieve high chemoselectivity. In this case, the authors chose thiol molecules with tail structure similar to that of the substrate. The van der Waals interaction between the substrates and the modifier favors the substrates being adsorbed via a vertical rather than horizontal pattern, whereby the hydrogenation of C═C bond was prevented.[200] For example, in the hydrogenation of cinnamaldehyde over Pt/Al_2O_3 under conditions of 50 °C and 4 MPa H_2, only when 3-phenylpropanethiol was used as the modifier could the selectivity be enhanced to 95% from 25% because of the similar length of the alkyl chain and the π−π stacking interactions between cinnamaldehyde and 3-phenylpropanethiol. On the contrary, the employment of 2-phenylethanethiol or 4-phenylbutanethiol with shorter or longer alkyl chain or alkanethiol without phenyl group resulted in inferior chemoselectivity (e.g., 60%) to unsaturated alcohol. Thiol modified Au nanocatalysts were also highly selective for the hydrogenation of α,β-unsaturated aldehydes/ketones.[191,201] For example, in the hydrogenation of benzalacetone at 0 °C under 0.1 MPa H_2, $Au_{25}(SC_2H_4Ph)_{18}/Fe_2O_3$ gave 100% selectivity to unsaturated alcohols with 43% conversion.[191]

Secondary phosphine oxides (SPOs) was also a good selectivity regulator in the hydrogenation of α,β-unsaturated aldehydes.[202] Au−SPOs showed good catalytic activity and selectivity for a broad scope of substrates with different structure and functional groups (Figure 19c). DFT calculations revealed that the Au−SPOs interfaces, which resemble the homogeneous Shvo−Noyori catalysts as well as FLPs,[72−75] enabled the heterolysis of H_2 to H^+ and H^- species binding to the O atom in SPOs and Au nanoparticles, respectively (Figure 19a,b).[83] The ionic H^+/H^- pairs kinetically favored the reduction of polar C═O bond over C═C bond via a concerted addition mechanism that is similar to the transfer hydrogenation.

DOI: 10.1021/acs.chemrev.9b00230
Chem. Rev. XXXX, XXX, XXX−XXX

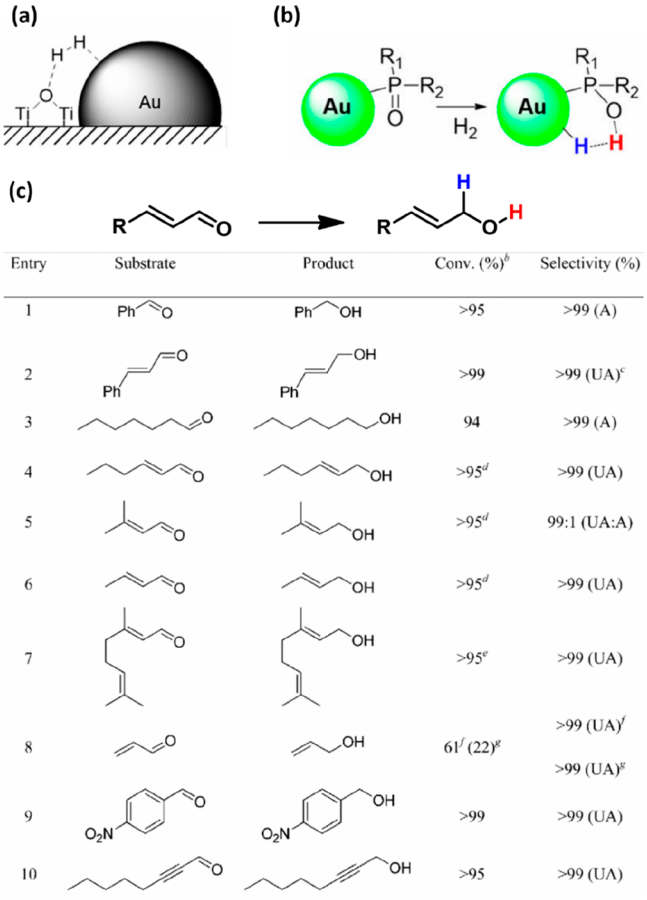

Entry	Substrate	Product	Conv. (%)[b]	Selectivity (%)
1	Ph, O	Ph, OH	>95	>99 (A)
2	Ph, O	Ph, OH	>99	>99 (UA)[c]
3	O	OH	94	>99 (A)
4	O	OH	>95[d]	>99 (UA)
5	O	OH	>95[d]	99:1 (UA:A)
6	O	OH	>95[d]	>99 (UA)
7	O	OH	>95[e]	>99 (UA)
8	O	OH	61[f] (22)[g]	>99 (UA)[f] >99 (UA)[g]
9	O_2N, O	O_2N, OH	>99	>99 (UA)
10	O	OH	>95	>99 (UA)

Figure 19. Comparison between heterolytic cleavage of dihydrogen at the edges of Au nanoparticles supported on TiO_2 (a) and at Au-SPOs interfaces (b); (c) substrate scope of the hydrogenation of α,β-unsaturated aldehydes catalyzed by Au-SPOs. Adapted with permission from ref 202. Copyright 2014 American Chemical Society.

Aspartic acid was also employed to modify nonporous Al_2O_3 supported Pt catalyst Pt/n-Al_2O_3.[203] Under reaction conditions of 30 °C and 1 MPa, 91% selectivity was obtained at 99% conversion, and the TOF reached 3746 h^{-1}. In addition, the catalyst could be reused for 5 times without noticeable decay of the activity.

Although the modification of nanocatalysts with organic molecules could improve the chemoselectivity in the hydrogenation of α,β-unsaturated aldehydes/ketones, the catalytic activity was usually greatly decreased due to the covering of the metal active sites. In addition, these organic modifiers might leach into the reaction system during reaction and thus led to issues of contamination of the products.

5.2. Metal Nanoparticles Confined in Porous Materials

Confinement of metal nanoparticles in ordered or disordered porous materials, such as zeolites, MOFs, and CNTs, is an effective strategy to modulate the accessibility of the metal nanoparticles to the reactants and consequently the chemoselectivity. Specifically, when the free diameter of the reactant with two functional groups is larger than the size of the pore, it is unlikely for the two functional groups to reach the active metal simultaneously. Instead, only the terminal groups (e.g., the carbonyl group in α,β-unsaturated aldehydes/ketones) can be selectively transformed.

Porous SiO_2 materials were widely used to encapsulate active metal nanoparticles. Taniya and co-workers fabricated SiO_2 encapsulated PtSn nanoparticles, which gave higher selectivity (66.7%) to crotyl alcohol than SiO_2 supported PtSn nanoparticles (38.0% selectivity) at comparable conversion level in the hydrogenation of crotonaldehyde.[204] Similar results were obtained by Zaera and co-workers who modified Pt/Al_2O_3 catalyst with submonolayer of SiO_2 through ALD technique.[205] When a half monolayer of SiO_2 was deposited, >85% yield of cinnamyl alcohol could be obtained in the hydrogenation of cinnamaldehyde under reaction conditions of 27 °C and 3 MPa H_2. Characterization by CO and pyridine adsorption FTIR revealed that upon SiO_2 deposition, the bridging Pt sites were mainly covered, and strong Lewis/Brønsted acidic sites were created at the SiO_2−Al_2O_3 interfacial sites. Both factors suppressed the adsorption of C═C bond yet promoted the activation of C═O bond and contributed to the high chemoselectivity. The similar selectivity enhancement was observed in the hydrogenation of furfural to furfuryl alcohol over a Fe(NiFe)O_4−SiO_2 nanocomposite coated by porous SiO_2.[206]

Besides SiO_2, CeO_2 was also employed to encapsulate metal nanoparticles. Core−shell structured Ag@CeO_2 and Au@CeO_2 catalysts were fabricated by Kaneda and co-workers.[179,194] In the three-phase hydrogenation of unsaturated aldehydes, Ag@CeO_2 gave >99% selectivity to unsaturated alcohols than Ag/CeO_2 (86%) where Ag nanoparticles were loaded on the surface of CeO_2, manifesting the importance of reduced Ag ensembles as well as the Ag−CeO_2 interfacial sites for the superior catalytic performances.[194] Besides Ag@CeO_2, Au@CeO_2, and Ir@CeO_2 also provided high chemoselectivity to the unsaturated alcohols, whereas the other metals encapsulated by CeO_2, such as Pt, Pd, Ru, and Rh, were totally nonselective for the reaction. The metal specificity might be related to the dissociation manner of H_2, i.e., H_2 underwent heterolysis at the Ag(Au, Ir)-interfaces, whereas preferential homolysis on the surface of Pt(Pd, Ru, Rh) nanoparticles. However, these reactions were performed under harsh conditions of 150 °C and 1.5 MPa H_2, indicating the low atomic efficiency of the active metals owing to the covering of CeO_2.

Metal organic frameworks (MOFs) with regular pores and high specific surface areas, were also used to encapsulate metal nanoparticles. Huang et al. selected UIO-66, a kind of MOF material, to encapsulate Pt nanoparticles.[207] The UIO-66 itself comprises tetrahedral and octahedral cages with free dimensions of 7.5 and 12 Å, respectively, and access to these cages is provided by narrow triangular windows with a free diameter close to 6 Å, which would only allow α,β-unsaturated aldehydes to contact with Pt nanoparticles in the end-on manner. As expected, in the liquid-phase hydrogenation of cinnamaldehyde under reaction conditions of 80 °C and 4 MPa H_2, 91.7% selectivity to cinnamyl alcohol was achieved at 98.7% conversion over Pt@UIO-66. In addition, the catalyst could be easily recovered and reused for 10 times without decay in activity or selectivity, and TON value as high as 10900 was obtained. However, the mass transfer limited the catalytic activity to some degree so that long reaction time was required for the completion of the reaction (e.g., 44 h).

MIL-101 is also employed to fabricate core@shell structured Pt/MOFs@MOFs composites, where the core was composed of Pt nanoparticles with size of 3 nm supported on MIL-101, and a separate MIL-101 shell was grown onto the core by

DOI: 10.1021/acs.chemrev.9b00230
Chem. Rev. XXXX, XXX, XXX−XXX

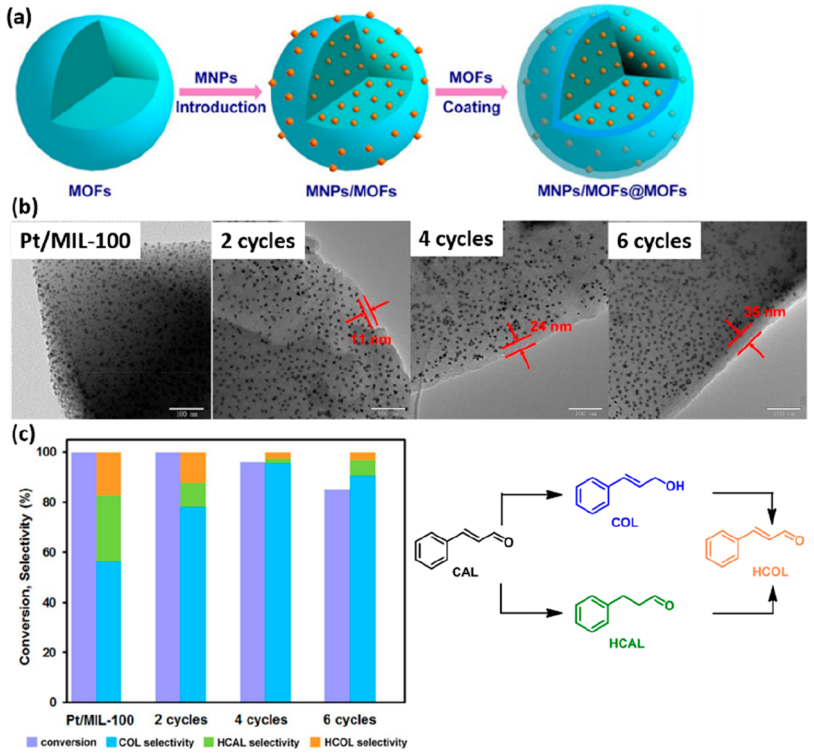

Figure 20. (a) Illustration of the preparation of MNPs/MOFs@MOFs nanocomposites. (b) TEM images of Pt/MIL-100 and Pt/MIL-100@MIL-100 prepared by two, four, and six assembly cycles, respectively. (c) Catalytic performances of Pt/MIL-100 and Pt/MIL-100@MIL-100 catalysts. Adapted with permission from ref 195. Copyright 2016 John Wiley and Sons.

liquid-phase epitaxy method (Figure 20a).[195] In the hydrogenation of cinnamaldehyde under reaction conditions of 25 °C and 0.1 MPa H_2, 96% selectivity to cinnamal alcohol was achieved at 95% conversion on Pt/MOFs@MOFs, whereas only 55% selectivity was obtained over Pt/MOFs. However, the thick shell (24−35 nm, Figure 20b) greatly hindered the mass transfer, leading to a lowered activity (Figure 20c).

In addition to geometric modulation, electronic modification was also proposed in such core@shell structured catalyst. Tang's group investigated the hydrogenation of cinnamaldehyde over sandwich structured MIL-101@Pt@MIL-101 catalyst.[208] DFT calculation revealed that the metal nodes in MIL-101, e.g., five-coordinated Fe and Cr trimers, could adsorb the carbonyl group in cinnamaldehyde, and XPS measurement showed that electrons could transfer from Pt nanoparticles to MIL-101(Fe). It was proposed that the carbonyl might be adsorbed on the metal nodes in MIL-101 and then was activated by the electrons from Pt tunneled through MIL-101. Other core@shell structured catalysts, such as Au@ZIF-8[209] and Pt/CeO_2@UIO-66-NH_2,[210] also showed promising chemoselectivity in the hydrogenation of α,β-unsaturated aldehydes/ketones.

Above all, the confinement of metal nanoparticles in porous materials indeed improved the chemoselectivity in the hydrogenation of α,β-unsaturated aldehydes/ketones. However, owing to the limited mass transfer, the catalytic activity was deteriorated to such a degree that harsh reaction condition or extended time was required to acquire an acceptable conversion level.

5.3. Bimetallic Nanocatalysts

Bimetallic nanoparticles usually exhibit superior catalytic activity and selectivity to their monometallic counterparts due to both geometric and electronic modifications.[30,247] In this respect, various bimetallic nanocatalysts have been developed for the selective hydrogenation of α,β-unsaturated aldehydes/ketones.

Fan and co-workers prepared SBA-15 supported monometallic Au and bimetallic Au−In catalysts.[192] In the hydrogenation of crotonaldehyde to crotyl alcohol under conditions of 120 °C and 2 MPa H_2, 75% chemoselectivity at 94% conversion was achieved on Au−In/SBA-15 catalyst, whereas only 55% selectivity on the Au/SBA-15. Bimetallic Ag−In nanoparticles supported on SBA-15 were also fabricated via a "two solvents" strategy, which gave 87% selectivity to crotyl alcohol at 99% conversion in the hydrogenation of crotonaldehyde under conditions of 140 °C and 2 MPa H_2.[193] DFT calculations showed that on Ag(111) surface without hydrogen adatoms (H), α,β-unsaturated aldehyde adsorbs in a η_1(O) mode via the terminal oxygen atom where the C═C bond tilts markedly.[48,248] However, at high H coverages, the C═C can also be saturated. Therefore, the In component in AgIn bimetallic nanoparticles might fulfill two roles. On one hand, it reduces the coverage of hydride on Ag surface by reducing the ensemble of Ag; on the other hand, it serves as a Lewis acid and promotes the polarization of C═O group and thus facilitates its reduction.

Similarly, the Au−Ag/SBA-15 catalyst showed much higher activity (TOF = 183.3 h^{-1}) than either Au/SBA-15 (TOF = 31.2 h^{-1}) or Ag/SBA-15 (TOF = 41.1 h^{-1}) and enhanced selectivity to unsaturated alcohols (from 55.3% on Au/SBA-15 to 72.3% over Au−Ag/SBA-15) in the hydrogenation reaction of crotonaldehyde.[211] The enhanced catalytic activity was ascribed to the easier dissociation of H_2 on bimetallic Au−Ag nanoparticles, as revealed by kinetic studies that the apparent activation energy on Au−Ag nanoparticles (32.9−58.8 kJ/mol)

DOI: 10.1021/acs.chemrev.9b00230
Chem. Rev. XXXX, XXX, XXX−XXX

was much lower than that on Au (71.5 kJ/mol) or Ag (67.9 kJ/mol). Au−Ir bimetallic nanoparticles supported on TiO_2 also showed good catalytic performance in the hydrogenation of cinnamaldehyde.[212] Under reaction conditions of 100 °C and 2 MPa H_2, the reaction rate was enhanced by 5-fold with the addition of Ir, which as ascribed to the higher ability of Ir to dissociate H_2.

Pt−Co (Fe, Sn) based bimetallic catalysts were widely investigated for the selective hydrogenation of α,β-unsaturated aldehydes/ketones.[213−220,249] On one hand, upon reduction at high temperature, the Co (Fe, Sn) ingredient can formed alloys with Pt, by which the ensemble of Pt is reduced. On the other hand, the partially reduced CoO_x (FeO_x and SnO_x), where the metal cations are coordinatedly unsaturated, can act as a Lewis acid and promote the preferential adsorption and polarization of the carbonyl group. Both of them contribute to the chemoselectivity. For example, in the hydrogenation of cinnamaldehyde, Pt−Co/rGO (reduced graphene oxides) afforded 89.5% selectivity at 94.6% conversion under reaction conditions of 40 °C and 2 MPa H_2.[213] When loaded on mixed metal oxides derived from layered double hydroxides precursors, Pt/MgCoAl-MMO catalyst gave 99% yield of cinnamyl alcohol under conditions of 80 °C and 2 MPa H_2.[215] In the hydrogenation of furfural to furfuryl alcohol, 87.4% yield of furfuryl alcohol was obtained on Pt−Fe bimetallic catalysts.[250] Supported RuFe alloy nanoparticles also showed high catalytic performance in the hydrogenation of cinnamaldehyde, and 96.7% selectivity to cinnamal alcohol was obtained at 96.2% conversion under reaction conditions of 130 °C and 2 MPa H_2.[221] CO adsorption FTIR measurements revealed that charge transfer occurred from both the support and Fe to Ru, which made Ru be negatively charged and thus favored the adsorption of electrophilic carbonyl group. In addition, the Fe cation could assist the activation of C═O bond, which also contributed to the high chemoselectivity. By contrast, Pd−Fe catalysts preferred to reduce the C═C rather than C═O bond, which was attributed to different percentage of d-character.[251]

Ni-based alloy catalysts provide an alternative and less-expensive route to the selective hydrogenation reactions.[222−224] Carbonaceous materials loaded Ni−Co alloy catalysts gave 62% selectivity to unsaturated alcohols at 63% conversion.[222] In the hydrogenation of furfural under reaction conditions of 180 °C and 3 MPa H_2, >99% selectivity to furfuryl alcohol could be obtained at full conversion over bimetallic Ni−In alloy catalysts supported on amorphous alumina.[224]

5.4. Monometallic Nanoparticles Supported on Reducible Oxides

As aforementioned, some reducible oxides (such as Fe_3O_4, CoO_x, SnO_x, and InO_x) could form alloys with the active metal when treated at high temperatures under reducing atmosphere,[215,217,219,221,222,224] by which the metal ensembles could be decreased and the chemoselectivity was improved. However, for reducible oxides that cannot form alloys with active metals (such as CeO_2, TiO_2), they can modify the geometric and electronic structure of the active species through SMSI (strong metal support interaction) effect or promote the polarization of C═O bond by coordinating to the O end. Consequently, good to excellent chemoselectivity could still be achieved.[196,225,226]

Urbano and co-workers prepared series of reducible oxide (including Fe_2O_3, Fe_3O_4, ZrO_2, ZnO, TiO_2, and SnO_2) supported Pt nanocatalysts and investigated their catalytic performance in the hydrogenation of crotonaldehyde.[225] Among others, the Pt/ZnO gave the best catalytic performance, and 90% selectivity to crotyl alcohol was obtained at about 40% conversion under conditions of 30 °C and 0.4 MPa. XPS measurement showed the presence of Lewis acidic ZnO_xCl_y species, which could preferentially activate the carbonyl group and might be responsible for the high chemoselectivity. Under similar reaction conditions, Pt nanoparticles supported on ZrO_2, TiO_2, and Fe_3O_4, however, gave the saturated butanal as the main product.

Besides ZnO, CrO_x could also be a good promoter in the hydrogenation reactions. It was reported that the addition of Cr to Pt/ZnO increased the surface area of the support, promoted the reduction of Pt, and thus greatly enhanced the catalytic activity in the hydrogenation of cinnamaldehyde.[227] Under conditions of 110 °C and 7 MPa H_2, 96% selectivity to cinnamyl alcohol was obtained at full conversion. Dragoi and co-workers studied SBA-15 supported Cu−Cr bimetallic catalysts in the three-phase hydrogenation of *trans*-cinnamaldehyde.[228] Under conditions of 150 °C, 0.1 MPa H_2, 50% selectivity to cinnamyl alcohol could be obtained over CuCr/SBA-15 with 11% conversion, whereas on Cu/SBA-15 and Cr/SBA-15 catalysts, the conversion was negligible (<1.5%) and the chemoselectivity was poor.

Manganese oxide octahedral molecular sieve (OMS-2) supported Pt nanoparticles were investigated for the hydrogenation of α,β-unsaturated aldehydes/ketones.[229] In the hydrogenation of ketoisophorone under conditions of 100 °C and 1 MPa H_2, 91% selectivity to the unsaturated alcohol was obtained at 70% conversion, and in the hydrogenation of cinnamaldehyde, 80% selectivity to cinnamyl alcohol was achieved at 96% conversion. However, when the OMS-2 itself was employed as the catalyst, the C═C group was preferentially reduced in both cases, and the catalytic activity was much lower than that of Pt/OMS-2.

$Ru(OH)_x/ZrO_2$ composites were reported to be highly selective and efficient catalysts for the hydrogenation of 5-hydroxymethyl-2-furaldehyde to 2,5-bis(hydroxymethyl)-furans.[197] The catalysts were prepared by impregnation of ZrO_2 with $RuCl_3$ aqueous solution without post treatment. XRD and HRTEM characterizations showed that Ru did not incorporate into the lattice of ZrO_2 but form $Ru(OH)_x$ hydroxide on the surface of ZrO_2. Under reaction conditions of 120 °C and 1.5 MPa H_2, >99% selectivity to C═O hydrogenation was achieved at nearly full conversion of the substrate. It is known that, in ZrO_2, the coordinatively unsaturated Zr^{4+} and O^{2-} act as Lewis acid and base, respectively. When Ru was loaded, it should coordinate to the O^{2-} cations, which strengthened the Lewis acidity of $Ru(OH)_x$. Consequently, a great many Lewis acid−base pairs existed in the $Ru(OH)_x/ZrO_2$ catalysts, which could not only heterolytically split H_2 into ionic H^+ and H^- species, but also activate the carbonyl group, and consequently gave rise to high activity and selectivity. The promotional effect of Zr and Zn in the hydrogenation of furfural to furfural alcohol was also observed over a Cu−Cr−Zn−Zr based catalyst.[230]

CeO_2 is another kind of reducible oxide known for the facile redox cycle of the cerium ion ($Ce^{4+} \leftrightarrow Ce^{3+}$), where Ce^{3+} could serve as Lewis acid sites. Fan's group prepared CeO_2 supported Au nanoparticles, which gave 87% selectivity to crotyl alcohol

DOI: 10.1021/acs.chemrev.9b00230
Chem. Rev. XXXX, XXX, XXX−XXX

at 88% conversion under reaction conditions of 100 °C and 1 MPa H_2 in the hydrogenation of crotonaldehyde.[231] CeO_2 supported Cu nanoparticles also afforded high selectivity (72%) in the liquid-phase hydrogenation of cinnamaldehyde under conditions of 100 °C, 1 MPa H_2.[232] CeO_2 can also form composites with another oxide, by which the concentration of oxygen vacancies can be greatly improved. CeO_2−ZrO_2 composite supported Pt nanoparticles with sizes of 4.3−4.7 nm were investigated in the liquid-phase selective hydrogenation of cinnamaldehyde under reaction conditions of 60 °C and 1 MPa H_2.[233] Pt/CeO_2 exhibited higher catalytic activity than Pt/ZrO_2, that is, 80% conversion was obtained over Pt/CeO_2 with TOF of 7567 h^{-1}, whereas 59% conversion on Pt/ZrO_2 with TOF of 4505 h^{-1}. However, 99% selectivity was achieved on Pt/ZrO_2, which was superior to that of Pt/CeO_2 (79%). Impressively, the catalytic performance was greatly enhanced when Pt was supported on CeO_2−ZrO_2, i.e., 95% conversion was achieved with TOF as high as 10423 h^{-1}, meanwhile, the chemoselectivity was maintained at a high level (94%). The incorporation of ZrO_2 into CeO_2 enhanced the redox behavior and the mobility/storage capacity of oxygen. XPS showed that with an increase of Zr/Ce ratios, the binding energy of Pt species presented a negative shift, while the Ce^{III}/(Ce^{III} + Ce^{IV}) ratios increased initially and reached the maximum at Zr/Ce = 1 and then decreased with a further increase of Zr/Ce ratios. In addition, both of the amount and strength of the Lewis acid steadily increased with an increase of the Zr content. The chemoselectivity increased with an increase of the amount and strength of the Lewis acid, and the catalytic activity was the highest when the amount of oxygen vacancies reached the maximum.

Ga_2O_3 is also a promising support for metal nanoparticles in the selective hydrogenation reactions. Inoue and co-workers prepared Ru nanoparticles supported on *p*-block metal oxides (Ga_2O_3, In_2O_3, SnO_2, SiO_2, GeO_2) and evaluated them in the liquid-phase hydrogenation of citral.[234] Under reaction conditions of 120 °C and 1.3 MPa, both of the conversion and chemoselectivity increased following the order of β-Ga_2O_3 > In_2O_3 > SnO_2 > SiO_2 > GeO_2. In addition, among the different polymorphic Ga_2O_3 investigated, GaOOH stood out to give the best catalytic performance, and 96.8% selectivity was obtained at 55.3% conversion.

TiO_2 is well-known for the SMSI when treating the supported metal nanoparticles at high temperature under reducing conditions. Carbon xerogels−TiO_2 composites were used as supports of Pt nanoparticles, where the role of carbon xerogels was to prevent the phase transformation of TiO_2 from anatase to rutile at high temperature.[235] In the hydrogenation of citral under conditions of 90 °C and 0.83 MPa H_2, 3 wt % Pt/60C−40TiO_2 gave the best performance, and >90% selectivity to unsaturated alcohols could be obtained at full conversion. During the high temperature prereduction of the catalyst, SMSI occurred where the partially reduced TiO_x species migrated onto Pt nanoparticles. Accordingly, the assemblies of accessible Pt atoms were reduced, and thus the adsorption of the C═C group was suppressed. Similarly, TiO_2−C composite supported Ru nanoparticles afforded 97% selectivity to furfuryl alcohol at full conversion in the hydrogenation of furfural under reaction conditions of 40 °C and 4 MPa H_2.[236] Besides TiO_2, Mo_2C and MoO_x (H-MoO_x) could also modify the supported metal nanoparticles by high temperature reduction, and good to excellent catalytic performances were obtained in the hydrogenation of α,β-unsaturated aldehyde.[198,237]

5.5. Reaction Parameters Affecting the Selectivity

Besides the geometric and electronic structure of the active sites, the reaction parameters (such as solvent, reaction temperature) also had profound effect on the catalytic activity and selectivity in the hydrogenation reactions.

The solvent was considered to play a critical role in modulating the selectivity in the hydrogenation of furfural catalyzed by g-C_3N_4 nanosheets (TECN) supported Pt nanoparticles.[238] A selectivity of >99% to furfuryl alcohol at >99% conversion could only be achieved in strong polar aqueous media. With the decrease of polarity of the solvent, both the conversion and selectivity decreased. For example, the conversion was 67.4% in ethanol solvent, while 8.3% in octane. In addition, the selectivity to furfuryl alcohol was only 65.8% in octane, and 34.2% furan was produced. The solvent was considered to modulate the adsorption pattern of furfural on the catalyst. That is, in polar solvent (e.g., H_2O) the carbonyl group might preferentially interact with the hydrophilic catalyst in η_1(O) manner and thus high selectivity to C═O hydrogenation was obtained, whereas in nonpolar solvent, the aromatic furan ring might also interact with the catalyst adopting a "lying down" adsorption mode, which facilitated the decarbonylation reaction to yield furan. Furthermore, the TECN support has abundant N atoms with high electron density, which repel the nucleophilic C═C group and thus contribute to the selectivity. In agreement with this mechanism, the Pt nanoparticles supported on N doped carbon materials derived from bamboo shoots gave 99% selectivity to furfuryl alcohol at 99% conversion under reaction conditions of 100 °C and 1 MPa H_2 in aqueous media.[239]

Similarly, Kyriakou and co-workers discovered that both reaction temperature and solvent greatly affected the selectivity in the hydrogenation of furfural over supported Pt nanoparticles.[252] When the reaction was conducted at 70 °C, side reactions such as decarbonylation and acetalization proceeded readily, and a great portion of furan and acetal were produced, whereas at 50 °C the selectivity to furfuryl alcohol could reach as high as 99%. The employment of polar solvent (such as methanol, ethanol) facilitated the formation of furfuryl alcohol, whereas nonpolar ones (e.g., toluene) promoted the production of furan, which was in good agreement of Mu's work.[238] Under optimized reaction conditions, Pt nanoparticles supported on MgO, SiO_2, Al_2O_3, and CeO_2 all gave 90−99% chemoselectivity to furfuryl alcohol with 35−80% conversion. Similar solvent effect was also observed in other catalytic systems, such as fullerene supported Ru catalysts,[253] and nitrogen-doped porous carbon (CPNs) supported Co catalysts Co@CPNs.[240]

As a remarkable solvent effect was observed in the hydrogenation of α,β-unsaturated aldehyde, i.e., both of the reaction rate and the selectivity to unsaturated alcohols, were greatly improved in polar solvent, e.g., H_2O. Yang and co-workers investigated the promotional role of water in the hydrogenation of cinnamaldehyde catalyzed by CNTs supported bimetallic Pt_3Fe nanoparticles.[241] In the hydrogenation reaction under conditions of 60 °C and 2 MPa H_2, the highest specific reaction rate was achieved in H_2O (1250 h^{-1}), which was much higher than that (100−750 h^{-1}) in organic solvent, such as cyclohexane, ethyl acetate, and 2-propanol. In addition, the selectivity to unsaturated alcohol as

DOI: 10.1021/acs.chemrev.9b00230
Chem. Rev. XXXX, XXX, XXX−XXX

high as 95.9% could be obtained at 98.1% conversion, which was also superior to those obtained in organic solvents. To shed light on the promotional role of H_2O, isotopic studies employing D_2O as solvent and H_2 as hydrogen source were carried out. It was found that without H_2, only H−D exchange between D_2O and the hydroxide group in cinnamal alcohol proceeded. Whereas in the presence of H_2, either C═C or C═O bond could be deuterated. In addition, HD and D_2 species were detected during the reaction. Therefore, it was proposed that water mediated and promoted the spillover process of hydrogen atom. In addition, H_2O also enhanced the polarity of the catalyst surface, either in the H_3O^+ or dissociated OH^-/H^+ form, which facilitated the adsorption of the polar carbonyl group in the end-on orientation and thus improved the chemoselectivity.

When using carbonaceous materials as support of Pt nanoparticles, the graphitic degree of the support was found to have profound influence on the catalytic performance.[242] In the hydrogenation reaction of cinnamaldehyde over Pt/C under reaction conditions of 60 °C and 1 MPa H_2, with an increase of the graphitic degree of the carbon nanosheets, the conversion was enhanced from 14.4% to 87.5%, meanwhile the selectivity to cinnamal alcohol significantly increased from 16.7% to 90.5%. Rong and co-workers obtained similar results.[243] They prepared Pt nanoparticles with size of 2.3−2.5 nm supported on three carbonaceous materials, i.e., reduced graphene oxide (rGO), carbon nanotubes (CNTs), and activated carbon (AC)). Among these catalysts, Pt/rGO with the highest graphitic degree gave the best catalytic activity and selectivity to unsaturated alcohol. For example, under reaction conditions of 40 °C and 2 MPa H_2, 69.6% selectivity to cinnamyl alcohol was obtained at 89.6% conversion, whereas the selectivity was 48.3% and 30.9% over Pt/CNTs and Pt/AC, respectively. The higher graphitic degree of the carbonaceous materials was considered to result in lower oxidation state of Pt nanoparticles, which had stronger adsorption to C═O bond than to C═C group and thus led to higher chemoselectivity to α,β-unsaturated alcohols.[254,255]

5.6. Single-Atom Catalysts

The employment of single-atom catalysts (SACs) in the selective hydrogenation reactions of α,β-unsaturated aldehydes/ketones has been relatively less explored. Meyer and co-workers investigated Pd−Ag SAA catalyst for the hydrogenation of acrolein in the fixed-bed continuous reactor[244] Under reaction conditions of 200 °C and 0.5 MPa H_2, Pd/SiO_2 was quite active for the reaction, yet the selectivity to unsaturated alcohol was zero. By contrast, 37% selectivity to allyl alcohol was achieved although the activity was low over the Ag/SiO_2. The Pd_1Ag_{800}/SiO_2 SAA catalyst combined the merits of monometallic Ag and Pd, affording 31% selectivity to allyl alcohol and 2-fold enhancement in the activity. The promotional role of Pd single atoms was ascribed to the enhanced ability to dissociate H_2 and the suppression of adsorption of C═C on single atoms. Xu and co-workers found that in the hydrogenation of α,β-unsaturated carbonyl compounds, the construction of Au−Pd SAA structure greatly improved the catalytic activity.[245] For example, in the hydrogenation of furfural, the conversion was enhanced from 1% to 10% over $Pt_{0.05}$^Au/SiO_2 catalyst, and the selectivity to furfuryl alcohol was above 99%. Kinetic studies showed that the reaction order with respect to H_2 decreased from 1.65 on Au/SiO_2 to 1.29 over $Pt_{0.05}$^Au/SiO_2, suggesting the ability of the catalyst to cleave H_2 was enhanced, which contributed to the high catalytic activity.[256] Recently, Ni−N−C SAC was investigated for the hydrogenation of furfural to furfuryl alcohol.[246] The catalyst was prepared by pyrolysis of $Ni(OAc)_2$ and cucurbit[6]uril at 800 °C under the atmosphere of H_2−Ar (10/90, v/v). Under reaction conditions of 140 °C and 1.4 MPa (200 psi) H_2, a high selectivity of 98% to furfuryl alcohol could be achieved at a furfural conversion of 99%. Although Ni nanoparticles were observed in the catalysts, the metal single atoms were probably the true active sites in such M−N−C based catalysts.[80]

5.7. Summary

To summarize, the chemoselective hydrogenation of C═O bond in α,β-unsaturated aldehydes/ketones is an important approach to producing unsaturated alcohols for pharmaceuticals and agrochemicals industry, yet it remains challenging because the C═C is more prone to be saturated. To tackle this challenge, various methodologies, e.g., selective poisoning, encapsulation by porous materials, and construction of bimetallic nanoparticles have been developed.

Now, it has been accepted that bifunctional sites are required for the catalysts, i.e., Lewis acid sites (e.g., transition metal cations) for the activation of C═O bond, and active metal site (e.g., metal nanoparticles) for H_2 dissociation (preferentially in heterolysis manner because H^+/H^- kinetically favor the hydrogenation of polar bond). In particular, the adsorption of substrates in an end-on mode via the O atom on the Lewis acid site is the prerequisite to achieve high chemoselectivity. However, owing to the flexibility of the C═C−C═O moiety, the C═C bond is also able to get access to the active metal sites in intimate proximity and be saturated in nanocatalysts. To suppress the adsorption of C═C, the most efficient strategy is downsizing the active metal to single atom dispersion, and thus SACs are expected to exhibit superior chemoselectivity in the selective hydrogenation of α,β-unsaturated aldehydes/ketones. However, to the best of our knowledge, few SACs have been reported so far for this type of reactions yet.[244,246] It is therefore highly desired that more efforts will be devoted to investigating the catalytic performance of SACs in the selective hydrogenation of α,β-unsaturated aldehydes/ketones in the near future. Besides, the influence of the type and valence state of transition metal cations as well as the solvent on the adsorption strength of the carbonyl group also needs more investigations.

6. CHEMOSELECTIVE HYDROGENATION OF FUNCTIONALIZED NITROARENES OVER SUPPORTED METAL NANOPARTICLES AND SINGLE ATOMS

Aromatic amines are key building blocks for fine chemicals (such as agrochemicals, dyes, pigments, and pharmaceuticals) and bulk chemicals (e.g., polymers). Generally, they are produced by reduction of the corresponding nitroarenes.[257,258] However, anilines used in life science applications are usually structurally decorated with diverse functional groups on the benzene ring, such as alkene, alkynes, amino, halogen, aldehydes, ketones, nitriles, esters, and amides. Therefore, the selective reduction of the $-NO_2$ groups while retaining the other reducible groups is a highly desirable yet rather difficult task. In particular, the substrate of nitrostyrene is considered to be the most challenging because the −C═C is extremely sensitive and thus more prone to reduce than $-NO_2$.[259]

DOI: 10.1021/acs.chemrev.9b00230
Chem. Rev. XXXX, XXX, XXX−XXX

Therefore, the chemoselective reduction of nitrostyrene is often regarded as a probe reaction to benchmark the selective performance of the investigated catalysts. On this ground, we summarize mainly the recent advances in the chemoselective hydrogenation of nitrostyrenes catalyzed by supported metal catalysts in this section.

Before referring to the catalysts, it would be better to understand the adsorption behavior of nitrostyrenes containing −C═C and $-NO_2$ groups (Figure 21), as the adsorption modes as well as adsorption strength of the two functional groups will determine the selectivity to a large extent.

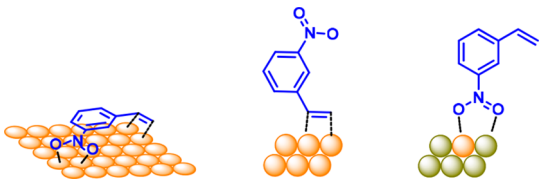

Figure 21. Possible adsorption patterns of 3-nitrostyrene on catalysts with different geometric structures. Adapted with permission from ref 277. Copyright 2016 The Royal Society of Chemistry (RSC).

The adsorption of the −C═C is structure sensitive.[23] As described in section 4, with the size decrease of the metal assemblies, the −C═C group is adsorbed in the mode of ethylidyne on 3-fold assemblies, di-σ mode on 2-fold, and π-bonded mode on isolated single atoms, with the adsorption strength ethylidyne > di-σ mode > π- mode. By contrast, the adsorption of the $-NO_2$ group is not dependent on the structure of the catalyst, because $-NO_2$ has an end-on geometry and the monodentate rather than bidentate adsorption mode is always preferred on the catalyst. For the electronic property, the −C═C group is electron-rich, whereas the $-NO_2$ is electron-deficient, and thus nucleophilic sites on the catalyst will favor the adsorption of $-NO_2$ while repelling the −C═C group, and vice versa. Therefore, to achieve high chemoselectivity to vinylamine in the hydrogenation of nitroarenes, the geometric and electronic structure of the active sites should be engineered to facilitate the preferential adsorption of $-NO_2$ group. When the $-NO_2$ group is preferentially adsorbed, it can be transformed through direct route or condensation route depending on the catalyst and the reaction conditions (Scheme 1).[260] In the direct route, the $-NO_2$ is reduced sequentially to nitroso, hydroxylamine, and finally amine, whereas in the condensation route, the intermediates of nitroso and hydroxylamine can couple to azoxy compound catalyzed by a base, which is further reduced to azo, hydrazo and finally aniline.

Traditionally, high selectivity to vinylaniline could be achieved by stoichiometric reduction of the nitrostyrene using sodium hydrosulfite, iron, tin, or zinc in ammonium hydroxide, however, this process produces stoichiometric waste and thus raises serious environmental concerns.[257] At present, this old and environmentally unfriendly method has been prohibited, and the chemoselective hydrogenation approaches are being explored. Catalyst is the key to the chemoselective hydrogenation, and the exploration of chemoselective catalysts can be dated back to 1952 when the famous Lindlar catalyst was reported.[22] Since then, a variety of noble metal catalysts modified by inorganic/organic compounds have been developed, such as $Pt/C-H_3PO_2-VO(acac)_2$, $Pt/CaCO_3-Pb\text{-}FeCl_2\text{-}nBu_4NCl$, $Rh/C-Fe(OAc)_2$, Pt/CNTs−

Scheme 1. Reaction Pathways of Hydrogenation of Nitroarenes to Anilines[a]

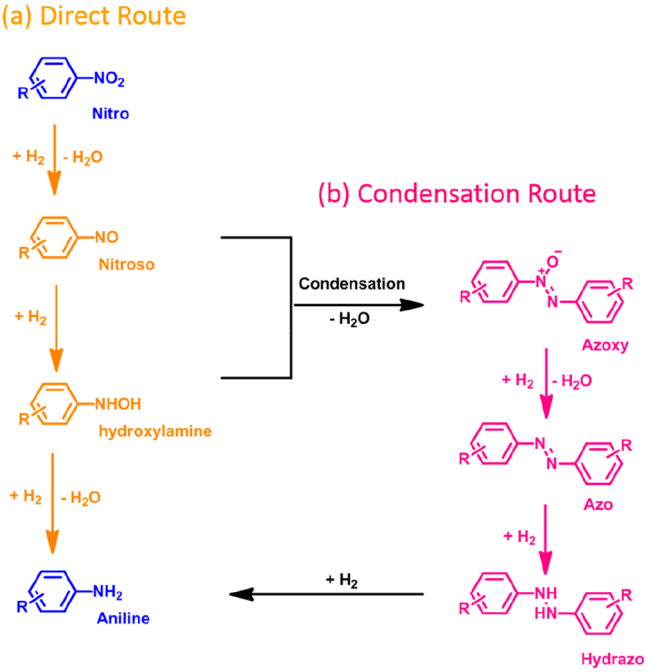

[a](a) Direct route; (b) condensation route. Reproduced with permission from ref 260. Copyright 2006 The American Association for the Advancement of Science.

ionic liquid,[261] and Pt/TiO_2-thiols.[262] In spite of high efficiency for enhancing chemoselectivity, this modification method suffers from the low catalytic activity based on total metal atom utilization efficiency owing to the covering of active metals by the additives. For example, the catalytic activity of Pt/TiO_2-thiols was significantly suppressed by 85−96% due to the poison by the sulfur-containing organic compounds.[262] In addition, the soluble additive not only led to environmental issues but also made the catalysts not be intrinsically heterogeneous. On this ground, great efforts have been devoted to developing highly selective and efficient nanocatalysts without soluble inorganic/organic compounds. A summary of the catalysts developed so far for the selective hydrogenation of functionalized nitroarenes (mainly nitrostyrene) is presented in Table 4.

6.1. Noble Metal Based Catalysts

Efforts to develop efficient and selective catalysts for the hydrogenation of functionalized nitroarenes, especially nitrostyrenes, have been going on for decades. However, it is not until 2006 that a breakthrough was made by Corma and coworkers.[263] They employed TiO_2 or Fe_2O_3 supported Au nanoparticles (3.5−4.0 nm) as catalysts, which afforded excellent chemoselectivity for the hydrogenation of a broad scope of nitroarenes with different functional groups. Especially for 3-nitrostyrene, the selectivity to 3-vinylaniline reached 96% at a high conversion of 98%.[263] For comparison, the TiO_2 supported bimetallic Au−Pt, Au−Pd and monometallic Pt/C, Pd/C gave quite low selectivity (<3%). Theoretical calculations show that the $-NO_2$ adsorb weakly on the Au(111) and Au(001) terraces, and that although a stronger adsorption occurs on low-coordinated atoms in Au nanoparticles, this adsorption is not selective,[57] suggesting Au nanoparticles alone cannot be responsible for the high

DOI: 10.1021/acs.chemrev.9b00230
Chem. Rev. XXXX, XXX, XXX−XXX

Table 4. Nanocatalysts and SACs for the Hydrogenation of Nitroarenes

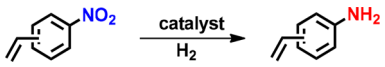

catalyst	T (°C)	P (bar)	conv (%)	selectivity (%)	TOF (h^{-1})	ref
Au/TiO_2	120	9	98.5	95.9	173	263
Au/Fe_2O_3	130	12	95.2	95.1	26	263
Pt/TiO_2	40	3	95.1	93.1	60	264
$Au-Pt/TiO_2$	80	8	94.5	93.4	550	265
$Au-Ni/SiO_2$	50	3	90.8	93.0	17.9	266
Pt/SiO_2	rt	10	90	70	73	267
Au/TiO_2	90	10	99	99	279	268
Au/Al_2O_3	160	30	100	89	6410	269
Ag/Al_2O_3	160	30	100	96	~510	270
Au/MgAl HT	50	20	100	98[a]	93	271
Au/ZnAl-HT	90	10	100	>99	76	272
Au-BP(DR)	100	0.5	96	94.8	1013	273
$Ag@CeO_2$	110	6	98	99	4.85	60
Pt@MFI	80	10	100	80		274
Pt/ZnO	75	10		97	744	275
PtZn/HPS	75	10	97	100	1020	276
$RhIn/SiO_2$	75	1	99	91	26.1	277
$Pt-Bi/TiO_2$	85	20	100	96	~170	278
$Ru-Mo/SiO_2$	30	3	97	98	9.7	279
$PtSn/MoO_x$	30	1	>60	93	338	280
Pd/CeO_2[c]	80	5	93.3	99.9	44059	281
$Au/Sn-TiO_2$	70	13	99	99.3	319	58
$Pt/Sn-TiO_2$	45	2	98.5	97.4	1802	58
Pt_1/FeO_x	80	10	88.8	91.1	11064	282
Pt_1/FeO_x	40	3	96.5	98.6	1514	283
$Na-Pt/FeO_x$	40	3	95.1	97.5	1083	284
Ni/TiO_2	120	15	93.0	90.2	15	264
Ni−Sn	150	30	100	87	0.9	285
LaCuSi	120	30	95[b]	95[b]	~900	286
Ni/AC_{OX}	40	3	97.9	97.1	2.5	287
Ni@C-650	140	5	>99	95.3	12.4	288
$Co_3O_4@C$	110	50	91[b]	91[b]		289
$Fe_2O_3@C$	120	50	96	97		290
Co@C	120	7	95	93	8.2	291
CoNi@C	120	7	>95	>97	450	292
$CoO_x@NCNTs$	110	30	98	98	2	293
Co/C−N	100	10	99	97	2.2	294
Co@C−N	110	30	53	88.7		295
Co−N−C	80	30	99[a,b]	99[a,b]	35.9	296
$Co-N_x/C$	110	3.5	100	97	393	297

[a]Azo was the product. [b]Yield. [c]The substrate is 4-nitrophenol.

selectivity in Au/TiO_2. On the contrary, the reducible supports (e.g., TiO_2, Fe_2O_3) played a critical role in governing the selectivity. FTIR measurements showed that the adsorption of the $-NO_2$ group was favored on TiO_2 or at the $Au-TiO_2$ interface, which was, however, not observed on inert support (e.g., SiO_2). Kinetic experiments showed that when fed separately, both the −C═C in styrene and the $-NO_2$ in nitrobenzene could be reduced on Au/TiO_2. However, when styrene and nitrobenzene was co-fed, the reduction of styrene was significantly suppressed, which was consistent with FTIR measurement results. Both of the results demonstrated that the preferential adsorption of the $-NO_2$ group on the TiO_2 support (or at the metal−TiO_2 interfaces) resulted in excellent chemoselectivity. It was noteworthy that the TiO_2 support (or the metal−TiO_2 interface) could also prohibit the formation of explosive hydroxylamine intermediate.[264] The unique capability of Au/TiO_2 to preferentially reduce the $-NO_2$ group was also demonstrated in the hydrogenation reaction of α,β-unsaturated nitrocompounds, where the $-NO_2$ and −C═C were conjugated.[298] It was found that for substrates with different structures, the $-NO_2$ was always preferentially hydrogenated over the Au/TiO_2, and the desired products of oximes were obtained with excellent yields.

Inasmuch as the unique property of TiO_2 to preferentially adsorb the $-NO_2$ group, one might suppose that TiO_2 supported VIII−X group metals such as Pt, Ru, and Ni should also have high selectivity similar to Au/TiO_2. However, these metals failed to give high selectivity when supported on TiO_2.[264] The reason might be that although TiO_2 can preferentially adsorb the $-NO_2$ group, yet the Pt, Ru, and Ni metals, which are quite different from Au, also have strong and nonselective interactions with both $-NO_2$ and −C═C

DOI: 10.1021/acs.chemrev.9b00230
Chem. Rev. XXXX, XXX, XXX−XXX

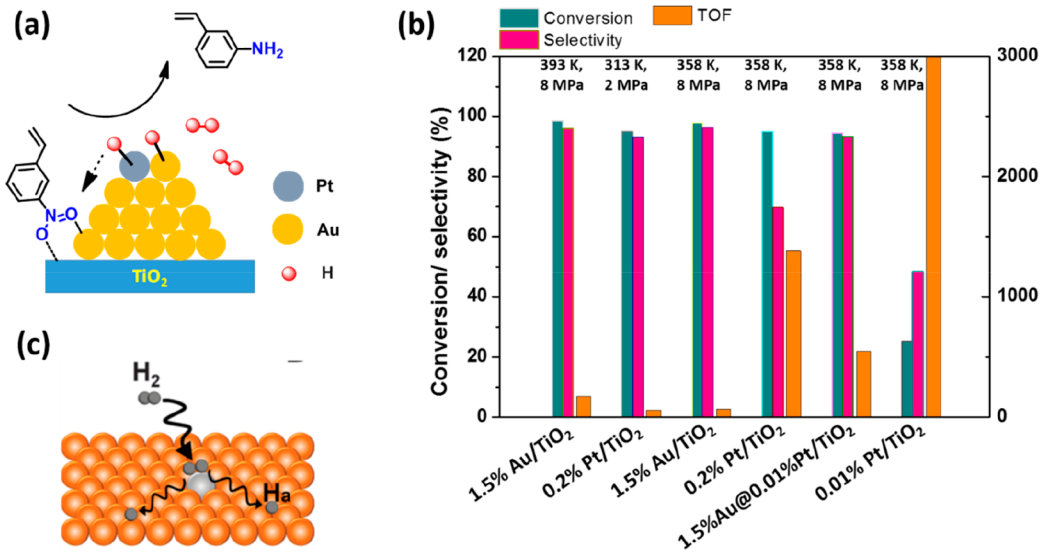

Figure 22. (a) Illustration of hydrogenation of 3-nitrostyrene over Au−Pt/TiO_2 catalyst; (b) catalytic performances of Au/TiO_2, Pt/TiO_2, and bimetallic AuPt/TiO_2 catalysts; (c) illustration of H_2 dissociation over isolated Pd atoms in Cu surface. (a) Reproduced with permission from ref 265. Copyright 2009 Elsevier. (c) Reproduced with permission from ref 153. Copyright 2012 The American Association for the Advancement of Science.

groups. An effective solution to this problem might be weakening the interaction of Pt with the reactant, at least the −C═C group therein. It has been established that the reduction of $-NO_2$ was structure insensitive, whereas the hydrogenation of −C═C was structure sensitive, thus it is rationalized that the adsorption of −C═C on Pt will be greatly weakened with the decrease of the size of Pt. On the basis of this recognition, Corma et al. developed an effective approach to transform nonselective supported VIII−X group metal nanoparticles to chemoselective catalysts by reducing the size or the exposed domains of the nanoparticles.[264,299] They first demonstrated this strategy by decreasing the size of Pt supported on Al_2O_3. It was found that when the size was decreased from a broad spectrum of 1−3 nm in 5 wt % Pt/Al_2O_3 to that narrowly centered at 1.5 nm in 0.2 wt % Pt/Al_2O_3, the selectivity to 3-vinylaniline increased from 0.6% to 60.2% at a high conversion level of 95%. To further decrease the size of Pt, they resorted to carbon supports with large surface area and abundant micropores, and in that case the selectivity was greatly enhanced to 90.5% at a 3-nitrostyrene conversion of 95.1% over 0.2 wt %Pt/C. In addition, the reaction could be conducted under conditions of 40 °C, 0.3 MPa H_2, which was milder than that of Au/TiO_2 (120 °C, 0.9 MPa H_2), indicating higher intrinsic catalytic activity for 0.2 wt % Pt/C. However, the 0.2 wt % Pt/C catalyst was not perfect, as a noticeable amount (25%) of explosive hydroxylamine accumulated at low conversion levels, which is dangerous for industrial application. By contrast, TiO_2 is the optimum support to avoid the production of hydroxylamine, as demonstrated by Au/TiO_2. Accordingly, TiO_2 supported Pt nanoparticles were synthesized by impregnation method. Nevertheless, the 0.2 wt % Pt/TiO_2 catalyst was nonselective because Pt nanoparticles with large size (>5 nm) were formed on TiO_2 phase boundaries. Then the authors tried to decrease the assemblies of accessible Pt atoms by the decoration of TiO_x induced by the strong metal support interaction (SMSI), which strategy should reach the same goal as the decrease of the size of Pt, and this time they succeeded. When the 0.2 wt % Pt/TiO_2 was reduced at higher temperature of 450 °C, it was clearly observed in HRTEM images that the Pt nanoparticles (particularly the terrace sites) were partially covered by TiO_x, which was also confirmed by CO adsorbed FTIR measurements. In the hydrogenation reaction of 3-nitrostyrene, the selectivity to 3-vinylaniline increased to 93.1% at a high conversion of 95.1%. More importantly, this strategy could be extended to other metals in VIII−X group, such as Ru and Ni. High selectivity of 90.2% and 96.3% could be achieved on Ni/TiO_2 and Ru/TiO_2 reduced at 450 °C at conversions of 93.0% and 95.1%, respectively. For other substrates with functional groups of −CHO, −CN, and −I, excellent yields of the corresponding products could be obtained over these catalysts.

Having established effective methodologies to achieve high chemoselectivity in the hydrogenation reaction of 3-nitrostyrene, Corma and co-workers tackled the challenge of low intrinsic activity of Au/TiO_2 and Pt/TiO_2 catalysts.[152,265] As aforementioned, although 1.5 wt % Au/TiO_2 showed excellent chemoselectivity, the activity was too low for practical applications (TOF = 173 h^{-1}), and thus the reactions need to be performed at harsh conditions (120 °C, 0.9 MPa H_2).[263] Although the 0.2 wt % Pt/TiO_2 could be selective under mild conditions (40 °C, 0.3 MPa H_2),[264,299] the TOF value was only 60 h^{-1} and the attempt to increase the reaction rate by increasing the temperature failed because the selectivity decreased at high temperature. In this regard, they aimed to enhance the catalytic activity of Au/TiO_2 because their high selectivity could be maintained at high temperature. On the basis of the H_2−D_2 exchange experiment, they discovered that the cleavage of H_2 was the rate-determining step in the hydrogenation reaction over gold.[265] Accordingly, they added trace amount of Pt into Au/TiO_2 with the purpose of promoting the H_2 cleavage without affecting the selectivity (Figure 22a). The results showed that the TOF value of the 1.5% Au@0.01% Pt/TiO_2 reached 550 h^{-1}, which was much higher than that of 0.2% Pt/TiO_2 and 1.5 wt % Au/TiO_2, and the selectivity was maintained at high level (>93.4%) (Figure 22b).[299] Although the distribution of Pt on the catalysts was difficult to be characterized by spectroscopic or microscopic techniques, it was supposed that Pt might exist as tiny clusters

DOI: 10.1021/acs.chemrev.9b00230
Chem. Rev. XXXX, XXX, XXX−XXX

or single atoms. These atomic dispersion of Pt species is reminiscent of Cu alloyed Pd single atoms,[153] where hydrogen molecules can be readily dissociated on Pd single atom and then flow to nearby Cu atoms by spillover (Figure 22c). Zhang, Wang, and co-workers adopted similar methodology to improve the catalytic activity of Au/SiO_2 by forming AuNi alloys based on their works on Au based bimetallic catalysts.[30,266] The monometallic Au/SiO_2 and Ni/SiO_2 catalysts were either not active enough or nonselective for the hydrogenation of 3-nitrostyrene, however, the bimetallic AuNi catalysts combined the merits of Au/SiO_2 and Ni/SiO_2.[266] In particular, the $AuNi_3/SiO_2$ showed the best catalytic performances, e.g., a selectivity of 93.0% was achieved at a conversion of 90.8%, and the TOF value was 21.9 h^{-1}, which was 4-fold higher than that of Au/SiO_2 (5.5 h^{-1}) under mild reaction conditions of 50 °C, 0.3 MPa H_2. Notably, SiO_2 supported Au nanoparticles (3.7 nm) here showed extremely high selectivity (99.6%) to 3-vinylamine, which was quite different from other reports where Au/SiO_2 was nonselective.[269] The reason might be the employment of APTES ((3-aminopropyl)triethoxysilane) grafted rather than pristine SiO_2 as the support, by which small sized Au nanoparticles could be obtained.[300] Meanwhile, the surface acidic/basic property of SiO_2 might be modified by the basic amine residue (APTES). It was also reported that in the hydrogenation of nitrostyrenes, the reduction of C═C was significantly inhibited by the presence of amines (e.g., triethylamine).[261] Similarly, when fibrous nanosilica was modified by polyethylenimine, the supported Pt nanoparticles (1.1 nm) and pseudosingle atom showed high selectivity (70%) to 3-vinylaniline at 90% conversion 3-nitrostyrene.[267] These results suggested that proper surface acidity/basicity of the support also had profound contribution to the chemoselectivity of the catalyst.[269,270]

Xiao and co-workers made attempts to improve the catalytic activity of Au/TiO_2 by deliberately placing the Au nanoparticles at the edge/corner sites rather than on the terraces of TiO_2.[268] The edge/corner sites are full of coordinatively unsaturated Ti^{3+} sites (i.e., oxygen vacancies), and thereby the electronic structure of Au nanoparticles was modified by the charge transfer from Ti^{3+} to Au.[301] In the hydrogenation reaction of 3-nitrostyrene under conditions of 90 °C, 1 MPa H_2, 4.5 h, high selectivity of 99% to 3-vinylamine was obtained at a conversion of 99%, and the TOF value reached 279 h^{-1}, much higher than that (173 h^{-1}) reported by Corma.[263] Kinetic studies revealed that when Au nanoparticles located on the terrace of TiO_2, the activation of $-NO_2$ was the rate-determining step, whereas the dissociation or diffusion of H_2 became critical when Au was placed at the corner/edge of TiO_2. Meanwhile, the apparent activation energy was significantly reduced from 40 to 26 kJ mol^{-1}. In agreement with kinetic studies, FTIR measurements also revealed that the defect-rich catalyst had strong adsorption to $-NO_2$ group, which might be responsible for the high intrinsic activity.

As aforementioned, in the hydrogenation of 3-nitrostyrene catalyzed by Au/TiO_2 (the size of Au was 3.5−4.0 nm), Corma et al. found that the catalysis was not dependent on the size of Au nanoparticles, and the reducible TiO_2 support was indispensable for the selectivity.[57,263] However, other groups had distinct discoveries that some nonreducible oxides such as Al_2O_3,[269,270] MgAl-HT,[271] and ZnAl-HT[272,302] supported Au nanoparticles could also perform well, and the selectivity was otherwise sensitive to the size of Au. For example, for the γ-Al_2O_3 supported Au catalysts,[269] with the decrease of the size of Au nanoparticles from 30 to 2.5 nm, the selectivity to 3-vinylaniline increased from 6% to 89%. In addition, the intrinsic activity of Au/Al_2O_3 (TOF = 6410 h^{-1}) was much higher than that of Au/TiO_2 (TOF = 1440 h^{-1}), although the selectivity was still lower than the latter (~95%). Similarly, γ-Al_2O_3 supported Ag nanoparticles also exhibited size-dependent catalytic performance.[270] When the size of Ag was in the range of 0.7−1.1 nm, the selectivity to 3-nitrostyrene was in the range of 88−96%. However, the selectivity decreased to 73% as the size of Ag nanoparticles increased to 3.4 nm and dramatically to zero when the size was further increased to 25 nm. In situ FTIR measurement results showed that the Al_2O_3 support, similar to TiO_2, could preferentially adsorb the $-NO_2$ group due to the acidic/basic pairs in γ-Al_2O_3.[57] The OH/D_2 isotope exchange experiment showed that molecular H_2 could heterolytically cleaved to ionic H^+/H^- pairs, which could preferentially transfer to the polar $-NO_2$ bond, leading to excellent chemoselectivity.

Au nanoparticles supported on Mg_4Al−HT also demonstrated a size-dependent catalytic performance in the hydrogenative coupling of 3-nitrostyrene to produce azo compounds.[271] When the Au loading decreased from 0.53 wt % to 0.11% (accompanied by the decrease of the size of Au), the selectivity was improved from 73% to 98%. Zhang, Liu, and co-workers developed ZnAl-HT supported Au catalysts (Au size: 1.7 nm) (Figure 23, top), which were highly selective for the preferential hydrogenation of $-NO_2$ group.[272] Interestingly, they are totally inactive for the hydrogenation of the −C═C bond in 3-nitrostyrene even when the reaction time was extensively prolonged. This behavior was in sharp contrast with other catalytic systems, where the hydrogenation of −C═C group was unavoidable when the $-NO_2$ group was completely converted.[152] The composition of the HT support played an important role in the catalysis.[302] When the support was MgAl−HT or CoAl−HT, high chemoselectivity could be obtained with negligible hydrogenation of the −C═C bond. By contrast, overhydrogenation occurred on Au/NiAl−HT (Figure 23, bottom). CO-adsorbed FTIR measurements showed that in the Au/NiAl−HT, the Ni (II) could be reduced to metallic Ni, which was responsible for the hydrogenation of −C═C bond. On the other hand, the residual sulfur which was introduced as the ligand of Au might also contribute to the high selectivity. As sulfur is one type of Lewis base, they, together with Au (Lewis acid) could form frustrated Lewis Pairs (FLPs), which would facilitate the heterolysis of H_2 to ionic H^+/H^-[202,303] and consequently promote the hydrogenation of polar $-NO_2$ group according to Atsushi Satsuma et al.[269]

Size-dependent catalysis was also observed in organic polymers supported Au catalysts. For instance, boronate self-assemblies supported Au nanoparticles (2.7 nm) afforded a high selectivity of 94.8% at 96% conversion of 4-nitrostyrene under reaction conditions of 100 °C, 0.5 MPa H_2 and 22 h, while larger Au nanoparticles with size of 5.5 nm gave much lower selectivity (72.7%) and activity (conversion 33%).[273] FTIR measurements revealed that the boronate support, prepared by condensation reaction of benzene-1,4-diboronic acid and pentaerythritol, had strong and preferential adsorption of $-NO_2$ group, which led to high chemoselectivity. However, the support was not stable enough that the catalytic activity decreased significantly (conversion 63%) in the second run.

DOI: 10.1021/acs.chemrev.9b00230
Chem. Rev. XXXX, XXX, XXX−XXX

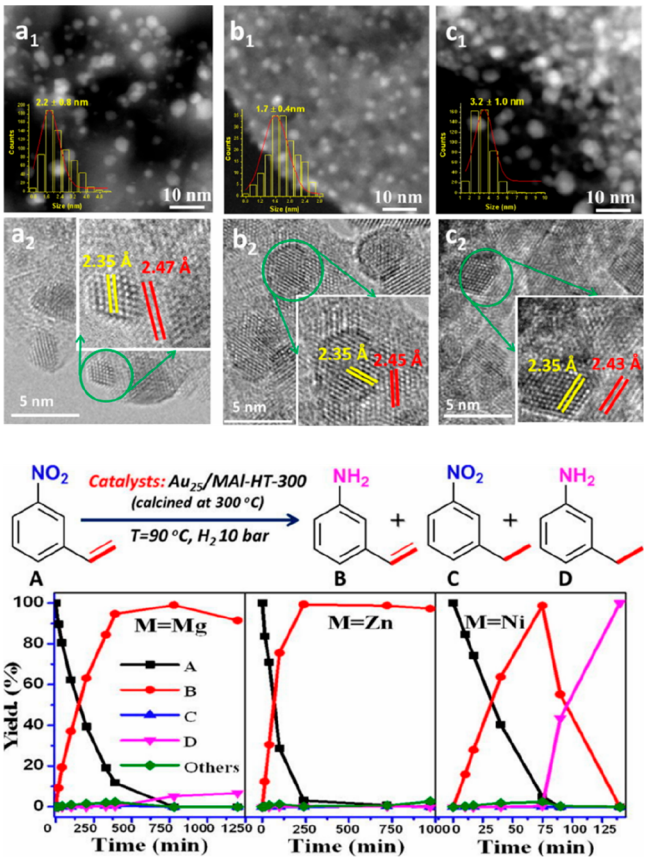

Figure 23. (top) HAADF−STEM and HRTEM images of the Au_{25}/MgAl−HT-300 (a_1, a_2), Au_{25}/ZnAl−HT-300 (b_1, b_2), and Au_{25}/NiAl−HT-300 (c_1, c_2) catalysts. (bottom) The distributions of the products with reaction time for the hydrogenation of 3-nitrostyrene over the three catalysts in the presence of H_2. Reproduced with permission from ref 272. Copyright 2018 Elsevier.

Inspired by the great success of employing small sized nanoparticles to achieve high chemoselectivity, other strategies to decrease the assemble size of metal nanoparticles, such as construction of core−shell structures,[60] forming alloys/intermetallics,[277] have been explored to construct chemoselective catalysts for the hydrogenation of nitrostyrenes. For example, core−shell structured Ag@CeO_2 nanocomposite exhibited >99% selectivity to 3-vinylaniline at a conversion of 98% under conditions of 110 °C and 0.6 MPa H_2 (Figure 24a,b).[60] However, the intrinsic activity of the catalyst was not high enough, which might arise from the low ability of IB group metals to dissociate H_2. The shell of the Ag@CeO_2 catalyst was assembled with spherical CeO_2 nanoparticles of 3−5 nm in diameter so that the spaces left between them allow for the core Ag NPs accessible to reactants (Figure 24a). The decoration of Ag NPs by CeO_2 not only decreased the size of exposed domains but also created a great many Ag−Ce interfaces which can heterolytically cleave H_2 (Figure 24c). The heterolysis of H_2 to ionic H^+/H^- was believed to play a vital role for the chemoselectivity, as they usually preferentially transferred to polar $-NO_2$ group rather than to nonpolar −C═C group. This core@shell strategy was also demonstrated in the Pt@MFI catalyst, which afforded 80% selectivity to 4-vinylaniline at full conversion of the substrate in the hydrogenation of 4-nitrostyrene under conditions of 80 °C and 1 MPa H_2.[274] On the contrary, the selectivity was zero on the nonencapsulated Pt/ZSM-5.

Construction of bimetallic alloys was another effective route to achieving high chemoselectivity in the target reaction. Kiwi-Minsker and co-workers prepared ZnO supported Pt nanoparticle with size of 2.5 nm.[275,276] Under a reaction condition of 70 °C and 1 MPa H_2, a 97% selectivity to 3-vinylaniline was obtained at full conversion of the substrate, and a TOF value as high as 744 h^{-1} was achieved. H_2-TPR, XRD together with XPS characterization results suggested the formation of PtZn alloys, whereby the exposed domains of Pt should be reduced via the separation of Zn and thus inhibit the structure sensitive hydrogenation of −C═C group. Similar to PtZn, PtBi bimetallic nanoparticles also showed 96% selectivity at full conversion under reaction condition of 85 °C and 2 MPa H_2 in the hydrogenation of 3-nitrostyrene.[278] XPS characterization indicated PtBi intermetallics might be formed, and the surface

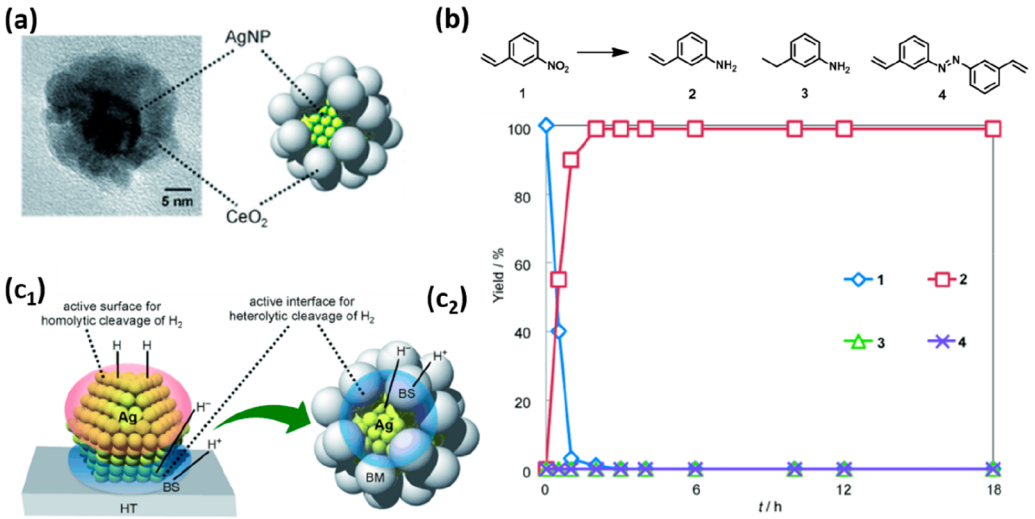

Figure 24. (a) HRTEM image and illustration of the single AgNPs@CeO_2 nanocomposite; (b) the catalytic performance of AgNPs@CeO_2 in the hydrogenation of 3-nitrostyrene; (c) illustration of H_2 dissociation over Ag/HT (c1) and AgNPs@CeO_2 (c2). On Ag/HT, H_2 undergoes heterolysis at Ag-support interface and homolysis on Ag nanoparticles. However, H_2 dissociates exclusively in the manner of heterolytic cleavage at the Ag-CeO_2 interface over AgNPs@CeO_2 catalyst. Reproduced with permission from ref 60. Copyright 2011 John Wiley and Sons.

DOI: 10.1021/acs.chemrev.9b00230
Chem. Rev. XXXX, XXX, XXX−XXX

of PtBi nanoparticles was rich of Bi. However, severe segregation of Bi on the surfaces was observed after the reaction, which led to deterioration of the activity, e.g., in the second run, the conversion decreased dramatically to 32.4% with a slight decrease of selectivity (93.2%).

Besides Pt, Rh based alloys and/or intermetallics also demonstrated improved chemoselectivity in the hydrogenation of nitrostyrene. Series of Rh-M (M = Bi, Fe, Ga, Ge, In, Ni, Pb, Sb, Sn, or Zn) alloys and/or intermetallics were screened by Komatsu and co-workers (Figure 25a,b).[277] Under reaction conditions of 0.5 h, 75 °C and 0.1 MPa, Rh/SiO_2 gave the highest conversion, yet the main product was 4-ethylnitrobenzene. Although the bimetallic $Rh-M/SiO_2$ showed inferior catalytic activity, the selectivity to 4-vinylamine was greatly improved. Among them, the $RhIn/SiO_2$ catalyst gave the highest selectivity (97%) to 4-aminostyrene at a conversion of 30%, followed by $RhSn/SiO_2$, which afforded a selectivity of ~95% with a conversion of ~40%. DFT calculation revealed that on extensive Rh terrace, the adsorption of −C═C was greatly favored by forming multiple coordination (Figure 25c). However, in RhIn ordered alloys, the Rh atoms were concave because of the larger atom radius of In than Rh, as well as the upshift of In atoms from the original plane resulted from the surface relaxation. Therefore, the steric hindrance provided by convex In atoms, together with the reduced assemblies of Rh by forming alloys, greatly suppressed the adsorption of −C═C bond (Figure 25d). However, the adsorption of $-NO_2$ through an end-on geometry was not affected by the change of the structure of catalysts.

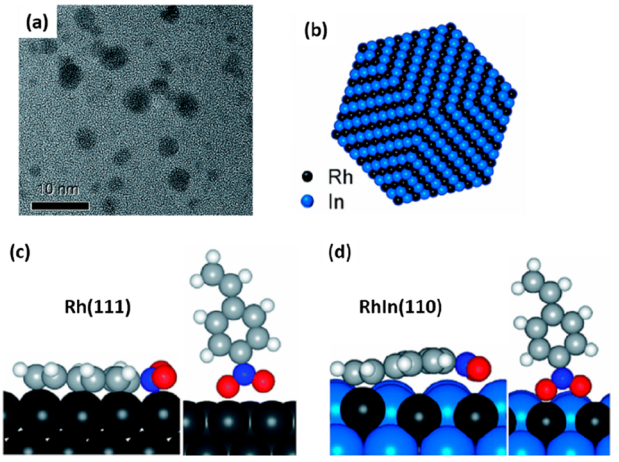

Figure 25. (a) HRTEM image and (b) illustration of RhIn intermetallics. The adsorption patterns of 4-nitrostyrene on Rh(111) (c) and RhIn(110) (d) surface. On Rh(111) surface, nitrostyrene can be adsorbed via "end-on" and "lying-down" patterns, whereas on RhIn(110) surface, the "lying-down" pattern is greatly prohibited. Adapted with permission from ref 277. Copyright 2016 The Royal Society of Chemistry (RSC).

Tomishige and co-workers found that when Ru/SiO_2 was modified by Re, Mo, or W, both activity and selectivity could be significantly improved.[279] In the hydrogenation of 3-nitrostyrene under conditions of 40 °C, 0.3 MPa H_2, 2 h, Ru/SiO_2 gave a trace conversion of 2.8% and a selectivity of 73.4% to 3-vinylamine. However, the conversion was enhanced to 15.3% and the selectivity was increased to 99.5% over the bimetallic $Ru-MoO_x/SiO_2$ catalyst. Similar promotional effect was also observed on $Ru-WO_x/SiO_2$ and $Ru-ReO_x/SiO_2$. When the reaction time was prolonged to 8 h, a high selectivity of 98% could be obtained at a conversion of 97%. Characterizations by TEM-EDX, H_2-TPR, and CO adsorption FTIR techniques revealed that metallic Ru nanoparticles were partially covered by MoO_x species, thereby the assemblies of Ru atoms should be reduced to some degree. Kinetic studies revealed that when Ru was modified with MoO_x, the reaction order with respect to 3-nitrostyrene concentration decreased from 0.8 to 0.1, indicating a strong adsorption and saturation coverage of the substrate on the catalyst surface. However, the reaction order with respect to H_2 pressure increased from 0.6 to 0.9, suggesting the dissolution or diffusion of H_2 was the rate-limiting step. The authors believed that H_2 might undergo heterolytic cleavage to ionic H^+/H^- pairs at the $Ru-MoO_x$ interfaces, by which the polar $-NO_2$ group was readily hydrogenated. MoO_x supported Pt−Sn bimetallic nano-

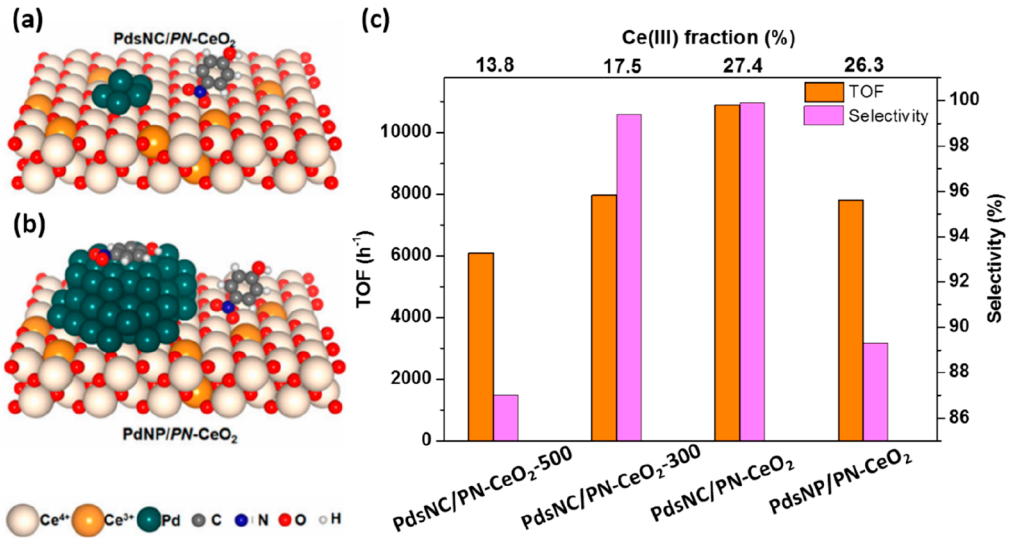

Figure 26. Adsorption patterns of 4-nitrophenol on PN−CeO_2 supported Pd clusters (a) and Pd nanoparticles (b); 4-nitrophenol adsorbs not only on CeO_2, but also on Pd nanoparticles. (c) Co-relationships between the concentration of oxygen vacancies (i.e., Ce(III)) of the catalysts and the TOF/selectivity. Adapted with permission from ref 281. Copyright 2016 American Chemical Society.

DOI: 10.1021/acs.chemrev.9b00230
Chem. Rev. XXXX, XXX, XXX−XXX

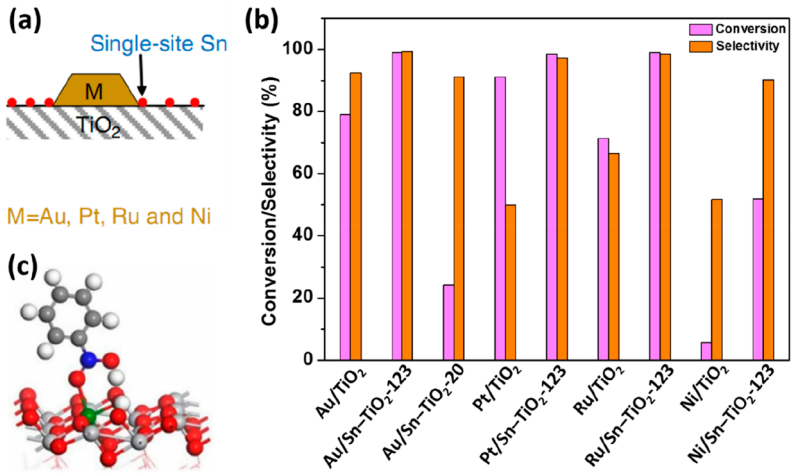

Figure 27. Illustration of (a) single site Sn promoted Au(Pt, Ru, Ni)/TiO_2 catalysts, and (c) adsorption pattern of nitrobenzene on oxygen vacancies sites of Sn-TiO_2 support. (b) catalytic performances of Au(Pt, Ru, Ni)/TiO_2 in the hydrogenation of 3-nitrostyrene. Adapted with permission from ref 58. Copyright 2018 Springer Nature.

particles also demonstrated high selectivity to vinylaniline in the hydrogenation of nitrostyrene under conditions of 30 °C and 0.1 MPa.[280] For example, 90% and 80% selectivity to 4-vinylaniline and 3-vinylaniline could be achieved at full conversion of the substrates, respectively. CO-TPD experiment revealed that with the introduction of Sn, the high temperature desorption peaks corresponding to CO adsorbed on bridging and 3-fold Pt sites decreased greatly, suggesting the continuous Pt ensembles were efficiently separated, which contributed to the high chemoselectivity.

The chemoselective catalysts for the hydrogenation of nitroarenes mentioned above generally employ reducible metal oxide as support (such as TiO_2, Fe_2O_3, ZnO, CeO_2),[60,263,275] therefore, their critical role in catalysis deserved investigation. Qu and co-workers prepared porous CeO_2 nanorods (PN−CeO_2) supported Pd clusters (<1 nm), which exhibited high catalytic activity (TOF = 44059 h^{-1}) for the hydrogenation of 4-nitrophenol.[281] FTIR measurements showed that the PN−CeO_2 with the higher concentration (30.8%) of oxygen vacancies had stronger adsorption of −NO_2 than nonporous CeO_2 nanorods and CeO_2 nanoparticles with lower oxygen vacancies portions of 15.7% and 9.3%, respectively. DFT calculation also indicated that the adsorption energy of nitro group on PN−CeO_2 was 6.6-fold higher than that on ideal (111) surface of CeO_2 without oxygen vacancies. Upon calcination under air, the concentration of oxygen vacancies in the catalyst decreased from 27.4% to 17.5%, while the reaction rate was reduced from 10900 to 7908 h^{-1}. Interestingly, the decreasing degree of the reaction rate (reduced by 1.4-fold) was in line with that of the oxygen vacancy concentration (decreased by 1.6-fold). These results demonstrated that the oxygen vacancies in CeO_2 served as the adsorption sites for the −NO_2 group (Figure 26a), and its concentration determined the reduction rate of −NO_2 (Figure 26c). On the other hand, the high dispersion of Pd clusters, which prohibited the coadsorption of several nitro groups and thus avoided possible side reactions of condensation of the intermediates (Figure 26b), was also an important factor for the high selectivity.

Similarly, Xiao's group also demonstrated that the oxygen vacancies in reducible metal oxides could preferentially adsorb the −NO_2 group in the hydrogenation of fuctionalized nitroarenes. They modified TiO_2 by doping of atomically dispersed Sn (Ti/Sn = 123, atomic ratio), and then deposited Au, Pt, Ru, and Ni on it by a deposition−precipitation (D−P) method (Figure 27a).[58] In the hydrogenation of 3-nitrostyrene, the doping of Sn significantly improved both the activity and selectivity. For example, Au/TiO_2 gave a selectivity to 3-vinylaniline of 93.9% at a conversion of 18.9% under the reaction conditions of 80 °C and 1.3 MPa H_2, whereas the Au/Sn−TiO_2-123 catalyst afforded 99.3% selectivity and 99.0% conversion. For other catalysts, such as Pt/Sn−TiO_2-123, Ru/Sn−TiO_2-123, and Ni/Sn−TiO_2-123, the selectivity was also greatly improved from 50.0−66.6% to 90.1−98.4%, along with the enhancement of activity (Figure 27b). It was found that upon treatment of the Sn−TiO_2-123 support with H_2 at 100 °C, oxygen vacancies were created, which then disappeared when the nitroarene was adsorbed. Meanwhile, FTIR measurement results showed that the −NO_2 could be strongly adsorbed on H_2-treated Au/Sn−TiO_2-123, whereas no adsorption band of −C═C on the catalyst was found. These results demonstrated that the oxygen vacancies in the support acted as active sites to adsorb the −NO_2 group (Figure 27c), which was in good agreement with that of Qu's group.[281] Thus, reducible oxides are the preferred choice of supports for the selective hydrogenation of nitroarenes because oxygen vacancies could be easily created on these metal oxides, especially at the metal−support interfacial sites.[304]

The driving force for the adsorption of −NO_2 group on oxygen vacancies arises from redox interaction. The oxygen vacancies, created by removal of one O atom while two electrons left, have high reduction potential so that they can even reduce CO_2 and H_2O to C and H_2 at high temperature, respectively.[305] Meanwhile, the −NO_2 is a weak oxidizer, therefore the oxygen vacancy is able to abstract one O atom in −NO_2 to yield −NO group, while the O atom filled in the vacancy is removed subsequently by H species dissociated on metal nanoparticles to generate H_2O, that is so-called reverse Mars−van Krevelen mechanism.[306] For the adsorption mode, the O atom in the −NO_2 group can interact with the metal cations (e.g., Ce(III)) nearby the oxygen vacancies in a perpendicular manner (i.e., end-on) based on DFT calculations.[281] Furthermore, in the −N═O hydrogenation steps in the catalytic circle, the metal cations neighboring to the oxygen

DOI: 10.1021/acs.chemrev.9b00230
Chem. Rev. XXXX, XXX, XXX−XXX

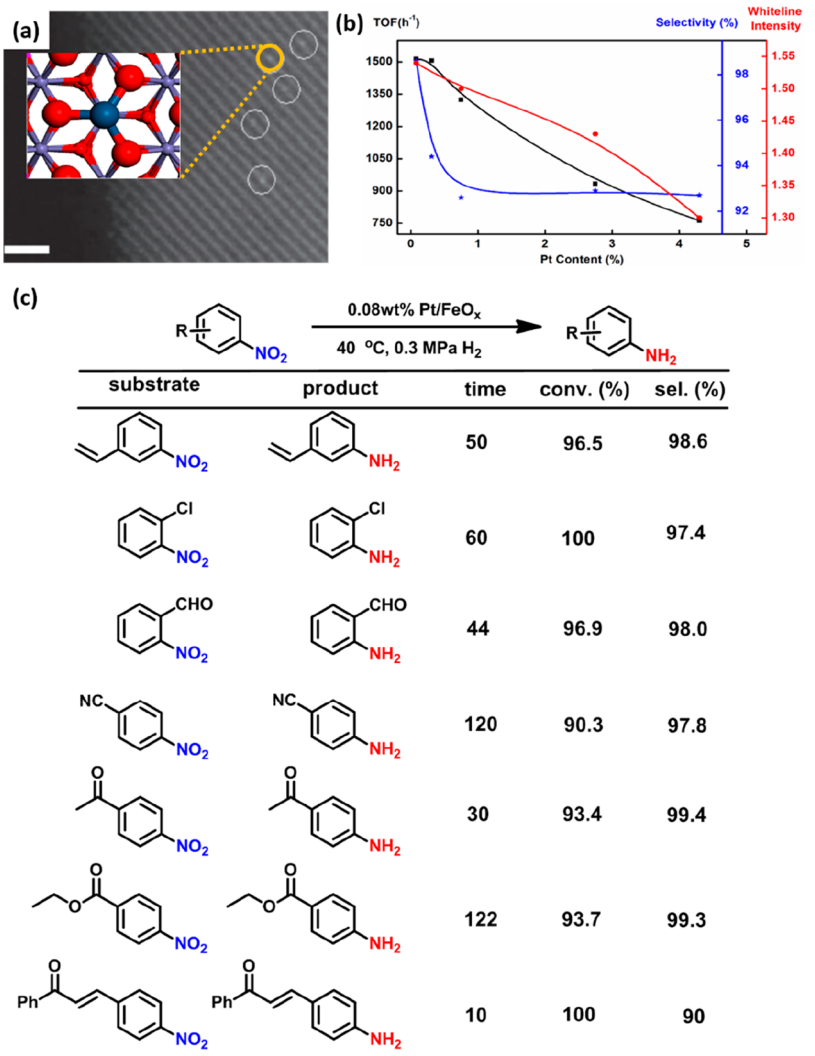

Figure 28. (a) HAADF−STEM images of 0.08% Pt/FeO_x−R200 SAC; the correlation between TOF/selectivity and the oxidation state (white-line intensity) of 0.08% Pt/FeOx−R200 SAC. (c) Substrate scope of the hydrogenation of functionalized nitroarenes. (b) Reproduced with permission from ref 44. Copyright 2018 Oxford University Press. (a,c) Reproduced with permission from ref 282. Copyright 2014 Springer Nature.

vacancies might act as Lewis acid to polarize the −N═O bond by binding to the O end (i.e., −N═O···Ce^{III}), which facilitates the hydride addition to this group and thus improves the chemoselectivity.

Taken together, some guidelines could be drawn for the design of efficient catalysts in the selective hydrogenation of nitroarenes. In these catalysts, oxygen vacancies (or interface sites) on the support fulfill the role of preferential adsorption of the $-NO_2$ group, whereas the small metal nanoparticles (or interface sites) are responsible for the dissociation of H_2 and may also contribute to the adsorption of $-NO_2$ and/or −C═C. In particular, the metal atoms in intimate contact with the support (i.e., interfacial sites) can contribute to both of the adsorption of $-NO_2$ and cleavage of H_2. Accordingly, it can be rationally deduced that if the nanoparticles are downsized to single atom dispersion (i.e., single-atom catalysts, SACs), the interfacial sites would reach the maximum on one hand, and on the other hand only one type of active sites would be present. As such, the adsorption of C═C bond would be completely suppressed, and both high activity and chemoselectivity to the $-NO_2$ hydrogenation would be achieved.

Motivated by the above hypothesis, Wang and co-workers explored Pt_1/FeO_x SAC for the chemoselective hydrogenation of nitroarenes.[282] At mild reaction conditions of 40 °C and 0.3 MPa H_2, the Pt_1/FeO_x SAC afforded a 98.6% selectivity to 3-vinylaniline at a high conversion of 96.5% (Figure 28c), which was the best among Pt based catalysts. Thanks to the high utilization efficiency of Pt atom, the TOF value reached as high as 11064 h^{-1}, which was 20-fold and 36.9-fold higher than that of the 1.5% Au@0.01% Pt/TiO_2 (TOF = 550 h^{-1})[265] and Pt/Sn−TiO_2-123 (TOF = 300 h^{-1}),[58] respectively. H_2-TPR experiment showed that when treated with H_2, not only the Pt(IV) in the catalyst precursor was reduced to $Pt^{\delta+}$($0 < \delta < 1$), but also the Fe(III) in the support was reduced to Fe(II), indicating the formation of oxygen vacancies. Interestingly, with a decrease of Pt loading (accompanied by the decrease of the size of Pt), the oxidation state of Pt, the molar ratio of reduced Fe species (Fe^{3+} to Fe^{2+}) to Pt species (Pt^{4+} to $Pt^{\delta+}$), and the selectivity to 3-vinylaniline all increased, and maximized at a Pt loading of 0.08 wt % (Figure 28b), where Pt existed as single atoms. These results suggested the maximization of oxygen vacancies, the slightly positive oxidation state of Pt, together with the single atom dispersion

DOI: 10.1021/acs.chemrev.9b00230
Chem. Rev. XXXX, XXX, XXX−XXX

of Pt in the 0.08 wt %Pt/FeO_x catalyst contributed to the high activity and selectivity. DFT calculation results showed the Pt single atoms occupied the Fe position in the support and coordinated to neighboring O atoms (Figure 28a).[39] These interfacial O atoms could be readily removed upon treatment by H_2, and the created oxygen vacancies then served as the adsorption sites for $-NO_2$ group. The employment of FeO_x as support was proved to be indispensable for the high selectivity, as inferior chemoselectivity was obtained over 0.08 wt % Pt/SiO_2 (46.9%) and 0.08 wt % Pt/Al_2O_3 (27.8%) in spite of small size of Pt (<1 nm). The 0.08 wt % Pt/FeO_x SAC also exhibited excellent catalytic performances in CO_2-expanded liquids, a type of solvent that is more environmentally benign than the traditional organic solvents.[283] For example, in CO_2-expanded toluene, a high selectivity of 96% was achieved at a conversion of 97.8%, while the amount of toluene could be reduced by 90%.

One major concern for the SACs is the extremely low density of the active sites (the Pt loading in the above example was only 0.08 wt %), which will undermine its potential for practical applications. It is therefore highly desired yet a great challenge to prepare a practically high loading SAC. Considering that alkali metals (e.g., Na) can promote the dispersion of Pt and meanwhile modify the electronic property of the metal, Wang and co-workers prepared alkali-metal promoted high-loading Pt/FeO_x (5 wt % Na−2.16 wt % Pt/FeO_x) and investigated their performances for the nitroarene reduction.[284] In the hydrogenation reaction of 3-nitrostyrene, a high selectivity of 97.5% to 3-vinylaniline was obtained at a conversion of 95.1%. Although the TOF value (1083 h^{-1}) was slightly lower than that of 0.08 wt % Pt/FeO_x (1514 h^{-1} at 40 °C),[282] the mass activity was enhanced by more than 20 times, which was attractive for practical application. Characterization results by Mössbauer spectroscopy and XAFS techniques showed that $NaFeO_2$ species formed on the surface of FeO_x, which species directly interacted with Pt by forming Pt−O−Na−O−Fe like species, and thereby a great many positively charged $Pt^{\delta+}$ ($0 < \delta < 1$) single atoms were formed. The authors also found the $NaFeO_2$ species could strengthen the adsorption of $-NO_2$ when compared with FeO_x, suggesting the more basic support will be favorable to the adsorption of acidic $-NO_2$ group. The dissociation of H_2 on the $Pt^{\delta+}$ single atoms, however, was not studied. It can be supposed that they may follow a heterolysis mechanism similar to that of Pd/TiO_2 SAC.[66] In that work, through kinetic isotope effect experiment and nuclear magnetic resonance measurements, Zheng and co-workers demonstrated that H_2 was heterolytically cleaved at the Pd−O interfaces, forming Pd−$H^{\delta-}$ and O−$H^{\delta+}$ species.

Above all, the modulation of the size of metal ensembles has been proved effective to tune the selectivity of the catalysts in the chemoselective hydrogenation of nitrostyrenes. Besides, the electronic structure of the active sites also had great influence on the catalytic performances. In the hydrogenation of nitrostyrenes, the $-NO_2$ group was electron-deficient, whereas the −C═C group was electron-rich. Accordingly, a proper density of electron on the catalytic sites should favor the adsorption of the $-NO_2$ rather than the −C═C group. For example, in TiO_x decorated Au, Pt, Ru, and Ni nanocatalysts developed by Corma's group,[264,299] the electronic structure of these metal nanoparticles might have been modified by TiO_x because charge transfer generally occurred simultaneously with SMSI. Analogously, in Pt based alloys/intermetallics, Pt sites should have high electron density due to charge transfer.[276,277] These electron-rich Pt sites have stronger affinity to electron-deficient $-NO_2$ group than did −C═C group and thus led to high selectivity. However, when there is too high electron density on the active sites, the catalytic performances will be quite different. Zheng's group reported that when the Pt nanowires were modified by ethylenediamine, interfacial electron transfer from N atoms to Pt occurred.[307] The electron-rich Pt atoms favored the adsorption of electron-deficient $-NO_2$ group, however, the reaction could not complete but stop at the *N*-hydroxylanilines stages because electron-rich Pt promoted the desorption of the intermediate *N*-hydroxylanilines, which is also electron-rich. Baiker and co-workers also observed that acidic reaction media facilitated the reduction of −C═C group, whereas basic solvent (e.g., triethylamine) significantly facilitated the reduction of $-NO_2$, yet the products were *N*-hydroxylanilines.[261]

6.2. Non-noble Metal Catalysts

Despite of the high activity and selectivity being achieved with the noble metal catalysts, the high price as well as the scarcity of the noble metals have prompted the intensive research on non-noble metal catalysts for the chemoselective hydrogenation of functionalized nitroarenes.

Nickel appears as the first choice thanks to its excellent activity for hydrogen dissociation. Corma and co-workers found that when the terraces of Ni nanoparticles were decorated by TiO_x induced by high temperature reduction (450 °C), highly selective Ni/TiO_2 catalysts could be obtained.[264] In the hydrogenation of 3-nitrostyrene under reaction conditions of 120 °C, 1.5 MPa H_2, 3 h, the selectivity to 3-vinylamine could reach 90.2% at a high conversion of 93.0% (TOF = 26 h^{-1}), whereas under otherwise identical conditions, the unmodified Ni catalyst only gave a selectivity of 55.3%. Shimazu et al. also made effective catalysts for the hydrogenation of nitrostyrene by alloying Ni with Sn.[285] Under reaction conditions of 110 °C and 3 MPa H_2, 99% selectivity to vinylaniline could be achieved. The authors proposed that the high chemoselectivity arose from the electrostatic interaction between Sn and $-NO_2$ group because Sn in the catalyst was electropositive, whereas O atoms in $-NO_2$ group were electronegative. However, the possible contribution of the weakened adsorption of −C═C on decreased assemblies of Ni atoms separated by Sn could not be excluded.

Hosono and co-workers investigated $LaCu_{0.67}Si_{1.33}$ intermetallic electride compounds for the selective hydrogenation of nitroarenes.[286] The $LaCu_{0.67}Si_{1.33}$ sample was featured with high electron density and low work function, which impart to them superior ability to donate electron to the adsorbed molecules, e.g., H_2. In the H_2−D_2 exchange reaction, the activation energy was only 14.8 kJ/mol, which was much lower than those (36.2−64.1 kJ/mol) on supported Au, Ag, and Cu catalysts. Accordingly, high catalytic activity (TOF= 5084 h^{-1}) was obtained in the hydrogenation of nitroarenes under condition of 120 °C and 3 MPa H_2. In addition, the high electron density of $LaCu_{0.67}Si_{1.33}$ also facilitated the preferential adsorption of electron-deficient $-NO_2$ group when other reducible functional groups (e.g., vinyl) were simultaneously present, leading to a high chemoselectivity to 4-vinylaniline (>95%).

In addition to alloying, the engineering of the support surface can also alter the selectivity of Ni nanoparticles. Wang and co-workers pretreated activated carbon with nitric acid in

DOI: 10.1021/acs.chemrev.9b00230
Chem. Rev. XXXX, XXX, XXX−XXX

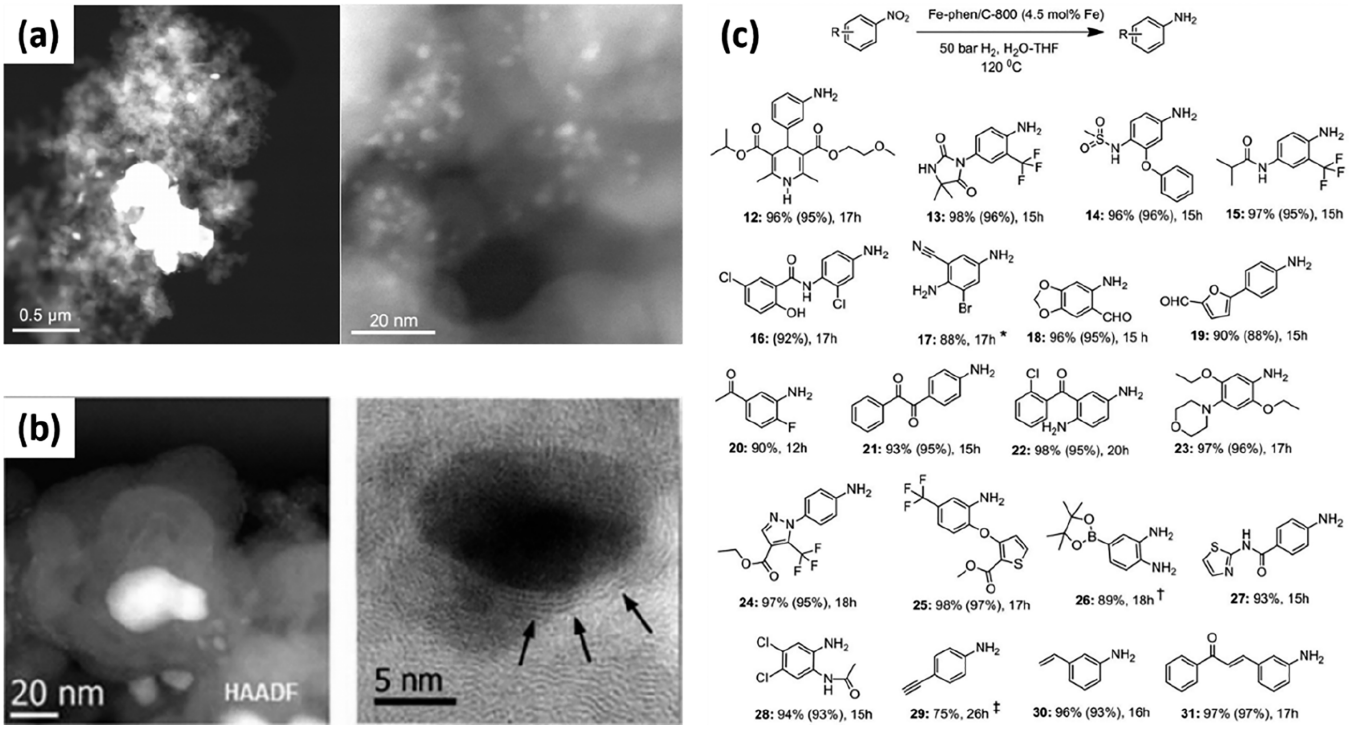

Figure 29. HAADF-STEM images of Co_3O_4−N/C catalyst (a) and Fe_2O_3−N/C catalysts (b); (c) substrate scope of hydrogenation of nitroarenes over Fe_2O_3−N/C catalysts. (a) Adapted with permission from ref 289. Copyright 2013 Springer Nature. (b,c) Adapted with permission from ref 290. Copyright 2013 The American Association for the Advancement of Science.

an attempt to create oxygen-containing functional groups and then supported Ni species with this surface-modified carbon. The resultant catalyst gave rise to high catalytic activity and chemoselectivity in the hydrogenation of functionalized nitroarenes and α,β-unsaturated nitroarenes.[287] For example, a high selectivity of 97.1% to 3-vinylamine could be obtained at 3-nitrostyrene conversion of 97.9%. Good to excellent yields (71−95%) of the desired oximes could also be obtained via hydrogenation of α,β-unsaturated nitroarenes. Notably, the hydrogenation reaction of nitroarenes was conducted under conditions of 40 °C and 0.3 MPa H_2, which was much milder than those reported in the literatures.[263,264,272] The large number of oxygen-containing groups on the acid-treated carbon support not only promoted the high dispersion of Ni precursors on the support and thus small sized Ni nanoparticles (average size: 5.5 ± 0.8 nm) were formed, but also facilitated the preferential adsorption of $-NO_2$. Both of the factors contributed to the high chemoselectivity.

Similarly, the porous graphitic carbon encapsulated Ni nanoparticles (Ni@C) also gave promising chemoselectivity in the hydrogenation of funtionalized nitroarenes. The Ni@C based catalysts were prepared via thermolysis of Ni-containing MOF composed of $NiCl_2$ and *p*-benzenedicarboxylic acid at 650 °C under N_2 atmosphere.[288] In the hydrogenation of 3-nitrostyrene under reaction conditions of 140 °C and 0.5 MPa H_2, a high selectivity of 95.3% to 3-vinylamine could be achieved at full conversion, and TOF value was 12.5 h^{-1}. TEM measurement revealed that most of the Ni nanoparticles were partially covered by graphitic carbon layers. When the carbon layers were burned off, the obtained catalysts showed inferior catalytic activity (conversion 40.8%) and selectivity (88.7%), suggesting the critical role of the carbon layers, which might reduce the ensembles of Ni and led to high chemoselectivity. Corma and co-workers also prepared carbon encapsulated Ni nanoparticles by coating $Ni(OH)_2$ with glucose, followed by pyrolysis at 600 °C under Ar tmosphere.[292] The Ni nanoparticles with sizes of tens to hundreds of nanometers were also covered by graphitic carbon layers, however, a lower selectivity to 3-vinylamine of 80% was obtained under reaction conditions of 120 °C and 0.7 MPa H_2, which might arise from the larger size of Ni nanoparticles or assemblies of accessible Ni atoms.

In 2013, Beller and co-workers reported a kind of N-doped carbon supported Co_3O_4 or Fe_2O_3 nanoparticles, i.e., Co(Fe)−N−C based catalysts, which demonstrated excellent catalytic selectivity in the hydrogenation of a variety of functionalized nitroarenes.[289,290] For example, for the most challenging substrate 3-nitrostyrene, the yield of the desired product 3-aminostyrene reached above 90% over both Co_3O_4−N/C and Fe_2O_3−N/C. Furthermore, other substrates with various functional groups, such as amino, halogen, aldehydes, ketones, nitriles, esters, amides, and alkynes, were well tolerated (Figure 29c). Although the M−N−C (M = Fe, Co, Ni, etc.) based catalysts had been extensively investigated in electrochemical reactions earlier,[308−311] e.g., the oxygen reduction reaction (ORR), it was not until Beller and co-workers explored their catalysis in chemoselective hydrogenation reactions that these materials have attracted great research interest for green synthesis of fine chemicals.[312−320] In spite of excellent catalytic performances, the true active species of these materials have been in great debates, both in electrochemical reactions and fine chemical synthesis. M−N−C based catalysts were generally prepared by pyrolysis of mixtures of metal, nitrogen, and carbon precursors at high temperature (600−1000 °C) under inert atmosphere. Owing to the complicated transformations at high temperature, various species coexist in these materials,[321] such as metallic nanoparticles, metal oxide, metal carbide, and nitride,[322] and atomically dispersed M−N−C

DOI: 10.1021/acs.chemrev.9b00230
Chem. Rev. XXXX, XXX, XXX−XXX

species that can only be observed under HAADF−STEM with atomic resolution.[323,324] Depending on the choice of the precursors and preparation methods, different species have been claimed to be responsible for the catalysis. Beller and co-workers claimed that Co_3O_4 nanoparticles with size of 20−80 nm and even hundreds of nanometers partially shielded by graphitic carbon layers in Co_3O_4−N/C catalyst (Figure 29a),[289] or FeN_x species in Fe_2O_3−N/C catalysts (Figure 29b),[290] contributed to the overall catalytic activity in the hydrogenation reactions, respectively. They found that the choice of ligands of cobalt, and the pyrolysis temperature had great influence on the catalytic activity. For instance, only when phen (phen = 1,10-phenanthroline) was the ligand of cobalt and when the pyrolysis was conducted at 800 °C could the catalyst show the best performance. However, the origin of the impacts of ligands and pyrolysis temperature on catalysis was not investigated. Therefore, unambiguous identification of the genuine active sites in the as-prepared M−N−C catalysts is highly desired for the rational design of less expensive chemoselective catalysts.

Corma's group also studied the catalytic performances of Co−N−C based catalysts for the chemoselective hydrogenation of 3-nitrostyrene. They prepared the Co@C catalysts by reduction of Co−EDTA (Ethylenediaminetetraacetic acid) complexes using H_2 at 450 °C.[291] The as-prepared catalyst afforded a high selectivity to 3-aminostyrene of 93% at 95% conversion under reaction conditions of 120 °C, 0.7 MPa H_2. According to XPS measurement, most of the Co species in the fresh Co@C catalyst had zero chemical state. When the Co@C was oxidized under air at 250−450 °C, both the activity and selectivity declined. However, when the oxidized sample was again reduced by H_2, the catalytic performance was totally recovered, indicating the metallic Co nanoparticles were the active sites. The possible contribution of N-containing species to the catalysis was also investigated. When the Co@C was treated by dilute acid to remove the cobalt nanoparticles, the obtained material was totally inactive. Accordingly, the authors claimed that the doping of nitrogen into the carbon matrix contributed little to the catalytic activity.

Corma et al. also employed glucose instead of EDTA as the carbon source to prepare Co@C and bimetallic CoNi@C catalysts. Co_3O_4 nanoparticles were first synthesized, which were then subjected to hydrothermal treatment in glucose solution followed by pyrolysis of the obtained complex at 600 °C under Ar or N_2 atmosphere.[292] The as-prepared catalyst Co@C-glucose showed even higher catalytic activity than the Co@C-EDTA,[291] thus precluding the contribution of surface N specie in the Co@C-EDTA. In the CoNi@C catalyst because of the high ability of Ni to dissociate H_2, the catalytic activity was enhanced by 4-fold compared with the monometallic counterpart Co@C, meanwhile the selectivity to 3-aminostyrene was well preserved (>97%). The origin of the high chemoselectivity of Co@C catalyst was studied by diffuse reflectance infrared Fourier transform spectroscopy (DRIFTS) technique. The measurement results showed that the valence state of cobalt had great influence on the adsorption mode of the substrate molecules, that is, the $-NO_2$ group preferentially adsorbed on metallic cobalt nanoparticles, whereas the −C═C adsorbed strongly on cobalt oxide. Consequently, the preferential adsorption of $-NO_2$ over −C═C group on metallic Co nanoparticles led to the high chemoselectivity of Co@C. It is surprising that although the metallic Co nanoparticles in Co@C had large size of 20−150 nm, they did not adsorb the −C═C group at all, which was quite different from other metals, such as Pt, Ru, and Ni.[264] It might result from the decoration of the graphitic carbon layer, which reduced the domains of accessible Co atoms.

Wang and co-workers had different views with Corma. They found that in the Co−N−C based catalysts, the metallic cobalt, the graphitic carbon layer, and the doped nitrogen species played concerted roles in the hydrogenation of nitroarenes.[293] The catalysts were made by thermal condensation of mixtures of D-glucosamine hydrochloride, melamine, and $Co(NO_3)_2 \cdot 6H_2O$ at 900 °C under N_2 atmosphere. In the hydrogenation of 3-nitrostyrene performed at 110 °C and 3 MPa H_2, a high selectivity of 98% to 3-vinylamine was achieved at a conversion of 98%. The metallic Co was totally shielded by carbon shells, whereas the CoO_x nanoparticles was only partially covered by the carbon layers. When the catalyst was treated by acid, the conversion and selectivity was only slightly decreased, indicating the remaining metallic cobalt nanoparticles protected by carbon shells was more efficient than the CoO_x in catalysis. The N species in the carbon layer was also found to be indispensable for the catalysis, because catalysts without N-doping showed worse catalytic activity. DFT calculations revealed that the graphitic carbon layers, activated by both of the inner metallic Co nanoparticles and N-doping, served as the active sites for H_2 dissociation. The activation of H_2 on this type of core@shell structured catalysts might follow the electron tunneling mechanism,[325,326] where the electron from the metal could tunnel through the carbon shell with no more than three layers.[325]

Li and co-workers had similar viewpoint to Wang's, that the Co nanoparticles, together with the N-doping played vital roles in the hydrogenation of nitroarenes.[294] However, Gascon and co-workers claimed that both the Co/CoO_x nanoparticles and the CoN_x species invisible in TEM images contributed to the catalysis.[295] They prepared Co−N−C based catalysts by pyrolysis of ZIF-67 at 600−900 °C under Ar atmosphere. In the hydrogenation of 3-nitrostyrene, a selectivity of 88.7% to 3-vinylamine could be obtained at a conversion level of 53% under reaction conditions of 110 °C, 3 MPa, 1 h. When the as-made samples were treated with dilute HCl solution, the conversion of nitrobenzene decreased from 99% to 62% with the loading of cobalt from 37.4 wt % to 13.6 wt %, implying the Co based nanoparticles indeed took part in the catalysis. Characterization of the acid-treated materials by energy-dispersive X-ray spectroscopy (EDS) technique revealed that in some cloudy-like area, although Co nanoparticles were absent, cobalt-containing species were detected, which were ascribed to atomically dispersed $Co-N_x$ species. SCN^- poisoning experiments revealed that upon the addition of KSCN, the TON value decreased from 53 to 33, indicating the $Co-N_x$ species also contributed to the catalytic activity. Notably, during the acid leaching experiment, when aqua regia was employed instead of dilute HCl, the treated sample was totally inactive. The reason might be that aqua regia was strongly oxidative, which might also destroy the $Co-N_x$ species confined in the carbon matrix besides Co based nanoparticles.

The argument over the true active species in M−N−C (M = Fe, Co, Ni, etc.) based catalysts has never stopped. Zhang, Wang, and co-workers, based on extensive characterizations and control experimental results, demonstrated that in Co−N−C based catalysts, the CoO_x nanoparticles were just

DOI: 10.1021/acs.chemrev.9b00230
Chem. Rev. XXXX, XXX, XXX−XXX

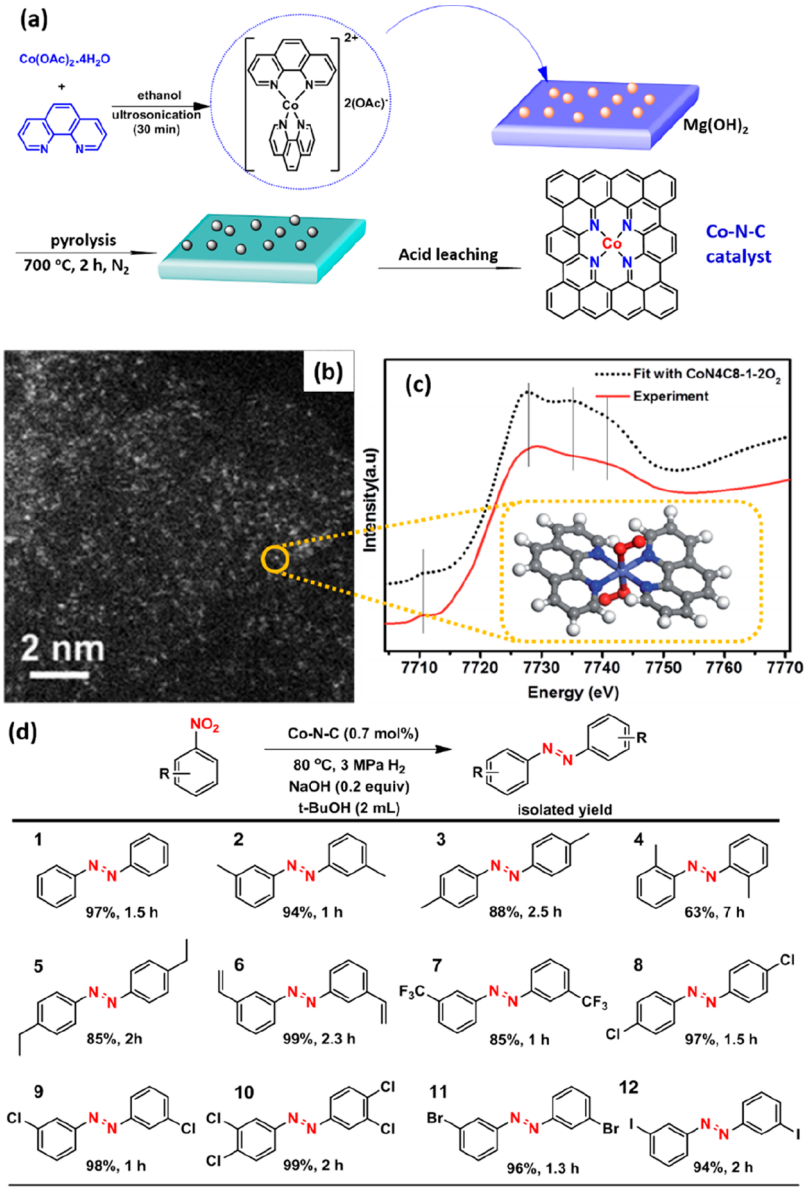

Figure 30. (a) Synthesis of Co−N−C SAC; (b) HAADF-STEM images of Co−N−C catalyst; (c) comparison between the K-edge XANES experimental spectrum of Co−N−C (solid red line) and the theoretical spectrum (black dotted line) calculated with the inset structure; (d) Substrate scope of the hydrogenation reaction. Reproduced with permission from ref 296. Copyright 2016 The Royal Society of Chemistry (RSC).

spectators, whereas the atomically dispersed Co−N_x moieties observed by Subångström-resolution high-angle annular dark-field scanning transmission electron microscopy (HAADF-STEM) technique, were the true active sites.[324] Subsequently, they prepared a self-supported Co−N−C material where the cobalt exclusively existed as single atoms (Figure 30a,b), which showed excellent catalytic performances in the hydrogenative coupling of functionalized nitroarenes to produce azo compounds (Figure 30d).[296] For the challenging substrate 3-nitrostyrene, the yield of the desirable product reached as high as 99%. It is noted that the reaction was conducted at 80 °C and 3 MPa H_2, where the temperature was much lower than that of the aforementioned Co−N−C based works (usually above 110 °C).[289,291] Characterization of the spent catalysts by HAADF−STEM as well as the XAFS techniques showed that cobalt was still dispersed as single atoms without sintering to clusters or nanoparticles, thus demonstrating unambiguously that the Co single atoms were the true active sites. The stability of the cobalt single atoms against aggregation was impressive, which might arise from their strong coordination with the pyridinic N in the carbon support. Therefore it is not surprising that in their later work, Ni−N−C single-atom catalysts with Ni loading of 7.5 wt % could even tolerate to harsh reaction conditions of 245 °C, 6 MPa H_2 in aqueous media without sintering.[80] By virtue of DFT calculation and XAFS technique, the structure of the Co−N−C moieties was identified to be CoN_4C_8−$2O_2$, where the Co(II) center atom coordinated with four pyridinic N atoms in the equatorial graphitic layer, while bonded weakly with two oxygen molecules in the polar direction (Figure 30c). The pyrolysis temperature had great influence on the catalytic activity, and the materials pyrolyzed at 700 °C showed the best catalytic activity. The reason, according to their another work of Fe−N−C single-atom catalysts, might be the formation of various M−N−C moieties with different structures and proportions at different temperatures.[327] On the basis of characterization

DOI: 10.1021/acs.chemrev.9b00230
Chem. Rev. XXXX, XXX, XXX−XXX

results of Mössbauer spectroscopy technique and selective poisoning experiments, four different Fe−N−C structures, i.e., medium spin Fe−N_4, medium spin Fe−N_5, low spin and high spin Fe−N_6, were identified. Particularly, the medium-spin Fe−N_5 species mainly formed at 700 °C showed much higher intrinsic catalytic activity (TOF = 5350 h^{-1}) than low-spin Fe−N_4 (TOF = 533 h^{-1}) and high-spin Fe−N_6 (TOF = 160 h^{-1}) species, which were dominantly formed at 600 and 800 °C, respectively. The origin of the high chemoselectivity of Co−N−C catalyst, on the basis of control experiment and ATR−FTIR measurements, was ascribed to the preferential adsorption of −NO_2.

That the CoN_x species was the true active site for the selective hydrogenation of nitroarenes was subsequently demonstrated by Zhang and co-workers.[297] They prepared the catalysts by pyrolysis of cobalt phthalocyanine supported on SiO_2 at 800 °C under N_2, followed by treatment with HF or NaOH. NaOH can only remove the SiO_2 support, whereas HF can dissolve both the SiO_2 and Co-containing nanoparticles. Under the reaction conditions of 110 °C and 0.35 MPa H_2, the HF treated sample showed almost identical catalytic activity to that treated with NaOH, suggesting the Co-containing nanoparticles were just spectators in catalysis, whereas the CoN_x species, which were not visible under traditional TEM, were the true active species. Even under mild reaction conditions of 40 °C and 0.1 MPa H_2, the HF treated sample could afford complete conversion of the substrate, although longer time was required, and the chemoselectivity to 3-aminestyrene could be as high as 97%. The reaction mechanism was also studied by kinetic experiments, and a direct reaction pathway was proposed, which was in contrast with that of Wang, Zhang, and co-workers, where the reaction followed a condensation route because of the presence of NaOH.[296] Unfortunately, the structure of the CoN_x species was not given.

In the above-mentioned Co−N−C based catalysts, two types of active species exist, one is the carbon decorated metallic Co nanoparticles and the other is the atomically dispersed Co−N−C moieties.[289,291,296,297] Which species is dominating the catalysis will be dependent on the preparation methods of the catalysts as well as the reaction conditions.

For Co-containing nanoparticles, two factors govern their chemoselectivity in the hydrogenation of nitrostyrenes. One is their chemical state. As demonstrated by Corma et al., the CoO_x species have strong adsorption to −C═C group, whereas only metallic Co nanoparticles can preferentially adsorb −NO_2.[291,292] As a thin layer of CoO_x tends to form on metallic Co when exposed to air, only when the CoO_x species were reduced could the catalysts exhibit high chemoselectivity. The other factor is the size of Co nanoparticles. Co-based nanoparticles obtained via high temperature pyrolysis generally have large size of tens to hundreds of nanometers, which favors the adsorption of the −C═C group. Therefore only when these nanoparticles were partially or totally covered by graphitic carbon layers can the hydrogenation of −C═C group was effectively suppressed. However, the decoration by carbon layers decreases their intrinsic activity, and thus the reactions need to be carried out under relatively high temperature and hydrogen pressure (e.g., temperature ≥110 °C).

By contrast, the atomically dispersed Co−N−C species are not sensitive to air and/or moisture, therefore they can be handled under ambient conditions.[296] In addition, the activation of H_2 on these single sites might follow a heterolysis rather than homolysis mechanism. Beller et al. found that the basic N species in the carbon matrix played a vital role in the heterolytic dissociation of H_2 into a hydride and a proton.[84] Zhang, Wang, and co-workers also demonstrated by DFT calculations that over the atomically dispersed Ni−N−C catalysts, H_2 underwent heterolysis to H^+ and H^-.[80] The Ni−N−C was believed to play a role similar to the frustrated Lewis pairs (FLP), which is well-known in homogeneous catalysis.[72−75] Therefore, the heterolytic dissociation of H_2, together with the high atom utilization of cobalt, furnished the catalysts with high catalytic activity and selectivity so that the reaction could be conducted under mild conditions (e.g., 40 °C and 1 atm H_2). However, the structure of Co−N−C species is greatly dependent on the metal precursor employed and the pyrolysis temperature. Generally, only transition metal complexes with N-containing aryl or macrocyclic ligands can generate highly efficient M−N−C catalysts because of the formation of graphitic carbon layers wherein the M−N−C moieties are imbedded.[309,328] The temperature also had great impact on the structure of M−N−C. For example, Zhang, Wang, and co-workers discovered that various structured Fe−N−C moieties could be formed at 600−800 °C, of which the Fe−N_5 species with the highest catalytic activity was mainly generated at 700 °C.[327] In addition, in all of the Fe−N−C species, the Fe−N_5 species only accounts for a small proportion (∼28%), leaving large room for the preparation of more active M−N−C based catalysts with homogeneous composition and structure on an atomic level (e.g., exclusively Fe−N_5 structure).

6.3. Summary

For the chemoselective hydrogenation of nitroarenes, heterogeneous catalysts from supported metal nanoparticles to single atoms have been developed so far. On the basis of the understanding of the reaction mechanism, some guidelines can be drawn for the design and development of efficient and selective catalysts.

First, the "geometric" modulation. As the hydrogenation of vinyl and nitro groups require different metal ensembles, i.e., the reduction of C═C bond is structure sensitive, whereas that of −NO_2 group is insensitive, decreasing the assemble of accessible metal atoms is able to suppress the hydrogenation of C═C while not affecting the −NO_2 group. Accordingly, many strategies have been developed to decrease the ensembles of metal nanoparticles, such as selective poisoning by organic surfactants, forming alloys, and partially covering the metal nanoparticles through SMSI. These methodologies moderately or even greatly improved the selectivity, however, the catalytic activity was more or less lost due to the low atom utilization efficiency. Among others, the construction of single-atom catalysts, where the metal ensembles are downsized to the lowest limit, prevents the reduction of vinyl group to the most extent, and thus shows superior selectivity to their nanoparticle counterparts.

Second, the "electronic" modification. The C═C and −NO_2 groups have different electron density, i.e., −C═C is electron-rich whereas the −NO_2 is electron-deficient. Therefore, nucleophilic sites on the catalysts should strongly adsorb −NO_2 while repelling the C═C group. Accordingly, methodologies to fabricate catalysts with high electron density, such as the employment of reducible metal oxide rich of oxygen vacancies as the support and the modification of the support

DOI: 10.1021/acs.chemrev.9b00230
Chem. Rev. XXXX, XXX, XXX−XXX

with organic amines, have been developed to achieve high selectivity for $-NO_2$ adsorption.

Third, the heterolytic dissociation of H_2. In this reaction pathway, H_2 is cleaved to ionic H^+/H^- pairs, which prefer to reduce the polar $-NO_2$ rather than the nonpolar C=C group. The heterolysis of H_2 is considered to occur on the metal−support interfacial sites that are maximized in SACs, thus rendering SACs with excellent chemoselectivity.

On the basis of the above analysis, SACs are more promising for the hydrogenation of functionalize nitroarenes than their nanoparticle counterparts. In fact, regarding the true active species, the nanocatalysts (e.g., partially covered by reducible oxide) share some similarities with SACs, i.e., in both cases the metal−support interfaces serve as the active species for the activation of both nitroarenes and hydrogen. However, subtle differences still exist in terms of coordination environment and electronic structures in the two catalytic systems. In SACs, the metal single atoms are exclusively surrounded by heteroatoms in the support, whereas in nanocatalysts, the metal atoms at the interface are still partially coordinated to the subsurface atoms within the nanoparticles, which might render interfacial atoms with higher electron density and consequently enhance the intrinsic catalytic activity. In this sense, by modulating the coordination environment and electronic structure of single atoms, both highly active and chemoselective SACs can be expected.

7. CONCLUSIONS AND PERSPECTIVES

In summary, the selective hydrogenation reactions are important transformations for both petrochemical and fine chemical industries, yet when two or multireducible functional groups coexist, the chemoselective reduction of the target one remains challenging. Typical reactions include the semihydrogenation of alkynes/dienes to monoenes, chemoselective hydrogenation of α,β-unsaturated aldehydes/ketones to unsaturated alcohols, and substituted nitroarenes to anilines. The common characteristics of the three types of reactions lie in that the chemoselectivity arises from the preferential adsorption of the desired group to the undesired one. In other words, the adsorption mode of the multifunctional group substrates (e.g., substituted nitroarenes or α,β-unsaturated aldehydes/ketones) or of the product (e.g., monoenes in the semihydrogenation of alkynes/dienes) dictates the chemoselectivity; only when the substrate adsorbs via an end-on mode or when the product adsorbs via a weak π-bonding mode on the active sites can a high chemoselectivity be obtained. Therefore, engineering the geometric configuration of the active sites so that it interacts with the reactant or product via the desired manner has become the most important strategy to accomplish the chemoselective hydrogenation. On the basis of experimental and theoretical studies, isolated active sites can perfectly meet the requirement for end-on adsorption of the multifunctional group substrates and π-bonding adsorption of monoenes. Toward the isolation of active sites, various approaches have been developed, including adsorption/grafting of N/S-containing organic molecules on the metal surface, partial covering of active metal surface by metal oxides either via doping or through SMSI, confinement of active metal NPs in micro- or mesopores of the supports, formation of bimetallic alloys or intermetallics or core@shell structures with a relatively inert metal (IB and IIB) or nonmetal element (B, C, S, etc.), and construction of SACs on reducible oxides or inert metals (SAAs) (Figure 1). All these approaches have been proved effective for the enhancement of chemoselectivity by virtue of isolation of active sites. By comparison of these approaches (Tables 1−4), one can see that SACs and intermetallics appear as the most promising as both of them provide a completely isolated environment of active sites. Moreover, in terms of atom utilization efficiency, SACs are more desirable because each and every catalytically active metal atoms are exposed and accessible to reactants, which is of particular importance for expensive noble metal catalysts.

Although exciting and encouraging advances have been made in the chemoselective hydrogenation reactions using the "active site isolation" strategy, some challenges are yet to be addressed in both fundamental studies and practical applications:

1. Achieving both high activity and chemoselectivity: For most of the approaches toward the "active site isolation", a high chemoselectivity is often accompanied with a certain loss of activity, the so-called "seesaw effect", which is particularly remarkable when the isolation of active metal atoms is accomplished by means of adsorption of organic modifiers or doping/encapsulation of inorganic oxides on the surface of metal NPs. In fact, even by forming alloys or intermetallics with the second metal, the enhancement of chemoselectivity is also, in many cases, at the cost of activity loss. The underlying reason is that the change of geometric structure is concomitant with the alteration of electronic structure, and the chemical bonding of the active metal with the modifier (organic or inorganic, or the second inert metal) will not only weaken the adsorption of the product molecules but also simultaneously weaken the adsorption of reactant molecules (e.g., H_2) based on the scaling relationship.[42,329] Therefore, to achieve high chemoselectivity without compromising the activity, one needs to develop novel strategies to break the limit of scaling relationship. One promising approach toward this direction is to construct single-atom catalysts with tunable coordination environment.[327,330] On one hand, the single-atom dispersion meets the "site isolation" requirement for high chemoselectivity; on the other hand, the coordination environment is tuned for electronic modification of the active site so that it can effectively activate the reactant molecules. The other effective approach is to fabricate the bifunctional catalysts where hydrogen activation and hydrogenation reaction occur at different sites. Both the single-atom alloy (SAA) catalysts and the reducible oxide supported single atoms belong to this approach.

2. Catalyst durability: Catalyst durability is even more important than activity for the practical applications. For liquid-phase hydrogenation reactions which are normally operated under mild conditions, the catalyst durability appears not a serious problem. Nevertheless, the catalysts modified with organic surfactants may take the risk of leaching of organic modifier in the liquid phase, which will destroy the isolation of active metal and eventually loss of chemoselectivity. Compared to the liquid-phase reactions, greater challenges are posed in the gas-phase hydrogenation reactions. For example, in the semihydrogenation of acetylene, most of the reported work only provided a short-term stability test (<100 h) and even in this case a declining tread in both activity and chemoselectivity is often observed. However, the industrial operations require at least a several-month stability. Considering that the phase segregation is ubiquitous in bimetallic alloys and the isolated single atoms tend to aggregate under reducing atmosphere, the stability of both SACs and SAAs

DOI: 10.1021/acs.chemrev.9b00230
Chem. Rev. XXXX, XXX, XXX−XXX

need to be carefully investigated for a long-term operation. Toward this goal, operando studies are required to provide a molecular understanding of the dynamics of the active site structure, and modifiers to stabilize and maintain the isolated site structure need to be developed in addition to the existing stabilizing effect by the support or the alloy structures.

3. Mechanism understanding: While it has been well accepted that the geometric effect, in particular the site isolation, predominates the chemoselectivity, the role of the spacer/isolator, including the support, the second metal, or the organic/inorganic modifiers should not be limited to the geometry modulator. Instead, it also functions as the electronic modifier. In this respect, the support or the second metal or the other modifiers should be chosen toward both isolating the active metal atoms and positively tuning the electronic properties of the active metal for activating H_2 molecules. This relies on both theoretical studies of different metal/modifier combinations for electronic interactions and atomic/molecular characterizations of the catalyst structure and interaction with the reactants with advanced operando technologies. On the other hand, reaction kinetics need to be investigated for a more comprehensive understanding of the reaction mechanism. In fact, the chemoselective hydrogenation of one group over the other groups is not only dependent on the active site structure but also on hydrogen coverage.[93,134] At a relatively high hydrogen coverage, deep hydrogenation of all the reducible groups can also occur. Therefore, it is important to make it clear how the active site structure influence the hydrogen coverage as well as the reaction rate, and how these can be tuned by operating parameters in addition to the catalyst itself.

Lastly, the fundamental principles drawn from the hydrogenation reactions may also be applicable for other reactions. For example, coking is the main problem for dehydrogenation of alkanes to produce alkenes industrially.[331] While SACs are known to effectively prohibit the formation of coke in semihydrogenation of acetylene, they might also be efficient catalysts for dehydrogenation reactions. Very recent reports have approved this deduction.[182,332−334]

AUTHOR INFORMATION

Corresponding Authors

*T.Z.: phone, +86-411-84379348; fax, +86-411-84685940; E-mail, taozhang@dicp.ac.cn.
*A.W.: E-mail, aqwang@dicp.ac.cn.

ORCID

Aiqin Wang: 0000-0003-4552-0360
Tao Zhang: 0000-0001-9470-7215

Notes

The authors declare no competing financial interest.

Biographies

Leilei Zhang was born in 1986. He graduated from Lanzhou University in 2008 and received his Ph.D. degree in 2014 from Dalian Institute of Chemical Physics, CAS, under the supervision of Profs. Aiqin Wang and Tao Zhang. His current research focuses on the construction of nano- and single-atom catalysts for green synthesis of fine chemicals.

Maoxiang Zhou was born in 1992. He received his B.S. degree in 2014 from Chongqing University. Since 2015, he has been studying for his Ph.D. degree at Dalian Institute of Chemical Physics, CAS, under the supervision of Prof. Aiqin Wang. His doctoral research is concerned with theoretical investigation on catalysis of the selective hydrogenolysis of polyols.

Aiqin Wang joined Prof. Tao Zhang's group after she received a Ph.D. degree in 2001 from the Dalian Institute of Chemical Physics (DICP) under the supervision of Profs. Dongbai Liang and Tao Zhang. In 2003, she moved to National Taiwan University as a postdoctoral fellow in Prof. Chung-Yuan Mou's group for synthesis and catalysis of gold-based alloy nanoparticles until 2005. Then she went back to DICP and joined Prof. Tao Zhang's group, where she was promoted to a full professor in 2009. Her current research interests involve catalysis by nanogold and gold alloy particles, catalytic conversion of biomass, and design and synthesis of new catalytic materials.

Tao Zhang received his Ph.D. degree in 1989 from Dalian Institute of Chemical Physics (DICP), Chinese Academy of Sciences. After one year at the University of Birmingham as a postdoctoral fellow, he joined DICP again in 1990, where he was promoted to a full professor in 1995. He is currently the vice president of the Chinese Academy of Sciences. His research interests are mainly focused on the design and synthesis of nano- and subnano-catalysts, the catalytic conversion of biomass, and environmental catalysis. He has won many important awards, such as the National Invention Prize (for three times), Distinguished Award of Chinese Academy of Sciences, Zhou Guang Zhao Foundation Award for Applied Science, and Excellent Scientist Award of Chinese Catalysis Society. Prof. Zhang is the author or coauthor of more than 300 peer-reviewed scientific publications. Over 100 patents were filed by him and co-workers. He serves as the Editor-in-Chief of the *Chinese Journal of Catalysis* and as an Editorial Board Member of *Applied Catalysis B*, *ACS Sustainable Chemistry & Engineering*, *ChemPhysChem*, and *Industrial & Engineering Chemistry Research*. He was elected as an Academician of the Chinese Academy of Sciences in 2013.

ACKNOWLEDGMENTS

We are grateful for the supports from the National Key Projects for Fundamental Research and Development of China (2018YFB1501602 and 2016YFA0202801), the National Natural Science Foundation of China (21690080, 21690084, 21673228, 21721004, 21606227), the Strategic Priority Research Program of the Chinese Academy of Sciences (XDB17020100), and Dalian National Laboratory for Clean Energy (DNL180303). We thank Y. Ren and H. Chen for assisting in the preparation of the Tables 1, 3, and 4.

REFERENCES

(1) Storch, H. H. Chemistry of Coal Hydrogenation. *Chem. Rev.* **1941**, *29*, 483−499.
(2) Brieger, G.; Nestrick, T. J. Catalytic transfer hydrogenation. *Chem. Rev.* **1974**, *74*, 567−580.
(3) Johnstone, R. A. W.; Wilby, A. H.; Entwistle, I. D. Heterogeneous Catalytic Transfer Hydrogenation and Its Relation to Other Methods for Reduction of Organic-Compounds. *Chem. Rev.* **1985**, *85*, 129−170.
(4) Grange, P. Catalytic Hydrodesulfurization. *Catal. Rev.: Sci. Eng.* **1980**, *21*, 135−181.
(5) Ho, T. C. Hydrodenitrogenation Catalysis. *Catal. Rev.: Sci. Eng.* **1988**, *30*, 117−160.
(6) Wang, D.; Astruc, D. The golden age of transfer hydrogenation. *Chem. Rev.* **2015**, *115*, 6621−6686.
(7) Meemken, F.; Baiker, A. Recent Progress in Heterogeneous Asymmetric Hydrogenation of C = O and C = C Bonds on Supported Noble Metal Catalysts. *Chem. Rev.* **2017**, *117*, 11522−11569.

DOI: 10.1021/acs.chemrev.9b00230
Chem. Rev. XXXX, XXX, XXX−XXX

(8) Alig, L.; Fritz, M.; Schneider, S. First-Row Transition Metal (De)Hydrogenation Catalysis Based On Functional Pincer Ligands. *Chem. Rev.* **2019**, *119*, 2681−2751.
(9) Wang, W.; Wang, S.; Ma, X.; Gong, J. Recent advances in catalytic hydrogenation of carbon dioxide. *Chem. Soc. Rev.* **2011**, *40*, 3703−3727.
(10) Deldari, H. Suitable catalysts for hydroisomerization of long-chain normal paraffins. *Appl. Catal., A* **2005**, *293*, 1−10.
(11) Escola, J. M.; Aguado, J.; Serrano, D. P.; García, A.; Peral, A.; Briones, L.; Calvo, R.; Fernandez, E. Catalytic hydroreforming of the polyethylene thermal cracking oil over Ni supported hierarchical zeolites and mesostructured aluminosilicates. *Appl. Catal., B* **2011**, *106*, 405−415.
(12) Crespo-Quesada, M.; Cárdenas-Lizana, F.; Dessimoz, A.-L.; Kiwi-Minsker, L. Modern Trends in Catalyst and Process Design for Alkyne Hydrogenations. *ACS Catal.* **2012**, *2*, 1773−1786.
(13) Kluson, P.; Cerveny, L. Selective hydrogenation over ruthenium catalysts. *Appl. Catal., A* **1995**, *128*, 13−31.
(14) Blaser, H. U.; Malan, C.; Pugin, B.; Spindler, F.; Steiner, H.; Studer, M. Selective hydrogenation for fine chemicals: Recent trends and new developments. *Adv. Synth. Catal.* **2003**, *345*, 103−151.
(15) McCue, A. J.; Anderson, J. A. Recent advances in selective acetylene hydrogenation using palladium containing catalysts. *Front. Chem. Sci. Eng.* **2015**, *9*, 142−153.
(16) Vilé, G.; Albani, D.; Almora-Barrios, N.; López, N.; Pérez-Ramírez, J. Advances in the Design of Nanostructured Catalysts for Selective Hydrogenation. *ChemCatChem* **2016**, *8*, 21−33.
(17) Noyori, R.; Hashiguchi, S. Asymmetric Transfer Hydrogenation Catalyzed by Chiral Ruthenium Complexes. *Acc. Chem. Res.* **1997**, *30*, 97−102.
(18) Climent, M. J.; Corma, A.; Iborra, S. Heterogeneous catalysts for the one-pot synthesis of chemicals and fine chemicals. *Chem. Rev.* **2011**, *111*, 1072−1133.
(19) Schoenbaum, C. A.; Schwartz, D. K.; Medlin, J. W. Controlling the surface environment of heterogeneous catalysts using self-assembled monolayers. *Acc. Chem. Res.* **2014**, *47*, 1438−1445.
(20) Vile, G.; Almora-Barrios, N.; Mitchell, S.; Lopez, N.; Perez-Ramirez, J. From the Lindlar catalyst to supported ligand-modified palladium nanoparticles: selectivity patterns and accessibility constraints in the continuous-flow three-phase hydrogenation of acetylenic compounds. *Chem. - Eur. J.* **2014**, *20*, 5926−5937.
(21) Niu, W.; Gao, Y.; Zhang, W.; Yan, N.; Lu, X. Pd-Pb Alloy Nanocrystals with Tailored Composition for Semihydrogenation: Taking Advantage of Catalyst Poisoning. *Angew. Chem., Int. Ed.* **2015**, *54*, 8271−8274.
(22) Lindlar, H. Ein neuer Katalysator für selektive Hydrierungen. *Helv. Chim. Acta* **1952**, *35*, 446−450.
(23) Hamm, G.; Schmidt, T.; Breitbach, J.; Franke, D.; Becker, C.; Wandelt, K. The Adsorption of Ethene on Pd(111) and Ordered Sn/Pd(111) Surface Alloys. *Z. Phys. Chem.* **2009**, *223*, 209−232.
(24) Lear, T.; Marshall, R.; Lopez-Sanchez, J. A.; Jackson, S. D.; Klapotke, T. M.; Baumer, M.; Rupprechter, G.; Freund, H. J.; Lennon, D. The application of infrared spectroscopy to probe the surface morphology of alumina-supported palladium catalysts. *J. Chem. Phys.* **2005**, *123*, 174706.
(25) Li, M. S.; Shen, J. Y. Microcalorimetric studies of O_2 and C_2H_4 adsorption on Pd/SiO_2 catalysts modified by Cu and Ag. *Thermochim. Acta* **2001**, *379*, 45−50.
(26) Zhou, K.; Li, Y. Catalysis based on nanocrystals with well-defined facets. *Angew. Chem., Int. Ed.* **2012**, *51*, 602−613.
(27) Strasser, P.; Koh, S.; Anniyev, T.; Greeley, J.; More, K.; Yu, C.; Liu, Z.; Kaya, S.; Nordlund, D.; Ogasawara, H.; et al. Lattice-strain control of the activity in dealloyed core-shell fuel cell catalysts. *Nat. Chem.* **2010**, *2*, 454−460.
(28) Hori, Y.; Takahashi, I.; Koga, O.; Hoshi, N. Selective formation of C2 compounds from electrochemical reduction of CO_2 at a series of copper single crystal electrodes. *J. Phys. Chem. B* **2002**, *106*, 15−17.
(29) Andersin, J.; Honkala, K. First principles investigations of Pd-on-Au nanostructures for trichloroethene catalytic removal from ground water. *Phys. Chem. Chem. Phys.* **2011**, *13*, 1386−1394.
(30) Wang, A.; Liu, X. Y.; Mou, C.-Y.; Zhang, T. Understanding the synergistic effects of gold bimetallic catalysts. *J. Catal.* **2013**, *308*, 258−271.
(31) Brodersen, S. H.; Grønbjerg, U.; Hvolbæk, B.; Schiøtz, J. Understanding the catalytic activity of gold nanoparticles through multi-scale simulations. *J. Catal.* **2011**, *284*, 34−41.
(32) Zhang, J.; Ellis, L. D.; Wang, B.; Dzara, M. J.; Sievers, C.; Pylypenko, S.; Nikolla, E.; Medlin, J. W. Control of interfacial acid−metal catalysis with organic monolayers. *Nat. Catal.* **2018**, *1*, 148−155.
(33) Chen, A.; Yu, X.; Zhou, Y.; Miao, S.; Li, Y.; Kuld, S.; Sehested, J.; Liu, J.; Aoki, T.; Hong, S.; et al. Structure of the catalytically active copper−ceria interfacial perimeter. *Nat. Catal.* **2019**, *2*, 334−341.
(34) Zhang, J.; Zhang, Q.; Feng, X. Support and Interface Effects in Water-Splitting Electrocatalysts. *Adv. Mater.* **2019**, *31*, 1808167.
(35) Liu, P.; Qin, R.; Fu, G.; Zheng, N. Surface Coordination Chemistry of Metal Nanomaterials. *J. Am. Chem. Soc.* **2017**, *139*, 2122−2131.
(36) Jiang, W.; Ji, W.; Au, C.-T. Surface/Interfacial Catalysis of (Metal)/Oxide System: Structure and Performance Control. *ChemCatChem* **2018**, *10*, 2125−2163.
(37) Yang, X. F.; Wang, A.; Qiao, B.; Li, J.; Liu, J.; Zhang, T. Single-atom catalysts: a new frontier in heterogeneous catalysis. *Acc. Chem. Res.* **2013**, *46*, 1740−1748.
(38) Wang, A.; Li, J.; Zhang, T. Heterogeneous single-atom catalysis. *Nat. Rev. Chem.* **2018**, *2*, 65−81.
(39) Qiao, B.; Wang, A.; Yang, X.; Allard, L. F.; Jiang, Z.; Cui, Y.; Liu, J.; Li, J.; Zhang, T. Single-atom catalysis of CO oxidation using Pt_1/FeO_x. *Nat. Chem.* **2011**, *3*, 634−641.
(40) Liu, J. Catalysis by Supported Single Metal Atoms. *ACS Catal.* **2017**, *7*, 34−59.
(41) Peng, Y.; Lu, B.; Chen, S. Carbon-Supported Single Atom Catalysts for Electrochemical Energy Conversion and Storage. *Adv. Mater.* **2018**, *30*, 1801995.
(42) Giannakakis, G.; Flytzani-Stephanopoulos, M.; Sykes, E. C. H. Single-Atom Alloys as a Reductionist Approach to the Rational Design of Heterogeneous Catalysts. *Acc. Chem. Res.* **2019**, *52*, 237−247.
(43) Liu, L.; Corma, A. Metal Catalysts for Heterogeneous Catalysis: From Single Atoms to Nanoclusters and Nanoparticles. *Chem. Rev.* **2018**, *118*, 4981−5079.
(44) Zhang, L.; Ren, Y.; Liu, W.; Wang, A.; Zhang, T. Single-atom catalyst: a rising star for green synthesis of fine chemicals. *Nat. Sci. Rev.* **2018**, *5*, 653−672.
(45) Védrine, J. Heterogeneous Catalysis on Metal Oxides. *Catalysts* **2017**, *7*, 341.
(46) Loffreda, D.; Delbecq, F.; Vigne, F.; Sautet, P. Chemo-regioselectivity in heterogeneous catalysis: competitive routes for C = O and C = C hydrogenations from a theoretical approach. *J. Am. Chem. Soc.* **2006**, *128*, 1316−1323.
(47) Delbecq, F.; Sautet, P. Competitive C = C and C = O Adsorption of α,β-Unsaturated Aldehydes on Pt and Pd Surfaces in Relation with the Selectivity of Hydrogenation Reactions - a Theoretical Approach. *J. Catal.* **1995**, *152*, 217−236.
(48) Brandt, K.; Chiu, M. E.; Watson, D. J.; Tikhov, M. S.; Lambert, R. M. Adsorption Geometry Determines Catalytic Selectivity in Highly Chemoselective Hydrogenation of Crotonaldehyde on Ag(111). *J. Phys. Chem. C* **2012**, *116*, 4605−4611.
(49) Ptushinskii, Y. G. Low-temperature adsorption of gases on metal surfaces (Review). *Low Temp. Phys.* **2004**, *30*, 1−26.
(50) Solymosi, F.; Pasztor, M. An infrared study of the influence of carbon monoxide chemisorption on the topology of supported rhodium. *J. Phys. Chem.* **1985**, *89*, 4789−4793.
(51) Chen, M. S.; Goodman, D. W. The structure of catalytically active gold on titania. *Science* **2004**, *306*, 252−255.

DOI: 10.1021/acs.chemrev.9b00230
Chem. Rev. XXXX, XXX, XXX−XXX

(52) Alonso, D. M.; Wettstein, S. G.; Dumesic, J. A. Bimetallic catalysts for upgrading of biomass to fuels and chemicals. *Chem. Soc. Rev.* **2012**, *41*, 8075−8098.
(53) Chen, M.; Kumar, D.; Yi, C. W.; Goodman, D. W. The promotional effect of gold in catalysis by palladium-gold. *Science* **2005**, *310*, 291−293.
(54) Jirkovsky, J. S.; Panas, I.; Ahlberg, E.; Halasa, M.; Romani, S.; Schiffrin, D. J. Single atom hot-spots at Au-Pd nanoalloys for electrocatalytic H_2O_2 production. *J. Am. Chem. Soc.* **2011**, *133*, 19432−19441.
(55) Slanac, D. A.; Hardin, W. G.; Johnston, K. P.; Stevenson, K. J. Atomic ensemble and electronic effects in Ag-rich AgPd nanoalloy catalysts for oxygen reduction in alkaline media. *J. Am. Chem. Soc.* **2012**, *134*, 9812−9819.
(56) Kitchin, J. R.; Norskov, J. K.; Barteau, M. A.; Chen, J. G. Role of strain and ligand effects in the modification of the electronic and chemical properties of bimetallic surfaces. *Phys. Rev. Lett.* **2004**, *93*, 156801.
(57) Boronat, M.; Concepcion, P.; Corma, A.; Gonzalez, S.; Illas, F.; Serna, P. A Molecular mechanism for the chemoselective hydrogenation of substituted nitroaromatics with nanoparticles of gold on TiO_2 catalysts: a cooperative effect between gold and the support. *J. Am. Chem. Soc.* **2007**, *129*, 16230−16237.
(58) Wang, L.; Guan, E.; Zhang, J.; Yang, J.; Zhu, Y.; Han, Y.; Yang, M.; Cen, C.; Fu, G.; Gates, B. C.; Xiao, F.-S. Single-site catalyst promoters accelerate metal-catalyzed nitroarene hydrogenation. *Nat. Commun.* **2018**, *9*, 1362.
(59) Teschner, D.; Borsodi, J.; Wootsch, A.; Revay, Z.; Havecker, M.; Knop-Gericke, A.; Jackson, S. D.; Schlogl, R. The roles of subsurface carbon and hydrogen in palladium-catalyzed alkyne hydrogenation. *Science* **2008**, *320*, 86−89.
(60) Mitsudome, T.; Mikami, Y.; Matoba, M.; Mizugaki, T.; Jitsukawa, K.; Kaneda, K. Design of a silver-cerium dioxide core-shell nanocomposite catalyst for chemoselective reduction reactions. *Angew. Chem., Int. Ed.* **2012**, *51*, 136−139.
(61) Harris, J.; Andersson, S. H_2 dissociation at metal surfaces. *Phys. Rev. Lett.* **1985**, *55*, 1583−1586.
(62) Klacar, S.; Grönbeck, H. H_2 dissociation over Ag/Al_2O_3: the first step in hydrogen assisted selective catalytic reduction of NO_x. *Catal. Sci. Technol.* **2013**, *3*, 183−190.
(63) German, E. D.; Abir, H.; Sheintuch, M. A Tunnel Model for Activated Hydrogen Dissociation on Metal Surfaces. *J. Phys. Chem. C* **2013**, *117*, 7475−7486.
(64) Frey, G. D.; Lavallo, V.; Donnadieu, B.; Schoeller, W. W.; Bertrand, G. Facile splitting of hydrogen and ammonia by nucleophilic activation at a single carbon center. *Science* **2007**, *316*, 439−441.
(65) Lu, J.; Aydin, C.; Browning, N. D.; Gates, B. C. Hydrogen activation and metal hydride formation trigger cluster formation from supported iridium complexes. *J. Am. Chem. Soc.* **2012**, *134*, 5022−5025.
(66) Liu, P.; Zhao, Y.; Qin, R.; Mo, S.; Chen, G.; Gu, L.; Chevrier, D. M.; Zhang, P.; Guo, Q.; Zang, D.; et al. Photochemical route for synthesizing atomically dispersed palladium catalysts. *Science* **2016**, *352*, 797−801.
(67) Doyle, A. M.; Shaikhutdinov, S. K.; Jackson, S. D.; Freund, H. J. Hydrogenation on metal surfaces: why are nanoparticles more active than single crystals? *Angew. Chem., Int. Ed.* **2003**, *42*, 5240−5243.
(68) Aleksandrov, H. A.; Kozlov, S. M.; Schauermann, S.; Vayssilov, G. N.; Neyman, K. M. How absorbed hydrogen affects the catalytic activity of transition metals. *Angew. Chem., Int. Ed.* **2014**, *53*, 13371−13375.
(69) Prins, R. Hydrogen spillover. Facts and fiction. *Chem. Rev.* **2012**, *112*, 2714−2738.
(70) Merte, L. R.; Peng, G.; Bechstein, R.; Rieboldt, F.; Farberow, C. A.; Grabow, L. C.; Kudernatsch, W.; Wendt, S.; Laegsgaard, E.; Mavrikakis, M.; et al. Water-mediated proton hopping on an iron oxide surface. *Science* **2012**, *336*, 889−893.
(71) Eisenstein, O.; Crabtree, R. H. Outer sphere hydrogenation catalysis. *New J. Chem.* **2013**, *37*, 21−27.
(72) Stephan, D. W. Frustrated Lewis pairs: from concept to catalysis. *Acc. Chem. Res.* **2015**, *48*, 306−316.
(73) Stephan, D. W. Frustrated Lewis Pairs. *J. Am. Chem. Soc.* **2015**, *137*, 10018−10032.
(74) Stephan, D. W.; Erker, G. Frustrated Lewis pair chemistry: development and perspectives. *Angew. Chem., Int. Ed.* **2015**, *54*, 6400−6441.
(75) Stephan, D. W.; Erker, G. Frustrated Lewis pairs: metal-free hydrogen activation and more. *Angew. Chem., Int. Ed.* **2010**, *49*, 46−76.
(76) Riley, C.; Zhou, S.; Kunwar, D.; De La Riva, A.; Peterson, E.; Payne, R.; Gao, L.; Lin, S.; Guo, H.; Datye, A. Design of Effective Catalysts for Selective Alkyne Hydrogenation by Doping of Ceria with a Single-Atom Promotor. *J. Am. Chem. Soc.* **2018**, *140*, 12964−12973.
(77) Juárez, R.; Parker, S. F.; Concepción, P.; Corma, A.; García, H. Heterolytic and heterotopic dissociation of hydrogen on ceria-supported gold nanoparticles. Combined inelastic neutron scattering and FT-IR spectroscopic study on the nature and reactivity of surface hydrogen species. *Chem. Sci.* **2010**, *1*, 731−738.
(78) Whittaker, T.; Kumar, K. B. S.; Peterson, C.; Pollock, M. N.; Grabow, L. C.; Chandler, B. D. H_2 Oxidation over Supported Au Nanoparticle Catalysts: Evidence for Heterolytic H_2 Activation at the Metal-Support Interface. *J. Am. Chem. Soc.* **2018**, *140*, 16469−16487.
(79) Vile, G.; Albani, D.; Nachtegaal, M.; Chen, Z.; Dontsova, D.; Antonietti, M.; Lopez, N.; Perez-Ramirez, J. A stable single-site palladium catalyst for hydrogenations. *Angew. Chem., Int. Ed.* **2015**, *54*, 11265−11269.
(80) Liu, W.; Chen, Y.; Qi, H.; Zhang, L.; Yan, W.; Liu, X.; Yang, X.; Miao, S.; Wang, W.; Liu, C.; et al. A Durable Nickel Single-Atom Catalyst for Hydrogenation Reactions and Cellulose Valorization under Harsh Conditions. *Angew. Chem., Int. Ed.* **2018**, *57*, 7071−7075.
(81) Lu, G.; Zhang, P.; Sun, D.; Wang, L.; Zhou, K.; Wang, Z.-X.; Guo, G.-C. Gold catalyzed hydrogenations of small imines and nitriles: enhanced reactivity of Au surface toward H_2 via collaboration with a Lewis base. *Chem. Sci.* **2014**, *5*, 1082−1090.
(82) Liu, C.; Abroshan, H.; Yan, C. Y.; Li, G.; Haruta, M. One-Pot Synthesis of $Au_{11}(PPh_2Py)_7Br_3$ for the Highly Chemoselective Hydrogenation of Nitrobenzaldehyde. *ACS Catal.* **2016**, *6*, 92−99.
(83) Almora-Barrios, N.; Cano, I.; van Leeuwen, P. W. N. M.; Lopez, N. Concerted Chemoselective Hydrogenation of Acrolein on Secondary Phosphine Oxide Decorated Gold Nanoparticles. *ACS Catal.* **2017**, *7*, 3949−3954.
(84) Formenti, D.; Topf, C.; Junge, K.; Ragaini, F.; Beller, M. Fe_2O_3/NGr@C- and Co−Co_3O_4/NGr@C-catalysed hydrogenation of nitroarenes under mild conditions. *Catal. Sci. Technol.* **2016**, *6*, 4473−4477.
(85) Formenti, D.; Ferretti, F.; Topf, C.; Surkus, A.-E.; Pohl, M.-M.; Radnik, J.; Schneider, M.; Junge, K.; Beller, M.; Ragaini, F. Co-based heterogeneous catalysts from well-defined α-diimine complexes: Discussing the role of nitrogen. *J. Catal.* **2017**, *351*, 79−89.
(86) Wang, J.; Zhao, X.; Lei, N.; Li, L.; Zhang, L.; Xu, S.; Miao, S.; Pan, X.; Wang, A.; Zhang, T. Hydrogenolysis of Glycerol to 1,3-propanediol under Low Hydrogen Pressure over WO_x-Supported Single/Pseudo-Single Atom Pt Catalyst. *ChemSusChem* **2016**, *9*, 784−790.
(87) Zhao, X.; Wang, J.; Yang, M.; Lei, N.; Li, L.; Hou, B.; Miao, S.; Pan, X.; Wang, A.; Zhang, T. Selective Hydrogenolysis of Glycerol to 1,3-Propanediol: Manipulating the Frustrated Lewis Pairs by Introducing Gold to Pt/WO_x. *ChemSusChem* **2017**, *10*, 819−824.
(88) Torres Galvis, H. M.; de Jong, K. P. Catalysts for Production of Lower Olefins from Synthesis Gas: A Review. *ACS Catal.* **2013**, *3*, 2130−2149.
(89) Bridier, B.; Perez-Ramirez, J. Cooperative effects in ternary Cu-Ni-Fe catalysts lead to enhanced alkene selectivity in alkyne hydrogenation. *J. Am. Chem. Soc.* **2010**, *132*, 4321−4327.

AQ

(90) Horiuti, I.; Polanyi, M. Exchange reactions of hydrogen on metallic catalysts. *Trans. Faraday Soc.* **1934**, *30*, 1164−1172.
(91) Benavidez, A. D.; Burton, P. D.; Nogales, J. L.; Jenkins, A. R.; Ivanov, S. A.; Miller, J. T.; Karim, A. M.; Datye, A. K. Improved selectivity of carbon-supported palladium catalysts for the hydrogenation of acetylene in excess ethylene. *Appl. Catal., A* **2014**, *482*, 108−115.
(92) Bridier, B.; Lopez, N.; Perez-Ramirez, J. Molecular understanding of alkyne hydrogenation for the design of selective catalysts. *Dalton Trans* **2010**, *39*, 8412−8419.
(93) McCue, A. J.; Guerrero-Ruiz, A.; Ramirez-Barria, C.; Rodríguez-Ramos, I.; Anderson, J. A. Selective hydrogenation of mixed alkyne/alkene streams at elevated pressure over a palladium sulfide catalyst. *J. Catal.* **2017**, *355*, 40−52.
(94) Osswald, J.; Giedigkeit, R.; Jentoft, R.; Armbruster, M.; Girgsdies, F.; Kovnir, K.; Ressler, T.; Grin, Y.; Schlogl, R. Palladium−gallium intermetallic compounds for the selective hydrogenation of acetylenePart I: Preparation and structural investigation under reaction conditions. *J. Catal.* **2008**, *258*, 210−218.
(95) Zhou, H.; Yang, X.; Li, L.; Liu, X.; Huang, Y.; Pan, X.; Wang, A.; Li, J.; Zhang, T. PdZn Intermetallic Nanostructure with Pd−Zn−Pd Ensembles for Highly Active and Chemoselective Semi-Hydrogenation of Acetylene. *ACS Catal.* **2016**, *6*, 1054−1061.
(96) Pei, G. X.; Liu, X. Y.; Wang, A.; Lee, A. F.; Isaacs, M. A.; Li, L.; Pan, X.; Yang, X.; Wang, X.; Tai, Z.; et al. Ag Alloyed Pd Single-Atom Catalysts for Efficient Selective Hydrogenation of Acetylene to Ethylene in Excess Ethylene. *ACS Catal.* **2015**, *5*, 3717−3725.
(97) Pei, G. X.; Liu, X. Y.; Wang, A.; Li, L.; Huang, Y.; Zhang, T.; Lee, J. W.; Jang, B. W. L.; Mou, C.-Y. Promotional effect of Pd single atoms on Au nanoparticles supported on silica for the selective hydrogenation of acetylene in excess ethylene. *New J. Chem.* **2014**, *38*, 2043−2051.
(98) Pei, G. X.; Liu, X. Y.; Yang, X.; Zhang, L.; Wang, A.; Li, L.; Wang, H.; Wang, X.; Zhang, T. Performance of Cu-Alloyed Pd Single-Atom Catalyst for Semihydrogenation of Acetylene under Simulated Front-End Conditions. *ACS Catal.* **2017**, *7*, 1491−1500.
(99) Molinier, M.; Ou, J. D.-Y.; Risch, M. A. Catalysts for selective hydrogenation of alkynes and alkadienes. U.S. Patent 2004176651. 2004.
(100) Studt, F.; Abild-Pedersen, F.; Bligaard, T.; Sorensen, R. Z.; Christensen, C. H.; Norskov, J. K. Identification of non-precious metal alloy catalysts for selective hydrogenation of acetylene. *Science* **2008**, *320*, 1320−1322.
(101) Luo, Y.; Alarcón Villaseca, S.; Friedrich, M.; Teschner, D.; Knop-Gericke, A.; Armbrüster, M. Addressing electronic effects in the semi-hydrogenation of ethyne by $InPd_2$ and intermetallic Ga−Pd compounds. *J. Catal.* **2016**, *338*, 265−272.
(102) Yan, H.; Cheng, H.; Yi, H.; Lin, Y.; Yao, T.; Wang, C.; Li, J.; Wei, S.; Lu, J. Single-Atom Pd_1/Graphene Catalyst Achieved by Atomic Layer Deposition: Remarkable Performance in Selective Hydrogenation of 1,3-Butadiene. *J. Am. Chem. Soc.* **2015**, *137*, 10484−10487.
(103) Huang, F.; Deng, Y.; Chen, Y.; Cai, X.; Peng, M.; Jia, Z.; Ren, P.; Xiao, D.; Wen, X.; Wang, N.; et al. Atomically Dispersed Pd on Nanodiamond/Graphene Hybrid for Selective Hydrogenation of Acetylene. *J. Am. Chem. Soc.* **2018**, *140*, 13142−13146.
(104) Vignola, E.; Steinmann, S. N.; Al Farra, A.; Vandegehuchte, B. D.; Curulla, D.; Sautet, P. Evaluating the Risk of C−C Bond Formation during Selective Hydrogenation of Acetylene on Palladium. *ACS Catal.* **2018**, *8*, 1662−1671.
(105) Teschner, D.; Revay, Z.; Borsodi, J.; Havecker, M.; Knop-Gericke, A.; Schlogl, R.; Milroy, D.; Jackson, S. D.; Torres, D.; Sautet, P. Understanding palladium hydrogenation catalysts: when the nature of the reactive molecule controls the nature of the catalyst active phase. *Angew. Chem., Int. Ed.* **2008**, *47*, 9274−9278.
(106) Armbrüster, M.; Behrens, M.; Cinquini, F.; Föttinger, K.; Grin, Y.; Haghofer, A.; Klötzer, B.; Knop-Gericke, A.; Lorenz, H.; Ota, A.; et al. How to Control the Selectivity of Palladium-based Catalysts in Hydrogenation Reactions: The Role of Subsurface Chemistry. *ChemCatChem* **2012**, *4*, 1048−1063.
(107) Tew, M. W.; Janousch, M.; Huthwelker, T.; van Bokhoven, J. A. The roles of carbide and hydride in oxide-supported palladium nanoparticles for alkyne hydrogenation. *J. Catal.* **2011**, *283*, 45−54.
(108) Shao, L.; Zhang, B.; Zhang, W.; Teschner, D.; Girgsdies, F.; Schlogl, R.; Su, D. S. Improved selectivity by stabilizing and exposing active phases on supported Pd nanoparticles in acetylene-selective hydrogenation. *Chem. - Eur. J.* **2012**, *18*, 14962−14966.
(109) Tew, M. W.; Miller, J. T.; van Bokhoven, J. A. Particle Size Effect of Hydride Formation and Surface Hydrogen Adsorption of Nanosized Palladium Catalysts: L_3 Edge vs K Edge X-ray Absorption Spectroscopy. *J. Phys. Chem. C* **2009**, *113*, 15140−15147.
(110) Yardimci, D.; Serna, P.; Gates, B. C. A Highly Selective Catalyst for Partial Hydrogenation of 1,3-Butadiene: MgO-Supported Rhodium Clusters Selectively Poisoned with CO. *ChemCatChem* **2012**, *4*, 1547−1550.
(111) Yardimci, D.; Serna, P.; Gates, B. C. Tuning Catalytic Selectivity: Zeolite- and Magnesium Oxide-Supported Molecular Rhodium Catalysts for Hydrogenation of 1,3-Butadiene. *ACS Catal.* **2012**, *2*, 2100−2113.
(112) Bachiller-Baeza, B.; Iglesias-Juez, A.; Castillejos-López, E.; Guerrero-Ruiz, A.; Michiel, M. D.; Fernández-García, M.; Rodríguez-Ramos, I. Detecting the Genesis of a High-Performance Carbon-Supported Pd Sulfide Nanophase and Its Evolution in the Hydrogenation of Butadiene. *ACS Catal.* **2015**, *5*, 5235−5241.
(113) McCue, A. J.; Guerrero-Ruiz, A.; Rodríguez-Ramos, I.; Anderson, J. A. Palladium sulphide − A highly selective catalyst for the gas phase hydrogenation of alkynes to alkenes. *J. Catal.* **2016**, *340*, 10−16.
(114) Gao, J.; Zhu, Q.; Wen, L.; Chen, J. TiO_2-modified nano-egg-shell Pd catalyst for selective hydrogenation of acetylene. *Particuology* **2010**, *8*, 251−256.
(115) Kim, E.; Shin, E. W.; Bark, C. W.; Chang, I.; Yoon, W. J.; Kim, W.-J. Pd catalyst promoted by two metal oxides with different reducibilities: Properties and performance in the selective hydrogenation of acetylene. *Appl. Catal., A* **2014**, *471*, 80−83.
(116) Zhang, L.; Ding, Y.; Wu, K. H.; Niu, Y.; Luo, J.; Yang, X.; Zhang, B.; Su, D. Pd@C core-shell nanoparticles on carbon nanotubes as highly stable and selective catalysts for hydrogenation of acetylene to ethylene. *Nanoscale* **2017**, *9*, 14317−14321.
(117) Lucci, F. R.; Liu, J.; Marcinkowski, M. D.; Yang, M.; Allard, L. F.; Flytzani-Stephanopoulos, M.; Sykes, E. C. Selective hydrogenation of 1,3-butadiene on platinum-copper alloys at the single-atom limit. *Nat. Commun.* **2015**, *6*, 8550.
(118) Kim, S. K.; Lee, J. H.; Ahn, I. Y.; Kim, W.-J.; Moon, S. H. Performance of Cu-promoted Pd catalysts prepared by adding Cu using a surface redox method in acetylene hydrogenation. *Appl. Catal., A* **2011**, *401*, 12−19.
(119) Lee, J. H.; Kim, S. K.; Ahn, I. Y.; Kim, W.-J.; Moon, S. H. Performance of Pd−Ag/Al_2O_3 catalysts prepared by the selective deposition of Ag onto Pd in acetylene hydrogenation. *Catal. Commun.* **2011**, *12*, 1251−1254.
(120) Han, Y.; Peng, D.; Xu, Z.; Wan, H.; Zheng, S.; Zhu, D. TiO_2 supported Pd@Ag as highly selective catalysts for hydrogenation of acetylene in excess ethylene. *Chem. Commun.* **2013**, *49*, 8350−8352.
(121) Armbruster, M.; Kovnir, K.; Behrens, M.; Teschner, D.; Grin, Y.; Schlogl, R. Pd-Ga intermetallic compounds as highly selective semihydrogenation catalysts. *J. Am. Chem. Soc.* **2010**, *132*, 14745−14747.
(122) Armbruster, M.; Wowsnick, G.; Friedrich, M.; Heggen, M.; Cardoso-Gil, R. Synthesis and catalytic properties of nanoparticulate intermetallic Ga-Pd compounds. *J. Am. Chem. Soc.* **2011**, *133*, 9112−9118.
(123) Ota, A.; Armbruster, M.; Behrens, M.; Rosenthal, D.; Friedrich, M.; Kasatkin, I.; Girgsdies, F.; Zhang, W.; Wagner, R.; Schlogl, R. Intermetallic Compound Pd_2Ga as a Selective Catalyst for the Semi-Hydrogenation of Acetylene: From Model to High Performance Systems. *J. Phys. Chem. C* **2011**, *115*, 1368−1374.

DOI: 10.1021/acs.chemrev.9b00230
Chem. Rev. XXXX, XXX, XXX−XXX

(124) Shao, L.; Zhang, W.; Armbruster, M.; Teschner, D.; Girgsdies, F.; Zhang, B.; Timpe, O.; Friedrich, M.; Schlogl, R.; Su, D. S. Nanosizing intermetallic compounds onto carbon nanotubes: active and selective hydrogenation catalysts. *Angew. Chem., Int. Ed.* **2011**, *50*, 10231−10235.
(125) Hu, M.; Zhao, S.; Liu, S.; Chen, C.; Chen, W.; Zhu, W.; Liang, C.; Cheong, W. C.; Wang, Y.; Yu, Y.; et al. MOF-Confined Sub-2 nm Atomically Ordered Intermetallic PdZn Nanoparticles as High-Performance Catalysts for Selective Hydrogenation of Acetylene. *Adv. Mater.* **2018**, *30*, 1801878.
(126) Feng, Q.; Zhao, S.; Wang, Y.; Dong, J.; Chen, W.; He, D.; Wang, D.; Yang, J.; Zhu, Y.; Zhu, H.; et al. Isolated Single-Atom Pd Sites in Intermetallic Nanostructures: High Catalytic Selectivity for Semihydrogenation of Alkynes. *J. Am. Chem. Soc.* **2017**, *139*, 7294−7301.
(127) Hugon, A.; Delannoy, L.; Louis, C. Supported gold catalysts for selective hydrogenation of 1,3-butadiene in the presence of an excess of alkenes. *Gold Bull.* **2008**, *41*, 127−138.
(128) Hugon, A.; Delannoy, L.; Krafft, J.-M.; Louis, C. Selective Hydrogenation of 1,3-Butadiene in the Presence of an Excess of Alkenes over Supported Bimetallic Gold−Palladium Catalysts. *J. Phys. Chem. C* **2010**, *114*, 10823−10835.
(129) Liu, X.; Mou, C.-Y.; Lee, S.; Li, Y.; Secrest, J.; Jang, B. W. L. Room temperature O_2 plasma treatment of SiO_2 supported Au catalysts for selective hydrogenation of acetylene in the presence of large excess of ethylene. *J. Catal.* **2012**, *285*, 152−159.
(130) Liu, X.; Li, Y.; Lee, J. W.; Hong, C.-Y.; Mou, C.-Y.; Jang, B. W. L. Selective hydrogenation of acetylene in excess ethylene over SiO_2 supported Au−Ag bimetallic catalyst. *Appl. Catal., A* **2012**, *439*−*440*, 8−14.
(131) Zhang, X.; Guo, Y. C.; Zhang, Z. C.; Gao, J. S.; Xu, C. M. High performance of carbon nanotubes confining gold nanoparticles for selective hydrogenation of 1,3-butadiene and cinnamaldehyde. *J. Catal.* **2012**, *292*, 213−226.
(132) Zhou, H.; Yang, X.; Wang, A.; Miao, S.; Liu, X.; Pan, X.; Su, Y.; Li, L.; Tan, Y.; Zhang, T. Pd/ZnO catalysts with different origins for high chemoselectivity in acetylene semi-hydrogenation. *Chin. J. Catal.* **2016**, *37*, 692−699.
(133) Hu, M.; Zhang, J.; Zhu, W.; Chen, Z.; Gao, X.; Du, X.; Wan, J.; Zhou, K.; Chen, C.; Li, Y. 50 ppm of Pd dispersed on $Ni(OH)_2$ nanosheets catalyzing semi-hydrogenation of acetylene with high activity and selectivity. *Nano Res.* **2018**, *11*, 905−912.
(134) Bridier, B.; López, N.; Pérez-Ramírez, J. Partial hydrogenation of propyne over copper-based catalysts and comparison with nickel-based analogues. *J. Catal.* **2010**, *269*, 80−92.
(135) Pei, G. X.; Liu, X. Y.; Wang, A.; Su, Y.; Li, L.; Zhang, T. Selective hydrogenation of acetylene in an ethylene-rich stream over silica supported Ag-Ni bimetallic catalysts. *Appl. Catal., A* **2017**, *545*, 90−96.
(136) Armbruster, M.; Kovnir, K.; Friedrich, M.; Teschner, D.; Wowsnick, G.; Hahne, M.; Gille, P.; Szentmiklosi, L.; Feuerbacher, M.; Heggen, M.; et al. $Al_{13}Fe_4$ as a low-cost alternative for palladium in heterogeneous hydrogenation. *Nat. Mater.* **2012**, *11*, 690−693.
(137) Chen, Y.; Chen, J. Selective hydrogenation of acetylene on SiO_2 supported Ni-In bimetallic catalysts: Promotional effect of In. *Appl. Surf. Sci.* **2016**, *387*, 16−27.
(138) Vile, G.; Bridier, B.; Wichert, J.; Perez-Ramirez, J. Ceria in hydrogenation catalysis: high selectivity in the conversion of alkynes to olefins. *Angew. Chem., Int. Ed.* **2012**, *51*, 8620−8623.
(139) Albani, D.; Capdevila-Cortada, M.; Vile, G.; Mitchell, S.; Martin, O.; Lopez, N.; Perez-Ramirez, J. Semihydrogenation of Acetylene on Indium Oxide: Proposed Single-Ensemble Catalysis. *Angew. Chem., Int. Ed.* **2017**, *56*, 10755−10760.
(140) Wang, Y.; Yang, J.; Gu, R.; Peng, L.; Guo, X.; Xue, N.; Zhu, Y.; Ding, W. Crystal-Facet Effect of γ-Al_2O_3 on Supporting CrO_x for Catalytic Semihydrogenation of Acetylene. *ACS Catal.* **2018**, *8*, 6419−6425.
(141) García-Mota, M.; Bridier, B.; Pérez-Ramírez, J.; López, N. Interplay between carbon monoxide, hydrides, and carbides in selective alkyne hydrogenation on palladium. *J. Catal.* **2010**, *273*, 92−102.
(142) McKenna, F.-M.; Anderson, J. A. Selectivity enhancement in acetylene hydrogenation over diphenyl sulphide-modified Pd/TiO_2 catalysts. *J. Catal.* **2011**, *281*, 231−240.
(143) Cooper, A.; Bachiller-Baeza, B.; Anderson, J. A.; Rodríguez-Ramos, I.; Guerrero-Ruiz, A. Design of surface sites for the selective hydrogenation of 1,3-butadiene on Pd nanoparticles: Cu bimetallic formation and sulfur poisoning. *Catal. Sci. Technol.* **2014**, *4*, 1446−1455.
(144) Osswald, J.; Kovnir, K.; Armbruster, M.; Giedigkeit, R.; Jentoft, R.; Wild, U.; Grin, Y.; Schlogl, R. Palladium−gallium intermetallic compounds for the selective hydrogenation of acetylenePart II: Surface characterization and catalytic performance. *J. Catal.* **2008**, *258*, 219−227.
(145) Kovnir, K.; Osswald, J.; Armbrüster, M.; Teschner, D.; Weinberg, G.; Wild, U.; Knop-Gericke, A.; Ressler, T.; Grin, Y.; Schlögl, R. Etching of the intermetallic compounds PdGa and Pd_3Ga_7: An effective way to increase catalytic activity? *J. Catal.* **2009**, *264*, 93−103.
(146) Prinz, J.; Pignedoli, C. A.; Stockl, Q. S.; Armbruster, M.; Brune, H.; Groning, O.; Widmer, R.; Passerone, D. Adsorption of small hydrocarbons on the three-fold PdGa surfaces: the road to selective hydrogenation. *J. Am. Chem. Soc.* **2014**, *136*, 11792−11798.
(147) Castillejos-López, E.; Agostini, G.; Di Michel, M.; Iglesias-Juez, A.; Bachiller-Baeza, B. Synergy of Contact between ZnO Surface Planes and PdZn Nanostructures: Morphology and Chemical Property Effects in the Intermetallic Sites for Selective 1,3-Butadiene Hydrogenation. *ACS Catal.* **2017**, *7*, 796−811.
(148) Huang, X.; Xia, Y.; Cao, Y.; Zheng, X.; Pan, H.; Zhu, J.; Ma, C.; Wang, H.; Li, J.; You, R.; et al. Enhancing both selectivity and coking-resistance of a single-atom Pd_1/C_3N_4 catalyst for acetylene hydrogenation. *Nano Res.* **2017**, *10*, 1302−1312.
(149) Feng, Y.; Zhou, L.; Wan, Q.; Lin, S.; Guo, H. Selective hydrogenation of 1,3-butadiene catalyzed by a single Pd atom anchored on graphene: the importance of dynamics. *Chem. Sci.* **2018**, *9*, 5890−5896.
(150) Segura, Y.; Lopez, N.; Perezramirez, J. Origin of the superior hydrogenation selectivity of gold nanoparticles in alkyne + alkene mixtures: Triple- versus double-bond activation. *J. Catal.* **2007**, *247*, 383−386.
(151) Boronat, M.; Corma, A. Origin of the different activity and selectivity toward hydrogenation of single metal Au and Pt on TiO_2 and bimetallic $Au-Pt/TiO_2$ catalysts. *Langmuir* **2010**, *26*, 16607−16614.
(152) Serna, P.; Boronat, M.; Corma, A. Tuning the Behavior of Au and Pt Catalysts for the Chemoselective Hydrogenation of Nitro-aromatic Compounds. *Top. Catal.* **2011**, *54*, 439−446.
(153) Kyriakou, G.; Boucher, M. B.; Jewell, A. D.; Lewis, E. A.; Lawton, T. J.; Baber, A. E.; Tierney, H. L.; Flytzani-Stephanopoulos, M.; Sykes, E. C. Isolated metal atom geometries as a strategy for selective heterogeneous hydrogenations. *Science* **2012**, *335*, 1209−1212.
(154) Zhang, X.; Shi, H.; Xu, B. Q. Catalysis by gold: isolated surface Au^{3+} ions are active sites for selective hydrogenation of 1,3-butadiene over Au/ZrO_2 catalysts. *Angew. Chem., Int. Ed.* **2005**, *44*, 7132−7135.
(155) Liu, Z. P.; Wang, C. M.; Fan, K. N. Single gold atoms in heterogeneous catalysis: selective 1,3-butadiene hydrogenation over Au/ZrO_2. *Angew. Chem., Int. Ed.* **2006**, *45*, 6865−6868.
(156) Zhang, X.; Shi, H.; Xu, B.-Q. Comparative study of Au/ZrO_2 catalysts in CO oxidation and 1,3-butadiene hydrogenation. *Catal. Today* **2007**, *122*, 330−337.
(157) Zhang, X.; Llabrés i Xamena, F. X.; Corma, A. Gold(III) − metal organic framework bridges the gap between homogeneous and heterogeneous gold catalysts. *J. Catal.* **2009**, *265*, 155−160.
(158) Comas-Vives, A.; Gonzalez-Arellano, C.; Corma, A.; Iglesias, M.; Sanchez, F.; Ujaque, G. Single-site homogeneous and

DOI: 10.1021/acs.chemrev.9b00230
Chem. Rev. XXXX, XXX, XXX−XXX

heterogeneized gold(III) hydrogenation catalysts: mechanistic implications. *J. Am. Chem. Soc.* **2006**, *128*, 4756−4765.
(159) Arcadi, A.; Di Giuseppe, S. Recent applications of gold catalysis in organic synthesis. *Curr. Org. Chem.* **2004**, *8*, 795−812.
(160) Gonzalez-Arellano, C.; Corma, A.; Iglesias, M.; Sanchez, F. Enantioselective hydrogenation of alkenes and imines by a gold catalyst. *Chem. Commun.* **2005**, *27*, 3451−3453.
(161) Rostrupnielsen, J. Coking on nickel catalysts for steam reforming of hydrocarbons. *J. Catal.* **1974**, *33*, 184−201.
(162) Studt, F.; Abild-Pedersen, F.; Bligaard, T.; Sorensen, R. Z.; Christensen, C. H.; Norskov, J. K. On the role of surface modifications of palladium catalysts in the selective hydrogenation of acetylene. *Angew. Chem., Int. Ed.* **2008**, *47*, 9299−9302.
(163) Mitsudome, T.; Kaneda, K. Gold nanoparticle catalysts for selective hydrogenations. *Green Chem.* **2013**, *15*, 2636−2654.
(164) Kahsar, K. R.; Schwartz, D. K.; Medlin, J. W. Selective Hydrogenation of Polyunsaturated Fatty Acids Using Alkanethiol Self-Assembled Monolayer-Coated Pd/Al_2O_3 Catalysts. *ACS Catal.* **2013**, *3*, 2041−2044.
(165) Mitsudome, T.; Takahashi, Y.; Ichikawa, S.; Mizugaki, T.; Jitsukawa, K.; Kaneda, K. Metal-ligand core-shell nanocomposite catalysts for the selective semihydrogenation of alkynes. *Angew. Chem., Int. Ed.* **2013**, *52*, 1481−1485.
(166) Albani, D.; Shahrokhi, M.; Chen, Z.; Mitchell, S.; Hauert, R.; Lopez, N.; Perez-Ramirez, J. Selective ensembles in supported palladium sulfide nanoparticles for alkyne semi-hydrogenation. *Nat. Commun.* **2018**, *9*, 2634.
(167) Chan, C. W.; Mahadi, A. H.; Li, M. M.; Corbos, E. C.; Tang, C.; Jones, G.; Kuo, W. C.; Cookson, J.; Brown, C. M.; Bishop, P. T.; et al. Interstitial modification of palladium nanoparticles with boron atoms as a green catalyst for selective hydrogenation. *Nat. Commun.* **2014**, *5*, 5787.
(168) Lee, K. H.; Lee, B.; Lee, K. R.; Yi, M. H.; Hur, N. H. Dual Pd and $CuFe_2O_4$ nanoparticles encapsulated in a core/shell silica microsphere for selective hydrogenation of arylacetylenes. *Chem. Commun.* **2012**, *48*, 4414−4416.
(169) Yang, S.; Cao, C.; Peng, L.; Zhang, J.; Han, B.; Song, W. A Pd-Cu_2O nanocomposite as an effective synergistic catalyst for selective semi-hydrogenation of the terminal alkynes only. *Chem. Commun.* **2016**, *52*, 3627−3630.
(170) Mitsudome, T.; Urayama, T.; Yamazaki, K.; Maehara, Y.; Yamasaki, J.; Gohara, K.; Maeno, Z.; Mizugaki, T.; Jitsukawa, K.; Kaneda, K. Design of Core-Pd/Shell-Ag Nanocomposite Catalyst for Selective Semihydrogenation of Alkynes. *ACS Catal.* **2016**, *6*, 666−670.
(171) Song, S.; Li, K.; Pan, J.; Wang, F.; Li, J.; Feng, J.; Yao, S.; Ge, X.; Wang, X.; Zhang, H. Achieving the Trade-Off between Selectivity and Activity in Semihydrogenation of Alkynes by Fabrication of (Asymmetrical Pd@Ag Core)@(CeO_2 Shell) Nanocatalysts via Autoredox Reaction. *Adv. Mater.* **2017**, *29*, 1605332.
(172) Tew, M. W.; Emerich, H.; van Bokhoven, J. A. Formation and Characterization of PdZn Alloy: A Very Selective Catalyst for Alkyne Semihydrogenation. *J. Phys. Chem. C* **2011**, *115*, 8457−8465.
(173) Shen, Y.; Yin, K.; An, C.; Xiao, Z. Design of a difunctional Zn-Ti LDHs supported PdAu catalyst for selective hydrogenation of phenylacetylene. *Appl. Surf. Sci.* **2018**, *456*, 1−6.
(174) Liu, J.; Shan, J.; Lucci, F. R.; Cao, S.; Sykes, E. C. H.; Flytzani-Stephanopoulos, M. Palladium−gold single atom alloy catalysts for liquid phase selective hydrogenation of 1-hexyne. *Catal. Sci. Technol.* **2017**, *7*, 4276−4284.
(175) Boucher, M. B.; Zugic, B.; Cladaras, G.; Kammert, J.; Marcinkowski, M. D.; Lawton, T. J.; Sykes, E. C.; Flytzani-Stephanopoulos, M. Single atom alloy surface analogs in $Pd_{0.18}Cu_{15}$ nanoparticles for selective hydrogenation reactions. *Phys. Chem. Chem. Phys.* **2013**, *15*, 12187−12196.
(176) Chen, Z.; Pronkin, S.; Fellinger, T. P.; Kailasam, K.; Vile, G.; Albani, D.; Krumeich, F.; Leary, R.; Barnard, J.; Thomas, J. M.; et al. Merging Single-Atom-Dispersed Silver and Carbon Nitride to a Joint Electronic System via Copolymerization with Silver Tricyanomethanide. *ACS Nano* **2016**, *10*, 3166−3175.
(177) Vile, G.; Perez-Ramirez, J. Beyond the use of modifiers in selective alkyne hydrogenation: silver and gold nanocatalysts in flow mode for sustainable alkene production. *Nanoscale* **2014**, *6*, 13476−13482.
(178) Mitsudome, T.; Yamamoto, M.; Maeno, Z.; Mizugaki, T.; Jitsukawa, K.; Kaneda, K. One-step Synthesis of Core-Gold/Shell-Ceria Nanomaterial and Its Catalysis for Highly Selective Semihydrogenation of Alkynes. *J. Am. Chem. Soc.* **2015**, *137*, 13452−13455.
(179) Urayama, T.; Mitsudome, T.; Maeno, Z.; Mizugaki, T.; Jitsukawa, K.; Kaneda, K. Green, Multi-Gram One-Step Synthesis of Core-Shell Nanocomposites in Water and Their Catalytic Application to Chemoselective Hydrogenations. *Chem. - Eur. J.* **2016**, *22*, 17962−17966.
(180) Ji, G.; Duan, Y.; Zhang, S.; Fei, B.; Chen, X.; Yang, Y. Selective Semihydrogenation of Alkynes Catalyzed by Pd Nanoparticles Immobilized on Heteroatom-Doped Hierarchical Porous Carbon Derived from Bamboo Shoots. *ChemSusChem* **2017**, *10*, 3427−3434.
(181) Deng, D.; Yang, Y.; Gong, Y.; Li, Y.; Xu, X.; Wang, Y. Palladium nanoparticles supported on mpg-C_3N_4 as active catalyst for semihydrogenation of phenylacetylene under mild conditions. *Green Chem.* **2013**, *15*, 2525−2531.
(182) Wu, Z.; Bukowski, B. C.; Li, Z.; Milligan, C.; Zhou, L.; Ma, T.; Wu, Y.; Ren, Y.; Ribeiro, F. H.; Delgass, W. N.; et al. Changes in Catalytic and Adsorptive Properties of 2 nm Pt_3Mn Nanoparticles by Subsurface Atoms. *J. Am. Chem. Soc.* **2018**, *140*, 14870−14877.
(183) Gallezot, P.; Richard, D. Selective hydrogenation of α,β-unsaturated aldehydes. *Catal. Rev.: Sci. Eng.* **1998**, *40*, 81−126.
(184) Yuan, Y.; Yao, S. Y.; Wang, M. N.; Lou, S. J.; Yan, N. Recent Progress in Chemoselective Hydrogenation of α,β-Unsaturated Aldehyde to Unsaturated Alcohol Over Nanomaterials. *Curr. Org. Chem.* **2013**, *17*, 400−413.
(185) Ide, M. S.; Hao, B.; Neurock, M.; Davis, R. J. Mechanistic Insights on the Hydrogenation of α,β-Unsaturated Ketones and Aldehydes to Unsaturated Alcohols over Metal Catalysts. *ACS Catal.* **2012**, *2*, 671−683.
(186) Liu, W.; Jiang, Y.; Dostert, K. H.; O'Brien, C. P.; Riedel, W.; Savara, A.; Schauermann, S.; Tkatchenko, A. Catalysis beyond frontier molecular orbitals: Selectivity in partial hydrogenation of multi-unsaturated hydrocarbons on metal catalysts. *Sci. Adv.* **2017**, *3*, e1700939.
(187) Yang, J. F.; Li, S. S.; Zhang, L. L.; Liu, X. Y.; Wang, J. H.; Pan, X. L.; Li, N.; Wang, A. Q.; Cong, Y.; Wang, X. D.; et al. Hydrodeoxygenation of furans over Pd-FeO_x/SiO_2 catalyst under atmospheric pressure. *Appl. Catal., B* **2017**, *201*, 266−277.
(188) Ponec, V. On the role of promoters in hydrogenations on metals; α,β-unsaturated aldehydes and ketones. *Appl. Catal., A* **1997**, *149*, 27−48.
(189) Wu, B.; Huang, H.; Yang, J.; Zheng, N.; Fu, G. Selective hydrogenation of α,β-unsaturated aldehydes catalyzed by amine-capped platinum-cobalt nanocrystals. *Angew. Chem., Int. Ed.* **2012**, *51*, 3440−3443.
(190) Jiang, H. J.; Jiang, H. B.; Zhu, D. M.; Zheng, X. L.; Fu, H. Y.; Chen, H.; Li, R. X. Cooperation between the surface hydroxyl groups of the support and organic additives in the highly selective hydrogenation of citral. *Appl. Catal., A* **2012**, *445*, 351−358.
(191) Zhu, Y.; Qian, H.; Drake, B. A.; Jin, R. Atomically precise $Au_{25}(SR)_{18}$ nanoparticles as catalysts for the selective hydrogenation of α,β-unsaturated ketones and aldehydes. *Angew. Chem., Int. Ed.* **2010**, *49*, 1295−1298.
(192) Yang, Q. Y.; Zhu, Y.; Tian, L.; Xie, S. H.; Pei, Y.; Li, H.; Li, H. X.; Qiao, M. H.; Fan, K. N. Preparation and characterization of Au-In/APTMS-SBA-15 catalysts for chemoselective hydrogenation of crotonaldehyde to crotyl alcohol. *Appl. Catal., A* **2009**, *369*, 67−76.
(193) Tian, L.; Yang, Q.; Jiang, Z.; Zhu, Y.; Pei, Y.; Qiao, M.; Fan, K. Highly chemoselective hydrogenation of crotonaldehyde over Ag-In/

DOI: 10.1021/acs.chemrev.9b00230
Chem. Rev. XXXX, XXX, XXX−XXX

SBA-15 fabricated by a modified "two solvents" strategy. *Chem. Commun.* **2011**, *47*, 6168−6170.
(194) Mitsudome, T.; Matoba, M.; Mizugaki, T.; Jitsukawa, K.; Kaneda, K. Core-shell AgNP@CeO_2 nanocomposite catalyst for highly chemoselective reductions of unsaturated aldehydes. *Chem. - Eur. J.* **2013**, *19*, 5255−5258.
(195) Liu, H. L.; Chang, L. N.; Chen, L. Y.; Li, Y. W. Nanocomposites of Platinum/Metal-Organic Frameworks Coated with Metal-Organic Frameworks with Remarkably Enhanced Chemoselectivity for Cinnamaldehyde Hydrogenation. *ChemCatChem* **2016**, *8*, 946−951.
(196) Wang, W.; Xie, Y.; Zhang, S. H.; Liu, X.; Haruta, M.; Huang, J. H. Selective Hydrogenation of Cinnamaldehyde Catalyzed by ZnO-Fe_2O_3 Mixed Oxide Supported Gold Nanocatalysts. *Catalysts* **2018**, *8*, 60.
(197) Han, J.; Kim, Y. H.; Jang, H. S.; Hwang, S. Y.; Jegal, J.; Kim, J. W.; Lee, Y. S. Heterogeneous zirconia-supported ruthenium catalyst for highly selective hydrogenation of 5-hydroxymethyl-2-furaldehyde to 2,5-bis(hydroxymethyl)furans in various n-alcohol solvents. *RSC Adv.* **2016**, *6*, 93394−93397.
(198) He, S.; Shao, Z. J.; Shu, Y.; Shi, Z.; Cao, X. M.; Gao, Q.; Hu, P.; Tang, Y. Enhancing Metal-Support Interactions by Molybdenum Carbide: An Efficient Strategy toward the Chemoselective Hydrogenation of α,β-Unsaturated Aldehydes. *Chem. - Eur. J.* **2016**, *22*, 5698−5704.
(199) Pang, S. H.; Schoenbaum, C. A.; Schwartz, D. K.; Medlin, J. W. Directing reaction pathways by catalyst active-site selection using self-assembled monolayers. *Nat. Commun.* **2013**, *4*, 2448.
(200) Kahsar, K. R.; Schwartz, D. K.; Medlin, J. W. Control of metal catalyst selectivity through specific noncovalent molecular interactions. *J. Am. Chem. Soc.* **2014**, *136*, 520−526.
(201) Li, G.; Zeng, C.; Jin, R. Thermally robust $Au_{99}(SPh)_{42}$ nanoclusters for chemoselective hydrogenation of nitrobenzaldehyde derivatives in water. *J. Am. Chem. Soc.* **2014**, *136*, 3673−3679.
(202) Cano, I.; Chapman, A. M.; Urakawa, A.; van Leeuwen, P. W. Air-stable gold nanoparticles ligated by secondary phosphine oxides for the chemoselective hydrogenation of aldehydes: crucial role of the ligand. *J. Am. Chem. Soc.* **2014**, *136*, 2520−2528.
(203) Liu, H.; Mei, Q.; Li, S.; Yang, Y.; Wang, Y.; Liu, H.; Zheng, L.; An, P.; Zhang, J.; Han, B. Selective hydrogenation of unsaturated aldehydes over Pt nanoparticles promoted by the cooperation of steric and electronic effects. *Chem. Commun.* **2018**, *54*, 908−911.
(204) Taniya, K.; Yu, C. H.; Tsang, S. C.; Ichihashi, Y.; Nishiyama, S. Preparation of SiO_2-encapsulated SnPt nanoparticle catalysts for selective hydrogenation of unsaturated aldehyde. *Catal. Commun.* **2011**, *14*, 6−9.
(205) Weng, Z. H.; Zaera, F. Sub-Monolayer Control of Mixed-Oxide Support Composition in Catalysts via Atomic Layer Deposition: Selective Hydrogenation of Cinnamaldehyde Promoted by (SiO_2-ALD)-Pt/Al_2O_3. *ACS Catal.* **2018**, *8*, 8513−8524.
(206) Halilu, A.; Ali, T. H.; Atta, A. Y.; Sudarsanam, P.; Bhargava, S. K.; Abd Hamid, S. B. Highly Selective Hydrogenation of Biomass-Derived Furfural into Furfuryl Alcohol Using a Novel Magnetic Nanoparticles Catalyst. *Energy Fuels* **2016**, *30*, 2216−2226.
(207) Guo, Z. Y.; Xiao, C. X.; Maligal-Ganesh, R. V.; Zhou, L.; Goh, T. W.; Li, X. L.; Tesfagaber, D.; Thiel, A.; Huang, W. Y. Pt Nanoclusters Confined within Metal Organic Framework Cavities for Chemoselective Cinnamaldehyde Hydrogenation. *ACS Catal.* **2014**, *4*, 1340−1348.
(208) Zhao, M.; Yuan, K.; Wang, Y.; Li, G.; Guo, J.; Gu, L.; Hu, W.; Zhao, H.; Tang, Z. Metal-organic frameworks as selectivity regulators for hydrogenation reactions. *Nature* **2016**, *539*, 76−80.
(209) Stephenson, C. J.; Whitford, C. L.; Stair, P. C.; Farha, O. K.; Hupp, J. T. Chemoselective Hydrogenation of Crotonaldehyde Catalyzed by an Au@ZIF-8 Composite. *ChemCatChem* **2016**, *8*, 855−860.
(210) Long, Y.; Song, S. Y.; Li, J.; Wu, L. L.; Wang, Q. S.; Liu, Y.; Jin, R. C.; Zhang, H. J. Pt/CeO_2@MOF Core@Shell Nanoreactor for Selective Hydrogenation of Furfural via the Channel Screening Effect. *ACS Catal.* **2018**, *8*, 8506−8512.
(211) Lin, H. Q.; Zheng, J. W.; Zheng, X. L.; Gu, Z. Q.; Yuan, Y. Z.; Yang, Y. H. Improved chemoselective hydrogenation of crotonaldehyde over bimetallic AuAg/SBA-15 catalyst. *J. Catal.* **2015**, *330*, 135−144.
(212) Zhao, J.; Ni, J.; Xu, J. H.; Xu, J. T.; Cen, J.; Li, X. N. Ir promotion of TiO_2 supported Au catalysts for selective hydrogenation of cinnamaldehyde. *Catal. Commun.* **2014**, *54*, 72−76.
(213) Rong, Z. M.; Sun, Z. H.; Wang, Y.; Lv, J. K.; Wang, Y. Selective Hydrogenation of Cinnamaldehyde to Cinnamyl Alcohol over Graphene Supported Pt-Co Bimetallic Catalysts. *Catal. Lett.* **2014**, *144*, 980−986.
(214) Tian, Z. B.; Li, Q. Y.; Hou, J. Y.; Pei, L.; Li, Y.; Ai, S. Y. Platinum nanocrystals supported on CoAl mixed metal oxide nanosheets derived from layered double hydroxides as catalysts for selective hydrogenation of cinnamaldehyde. *J. Catal.* **2015**, *331*, 193−202.
(215) Li, C. Y.; Ke, C. X.; Han, R. R.; Fan, G. L.; Yang, L.; Li, F. The remarkable promotion of in situ formed Pt-cobalt oxide interfacial sites on the carbonyl reduction to allylic alcohols. *Mol. Catal.* **2018**, *455*, 78−87.
(216) Zgolicz, P. D.; Rodriguez, V. I.; Vilella, I. M. J.; de Miguel, S. R.; Scelza, O. A. Catalytic performance in selective hydrogenation of citral of bimetallic Pt-Sn catalysts supported on $MgAl_2O_4$ and γ-Al_2O_3. *Appl. Catal., A* **2011**, *392*, 208−217.
(217) Stassi, J. P.; Zgolicz, P. D.; de Miguel, S. R.; Scelza, O. A. Formation of different promoted metallic phases in PtFe and PtSn catalysts supported on carbonaceous materials used for selective hydrogenation. *J. Catal.* **2013**, *306*, 11−29.
(218) Dai, L. X.; Zhu, W.; Lin, M.; Zhang, Z. P.; Gu, J.; Wang, Y. H.; Zhang, Y. W. Self-supported composites of thin Pt-Sn crosslinked nanowires for the highly chemoselective hydrogenation of cinnamaldehyde under ambient conditions. *Inorg. Chem. Front.* **2015**, *2*, 949−956.
(219) Shi, Y. S.; Yuan, Z. F.; Wei, Q.; Sun, K. Q.; Xu, B. Q. Pt-FeO_x/SiO_2 catalysts prepared by galvanic displacement show high selectivity for cinnamyl alcohol production in the chemoselective hydrogenation of cinnamaldehyde. *Catal. Sci. Technol.* **2016**, *6*, 7033−7037.
(220) Zhang, Y.; Chen, C.; Gong, W. B.; Song, J. Y.; Su, Y. P.; Zhang, H. M.; Wang, G. Z.; Zhao, H. J. One-pot redox synthesis of Pt/Fe_3O_4 catalyst for efficiently chemoselective hydrogenation of cinnamaldehyde. *RSC Adv.* **2017**, *7*, 21107−21113.
(221) Ye, T. N.; Li, J.; Kitano, M.; Sasase, M.; Hosono, H. Electronic interactions between a stable electride and a nano-alloy control the chemoselective reduction reaction. *Chem. Sci.* **2016**, *7*, 5969−5975.
(222) Malobela, L. J.; Heveling, J.; Augustyn, W. G.; Cele, L. M. Nickel-Cobalt on Carbonaceous Supports for the Selective Catalytic Hydrogenation of Cinnamaldehyde. *Ind. Eng. Chem. Res.* **2014**, *53*, 13910−13919.
(223) Rudolf, C.; Dragoi, B.; Ungureanu, A.; Chirieac, A.; Royer, S.; Nastro, A.; Dumitriu, E. NiAl and CoAl materials derived from takovite-like LDHs and related structures as efficient chemoselective hydrogenation catalysts. *Catal. Sci. Technol.* **2014**, *4*, 179−189.
(224) Rodiansono; Astuti, M. D.; Mujiyanti, D. R.; Santoso, U. T.; Shimazu, S. Novel preparation method of bimetallic Ni-In alloy catalysts supported on amorphous alumina for the highly selective hydrogenation of furfural. *Mol. Catal.* **2018**, *445*, 52−60.
(225) Hidalgo-Carrillo, J.; Aramendia, M. A.; Marinas, A.; Marinas, J. M.; Urbano, F. J. Support and solvent effects on the liquid-phase chemoselective hydrogenation of crotonaldehyde over Pt catalysts. *Appl. Catal., A* **2010**, *385*, 190−200.
(226) Li, W.; Fan, G. L.; Yang, L.; Li, F. Surface Lewis acid-promoted copper-based nanocatalysts for highly efficient and chemoselective hydrogenation of citral to unsaturated allylic alcohols. *Catal. Sci. Technol.* **2016**, *6*, 2337−2348.
(227) Ramos-Fernandez, E. V.; Ferreira, A. F. P.; Sepulveda-Escribano, A.; Kapteijn, F.; Rodriguez-Reinoso, F. Enhancing the catalytic performance of Pt/ZnO in the selective hydrogenation of

DOI: 10.1021/acs.chemrev.9b00230
Chem. Rev. XXXX, XXX, XXX−XXX

cinnamaldehyde by Cr addition to the support. *J. Catal.* **2008**, *258*, 52−60.
(228) Dragoi, B.; Ungureanu, A.; Chirieac, A.; Hulea, V.; Royer, S.; Dumitriu, E. Enhancing the performance of SBA-15-supported copper catalysts by chromium addition for the chemoselective hydrogenation of trans-cinnamaldehyde. *Catal. Sci. Technol.* **2013**, *3*, 2319−2329.
(229) Manyar, H. G.; Yang, B.; Daly, H.; Moor, H.; McMonagle, S.; Tao, Y.; Yadav, G. D.; Goguet, A.; Hu, P.; Hardacre, C. Selective Hydrogenation of α,β-Unsaturated Aldehydes and Ketones using Novel Manganese Oxide and Platinum Supported on Manganese Oxide Octahedral Molecular Sieves as Catalysts. *ChemCatChem* **2013**, *5*, 506−512.
(230) Sharma, R. V.; Das, U.; Sammynaiken, R.; Dalai, A. K. Liquid phase chemo-selective catalytic hydrogenation of furfural to furfuryl alcohol. *Appl. Catal., A* **2013**, *454*, 127−136.
(231) Wang, M. M.; He, L.; Liu, Y. M.; Cao, Y.; He, H. Y.; Fan, K. N. Gold supported on mesostructured ceria as an efficient catalyst for the chemoselective hydrogenation of carbonyl compounds in neat water. *Green Chem.* **2011**, *13*, 602−607.
(232) Gutierrez, V.; Nador, F.; Radivoy, G.; Volpe, M. A. Highly selective copper nanoparticles for the hydrogenation of α,β-unsaturated aldehydes in liquid phase. *Appl. Catal., A* **2013**, *464*, 109−115.
(233) Wei, S. P.; Zhao, Y. T.; Fan, G. L.; Yang, L.; Li, F. Structure-dependent selective hydrogenation of cinnamaldehyde over high-surface-area CeO_2-ZrO_2 composites supported Pt nanoparticles. *Chem. Eng. J.* **2017**, *322*, 234−245.
(234) Nishiyama, H.; Takeuchi, J.; Hayase, H.; Saito, N.; Inoue, Y. Remarkable Support Effects of Gallium Compounds on the Activity and Selectivity of Ru Metal Catalyst for Liquid-phase Citral Hydrogenation. *Chem. Lett.* **2008**, *37*, 1256−1257.
(235) Bailon-Garcia, E.; Carrasco-Marin, F.; Perez-Cadenas, A. F.; Maldonado-Hodar, F. J. Chemoselective Pt-catalysts supported on carbon-TiO_2 composites for the direct hydrogenation of citral to unsaturated alcohols. *J. Catal.* **2016**, *344*, 701−711.
(236) Zhang, Z. R.; Song, J. L.; Jiang, Z. W.; Meng, Q. L.; Zhang, P.; Han, B. X. Direct Synthesis of Ultrasmall Ruthenium Nanoparticles on Porous Supports Using Natural Sources for Highly Efficient and Selective Furfural Hydrogenation. *ChemCatChem* **2017**, *9*, 2448−2452.
(237) He, S.; Xie, L. F.; Che, M. W.; Chan, H. C.; Yang, L. C.; Shi, Z. P.; Tang, Y.; Gao, Q. S. Chemoselective hydrogenation of α,β-unsaturated aldehydes on hydrogenated MoO_x nanorods supported iridium nanoparticles. *J. Mol. Catal. A: Chem.* **2016**, *425*, 248−254.
(238) Chen, X.; Zhang, L.; Zhang, B.; Guo, X.; Mu, X. Highly selective hydrogenation of furfural to furfuryl alcohol over Pt nanoparticles supported on g-C_3N_4 nanosheets catalysts in water. *Sci. Rep.* **2016**, *6*, 28558.
(239) Liu, X.; Zhang, B.; Fei, B.; Chen, X.; Zhang, J.; Mu, X. Tunable and selective hydrogenation of furfural to furfuryl alcohol and cyclopentanone over Pt supported on biomass-derived porous heteroatom doped carbon. *Faraday Discuss.* **2017**, *202*, 79−98.
(240) Jiang, P. B.; Li, X. L.; Gao, W. B.; Wang, X.; Tang, Y.; Lan, K.; Wang, B.; Li, R. Highly selective hydrogenation of α,β-unsaturated carbonyl compounds over supported Co nanoparticles. *Catal. Commun.* **2018**, *111*, 6−9.
(241) Dai, Y. H.; Gao, X.; Chu, X. F.; Jiang, C. Y.; Yao, Y.; Guo, Z.; Zhou, C. M.; Wang, C.; Wang, H. M.; Yang, Y. H. On the role of water in selective hydrogenation of cinnamaldehyde to cinnamyl alcohol on PtFe catalysts. *J. Catal.* **2018**, *364*, 192−203.
(242) Han, Q.; Liu, Y. F.; Wang, D.; Yuan, F. L.; Niu, X. Y.; Zhu, Y. J. Effect of carbon nanosheets with different graphitization degrees as a support of noble metals on selective hydrogenation of cinnamaldehyde. *RSC Adv.* **2016**, *6*, 98356−98364.
(243) Sun, Z. H.; Rong, Z. M.; Wang, Y.; Xia, Y.; Du, W. Q.; Wang, Y. Selective hydrogenation of cinnamaldehyde over Pt nanoparticles deposited on reduced graphene oxide. *RSC Adv.* **2014**, *4*, 1874−1878.
(244) Aich, P.; Wei, H. J.; Basan, B.; Kropf, A. J.; Schweitzer, N. M.; Marshall, C. L.; Miller, J. T.; Meyer, R. Single-Atom Alloy Pd-Ag Catalyst for Selective Hydrogenation of Acrolein. *J. Phys. Chem. C* **2015**, *119*, 18140−18148.
(245) Hong, Y. C.; Sun, K. Q.; Zhang, G. R.; Zhong, R. Y.; Xu, B. Q. Fully dispersed Pt entities on nano-Au dramatically enhance the activity of gold for chemoselective hydrogenation catalysis. *Chem. Commun.* **2011**, *47*, 1300−1302.
(246) Nandi, S.; Saha, A.; Patel, P.; Khan, N. H.; Kureshy, R. I.; Panda, A. B. Hydrogenation of Furfural with Nickel Nanoparticles Stabilized on Nitrogen-Rich Carbon Core-Shell and Its Transformations for the Synthesis of γ-Valerolactone in Aqueous Conditions. *ACS Appl. Mater. Interfaces* **2018**, *10*, 24480−24490.
(247) Vetere, V.; Merlo, A. B.; Ruggera, J. F.; Casella, M. L. Transition Metal-based Bimetallic Catalysts for the Chemoselective Hydrogenation of Furfuraldehyde. *J. Braz. Chem. Soc.* **2010**, *21*, 914−920.
(248) Brandt, K.; Chiu, M. E.; Watson, D. J.; Tikhov, M. S.; Lambert, R. M. Chemoselective catalytic hydrogenation of acrolein on Ag(111): effect of molecular orientation on reaction selectivity. *J. Am. Chem. Soc.* **2009**, *131*, 17286−17290.
(249) Bertero, N. M.; Trasarti, A. F.; Moraweck, B.; Borgna, A.; Marchi, A. J. Selective liquid-phase hydrogenation of citral over supported bimetallic Pt-Co catalysts. *Appl. Catal., A* **2009**, *358*, 32−41.
(250) Liu, L. J.; Lou, H.; Chen, M. Selective hydrogenation of furfural over Pt based and Pd based bimetallic catalysts supported on modified multiwalled carbon nanotubes (MWNT). *Appl. Catal., A* **2018**, *550*, 1−10.
(251) Singh, U. K.; Vannice, M. A. Liquid-Phase Citral Hydrogenation over SiO_2-Supported Group VIII Metals. *J. Catal.* **2001**, *199*, 73−84.
(252) Taylor, M. J.; Durndell, L. J.; Isaacs, M. A.; Parlett, C. M. A.; Wilson, K.; Lee, A. F.; Kyriakou, G. Highly selective hydrogenation of furfural over supported Pt nanoparticles under mild conditions. *Appl. Catal., B* **2016**, *180*, 580−585.
(253) Leng, F. Q.; Gerber, L. C.; Axet, M. R.; Serp, P. Selectivity shifts in hydrogenation of cinnamaldehyde on electron-deficient ruthenium nanoparticles. *C. R. Chim.* **2018**, *21*, 346−353.
(254) Hu, D.; Fan, W. Q.; Liu, Z.; Li, L. Three-Dimensionally Hierarchical Pt/C Nanocomposite with Ultra-High Dispersion of Pt Nanoparticles as a Highly Efficient Catalyst for Chemoselective Cinnamaldehyde Hydrogenation. *ChemCatChem* **2018**, *10*, 779−788.
(255) Steffan, M.; Klasovsky, F.; Arras, J.; Roth, C.; Radnik, J.; Hofmeister, H.; Claus, P. Carbon-carbon double bond versus carbonyl group hydrogenation: Controlling the intramolecular selectivity with polyaniline-supported platinum catalysts. *Adv. Synth. Catal.* **2008**, *350*, 1337−1348.
(256) Sun, K. Q.; Hong, Y. C.; Zhang, G. R.; Xu, B. Q. Synergy between Pt and Au in Pt-on-Au Nanostructures for Chemoselective Hydrogenation Catalysis. *ACS Catal.* **2011**, *1*, 1336−1346.
(257) Blaser, H. U.; Siegrist, U.; Steiner, H. *Aromatic Nitro Compounds: Fine Chemicals Through Heterogeneous Catalysis* Sheldon, R. A., van Bekkum, H., Eds.; Wiley-VCH: Weinheim, 2001).
(258) Downing, R. S.; Kunkeler, P. J.; van Bekkum, H. Catalytic syntheses of aromatic amines. *Catal. Today* **1997**, *37*, 121−136.
(259) Blaser, H.-U.; Steiner, H.; Studer, M. Selective Catalytic Hydrogenation of Functionalized Nitroarenes: An Update. *ChemCatChem* **2009**, *1*, 210−221.
(260) Blaser, H. U. A golden boost to an old reaction. *Science* **2006**, *313*, 312−313.
(261) Beier, M. J.; Andanson, J.-M.; Baiker, A. Tuning the Chemoselective Hydrogenation of Nitrostyrenes Catalyzed by Ionic Liquid-Supported Platinum Nanoparticles. *ACS Catal.* **2012**, *2*, 2587−2595.
(262) Makosch, M.; Lin, W.-I.; Bumbálek, V.; Sá, J.; Medlin, J. W.; Hungerbühler, K.; van Bokhoven, J. A. Organic Thiol Modified Pt/TiO_2 Catalysts to Control Chemoselective Hydrogenation of Substituted Nitroarenes. *ACS Catal.* **2012**, *2*, 2079−2081.

DOI: 10.1021/acs.chemrev.9b00230
Chem. Rev. XXXX, XXX, XXX−XXX

(263) Corma, A.; Serna, P. Chemoselective hydrogenation of nitro compounds with supported gold catalysts. *Science* **2006**, *313*, 332−334.
(264) Corma, A.; Serna, P.; Concepcion, P.; Calvino, J. J. Transforming nonselective into chemoselective metal catalysts for the hydrogenation of substituted nitroaromatics. *J. Am. Chem. Soc.* **2008**, *130*, 8748−8753.
(265) Serna, P.; Concepción, P.; Corma, A. Design of highly active and chemoselective bimetallic gold−platinum hydrogenation catalysts through kinetic and isotopic studies. *J. Catal.* **2009**, *265*, 19−25.
(266) Wei, H.; Wei, X.; Yang, X.; Yin, G.; Wang, A.; Liu, X.; Huang, Y.; Zhang, T. Supported Au-Ni nano-alloy catalysts for the chemoselective hydrogenation of nitroarenes. *Chin. J. Catal.* **2015**, *36*, 160−167.
(267) Dhiman, M.; Polshettiwar, V. Ultrasmall nanoparticles and pseudo-single atoms of platinum supported on fibrous nanosilica (KCC-1/Pt): engineering selectivity of hydrogenation reactions. *J. Mater. Chem. A* **2016**, *4*, 12416−12424.
(268) Wang, L.; Zhang, J.; Wang, H.; Shao, Y.; Liu, X.; Wang, Y.-Q.; Lewis, J. P.; Xiao, F.-S. Activity and Selectivity in Nitroarene Hydrogenation over Au Nanoparticles on the Edge/Corner of Anatase. *ACS Catal.* **2016**, *6*, 4110−4116.
(269) Shimizu, K.; Miyamoto, Y.; Kawasaki, T.; Tanji, T.; Tai, Y.; Satsuma, A. Chemoselective Hydrogenation of Nitroaromatics by Supported Gold Catalysts: Mechanistic Reasons of Size- and Support-Dependent Activity and Selectivity. *J. Phys. Chem. C* **2009**, *113*, 17803−17810.
(270) Shimizu, K.-i.; Miyamoto, Y.; Satsuma, A. Size- and support-dependent silver cluster catalysis for chemoselective hydrogenation of nitroaromatics. *J. Catal.* **2010**, *270*, 86−94.
(271) Liu, X.; Li, H. Q.; Ye, S.; Liu, Y. M.; He, H. Y.; Cao, Y. Gold-catalyzed direct hydrogenative coupling of nitroarenes to synthesize aromatic azo compounds. *Angew. Chem., Int. Ed.* **2014**, *53*, 7624−7628.
(272) Tan, Y.; Liu, X. Y.; Zhang, L.; Wang, A.; Li, L.; Pan, X.; Miao, S.; Haruta, M.; Wei, H.; Wang, H.; et al. ZnAl-Hydrotalcite-Supported Au_{25} Nanoclusters as Precatalysts for Chemoselective Hydrogenation of 3-Nitrostyrene. *Angew. Chem., Int. Ed.* **2017**, *56*, 2709−2713.
(273) Matsushima, Y.; Nishiyabu, R.; Takanashi, N.; Haruta, M.; Kimura, H.; Kubo, Y. Boronate self-assemblies with embedded Au nanoparticles: preparation, characterization and their catalytic activities for the reduction of nitroaromatic compounds. *J. Mater. Chem.* **2012**, *22*, 24124−24131.
(274) Gu, J.; Zhang, Z.; Hu, P.; Ding, L.; Xue, N.; Peng, L.; Guo, X.; Lin, M.; Ding, W. Platinum Nanoparticles Encapsulated in MFI Zeolite Crystals by a Two-Step Dry Gel Conversion Method as a Highly Selective Hydrogenation Catalyst. *ACS Catal.* **2015**, *5*, 6893−6901.
(275) Berguerand, C.; Yarulin, A.; Cárdenas-Lizana, F.; Wärnå, J.; Sulman, E.; Murzin, D. Y.; Kiwi-Minsker, L. Chemoselective Liquid Phase Hydrogenation of 3-Nitrostyrene over Pt Nanoparticles: Synergy with ZnO Support. *Ind. Eng. Chem. Res.* **2015**, *54*, 8659−8669.
(276) Yarulin, A.; Berguerand, C.; Yuranov, I.; Cárdenas-Lizana, F.; Prokopyeva, I.; Kiwi-Minsker, L. Pt−Zn nanoparticles supported on porous polymeric matrix for selective 3-nitrostyrene hydrogenation. *J. Catal.* **2015**, *321*, 7−12.
(277) Furukawa, S.; Takahashi, K.; Komatsu, T. Well-structured bimetallic surface capable of molecular recognition for chemoselective nitroarene hydrogenation. *Chem. Sci.* **2016**, *7*, 4476−4484.
(278) Lan, M.; Zhang, B.; Cheng, H.; Li, X.; Wu, Q.; Ying, Z.; Zhu, Y.; Li, Y.; Meng, X.; Zhao, F. Chemoselective hydrogenation of 3-nitrostyrene to 3-aminostyrene over Pt-Bi/TiO_2 catalysts. *Mol. Catal.* **2017**, *432*, 23−30.
(279) Tamura, M.; Yuasa, N.; Nakagawa, Y.; Tomishige, K. Selective hydrogenation of nitroarenes to aminoarenes using a MoO_x-modified Ru/SiO_2 catalyst under mild conditions. *Chem. Commun.* **2017**, *53*, 3377−3380.
(280) Shu, Y.; Chan, H. C.; Xie, L.; Shi, Z.; Tang, Y.; Gao, Q. Bimetallic Platinum-Tin Nanoparticles on Hydrogenated Molybdenum Oxide for the Selective Hydrogenation of Functionalized Nitroarenes. *ChemCatChem* **2017**, *9*, 4199−4205.
(281) Zhang, S.; Chang, C. R.; Huang, Z. Q.; Li, J.; Wu, Z.; Ma, Y.; Zhang, Z.; Wang, Y.; Qu, Y. High Catalytic Activity and Chemoselectivity of Sub-nanometric Pd Clusters on Porous Nanorods of CeO_2 for Hydrogenation of Nitroarenes. *J. Am. Chem. Soc.* **2016**, *138*, 2629−2637.
(282) Wei, H.; Liu, X.; Wang, A.; Zhang, L.; Qiao, B.; Yang, X.; Huang, Y.; Miao, S.; Liu, J.; Zhang, T. FeO_x-supported platinum single-atom and pseudo-single-atom catalysts for chemoselective hydrogenation of functionalized nitroarenes. *Nat. Commun.* **2014**, *5*, 5634.
(283) Xu, G.; Wei, H.; Ren, Y.; Yin, J.; Wang, A.; Zhang, T. Chemoselective hydrogenation of 3-nitrostyrene over a Pt/FeO_x pseudo-single-atom-catalyst in CO_2-expanded liquids. *Green Chem.* **2016**, *18*, 1332−1338.
(284) Wei, H.; Ren, Y.; Wang, A.; Liu, X.; Liu, X.; Zhang, L.; Miao, S.; Li, L.; Liu, J.; Wang, J.; et al. Remarkable effect of alkalis on the chemoselective hydrogenation of functionalized nitroarenes over high-loading Pt/FeO_x catalysts. *Chem. Sci.* **2017**, *8*, 5126−5131.
(285) Yamanaka, N.; Hara, T.; Ichikuni, N.; Shimazu, S. Chemoselective Hydrogenation of Unsaturated Nitro Compounds to Unsaturated Amines by Ni-Sn Alloy Catalysts. *Chem. Lett.* **2018**, *47*, 971−974.
(286) Ye, T. N.; Lu, Y.; Li, J.; Nakao, T.; Yang, H.; Tada, T.; Kitano, M.; Hosono, H. Copper-Based Intermetallic Electride Catalyst for Chemoselective Hydrogenation Reactions. *J. Am. Chem. Soc.* **2017**, *139*, 17089−17097.
(287) Ren, Y.; Wei, H.; Yin, G.; Zhang, L.; Wang, A.; Zhang, T. Oxygen surface groups of activated carbon steer the chemoselective hydrogenation of substituted nitroarenes over nickel nanoparticles. *Chem. Commun.* **2017**, *53*, 1969−1972.
(288) Tang, B.; Song, W.-C.; Yang, E.-C.; Zhao, X.-J. MOF-derived Ni-based nanocomposites as robust catalysts for chemoselective hydrogenation of functionalized nitro compounds. *RSC Adv.* **2017**, *7*, 1531−1539.
(289) Westerhaus, F. A.; Jagadeesh, R. V.; Wienhofer, G.; Pohl, M. M.; Radnik, J.; Surkus, A. E.; Rabeah, J.; Junge, K.; Junge, H.; Nielsen, M.; et al. Heterogenized cobalt oxide catalysts for nitroarene reduction by pyrolysis of molecularly defined complexes. *Nat. Chem.* **2013**, *5*, 537−543.
(290) Jagadeesh, R. V.; Surkus, A. E.; Junge, H.; Pohl, M. M.; Radnik, J.; Rabeah, J.; Huan, H.; Schunemann, V.; Bruckner, A.; Beller, M. Nanoscale Fe_2O_3-based catalysts for selective hydrogenation of nitroarenes to anilines. *Science* **2013**, *342*, 1073−1076.
(291) Liu, L.; Concepción, P.; Corma, A. Non-noble metal catalysts for hydrogenation: A facile method for preparing Co nanoparticles covered with thin layered carbon. *J. Catal.* **2016**, *340*, 1−9.
(292) Liu, L.; Gao, F.; Concepción, P.; Corma, A. A new strategy to transform mono and bimetallic non-noble metal nanoparticles into highly active and chemoselective hydrogenation catalysts. *J. Catal.* **2017**, *350*, 218−225.
(293) Wei, Z.; Wang, J.; Mao, S.; Su, D.; Jin, H.; Wang, Y.; Xu, F.; Li, H.; Wang, Y. In Situ-Generated Co^0-Co_3O_4/N-Doped Carbon Nanotubes Hybrids as Efficient and Chemoselective Catalysts for Hydrogenation of Nitroarenes. *ACS Catal.* **2015**, *5*, 4783−4789.
(294) Wang, X.; Li, Y. Chemoselective hydrogenation of functionalized nitroarenes using MOF-derived co-based catalysts. *J. Mol. Catal. A: Chem.* **2016**, *420*, 56−65.
(295) Sun, X.; Olivos-Suarez, A. I.; Oar-Arteta, L.; Rozhko, E.; Osadchii, D.; Bavykina, A.; Kapteijn, F.; Gascon, J. Metal-Organic Framework Mediated Cobalt/Nitrogen-Doped Carbon Hybrids as Efficient and Chemoselective Catalysts for the Hydrogenation of Nitroarenes. *ChemCatChem* **2017**, *9*, 1854−1862.
(296) Liu, W.; Zhang, L.; Yan, W.; Liu, X.; Yang, X.; Miao, S.; Wang, W.; Wang, A.; Zhang, T. Single-atom dispersed Co-N-C catalyst:

DOI: 10.1021/acs.chemrev.9b00230
Chem. Rev. XXXX, XXX, XXX−XXX

structure identification and performance for hydrogenative coupling of nitroarenes. *Chem. Sci.* **2016**, *7*, 5758−5764.
(297) Zhou, P.; Jiang, L.; Wang, F.; Deng, K.; Lv, K.; Zhang, Z. High performance of a cobalt-nitrogen complex for the reduction and reductive coupling of nitro compounds into amines and their derivatives. *Sci. Adv.* **2017**, *3*, e1601945.
(298) Corma, A.; Serna, P.; Garcia, H. Gold catalysts open a new general chemoselective route to synthesize oximes by hydrogenation of α,β-unsaturated nitrocompounds with H_2. *J. Am. Chem. Soc.* **2007**, *129*, 6358−6359.
(299) Serna, P.; Corma, A. Transforming Nano Metal Nonselective Particulates into Chemoselective Catalysts for Hydrogenation of Substituted Nitrobenzenes. *ACS Catal.* **2015**, *5*, 7114−7121.
(300) Liu, X.; Wang, A.; Yang, X.; Zhang, T.; Mou, C.-Y.; Su, D.-S.; Li, J. Synthesis of Thermally Stable and Highly Active Bimetallic Au−Ag Nanoparticles on Inert Supports. *Chem. Mater.* **2009**, *21*, 410−418.
(301) Wang, L.; Wang, H.; Rice, A. E.; Zhang, W.; Li, X.; Chen, M.; Meng, X.; Lewis, J. P.; Xiao, F. S. Design and Preparation of Supported Au Catalyst with Enhanced Catalytic Activities by Rationally Positioning Au Nanoparticles on Anatase. *J. Phys. Chem. Lett.* **2015**, *6*, 2345−2349.
(302) Tan, Y.; Liu, X. Y.; Li, L.; Kang, L.; Wang, A.; Zhang, T. Effects of divalent metal ions of hydrotalcites on catalytic behavior of supported gold nanocatalysts for chemoselective hydrogenation of 3-nitrostyrene. *J. Catal.* **2018**, *364*, 174−182.
(303) Cano, I.; Huertos, M. A.; Chapman, A. M.; Buntkowsky, G.; Gutmann, T.; Groszewicz, P. B.; van Leeuwen, P. W. Air-Stable Gold Nanoparticles Ligated by Secondary Phosphine Oxides as Catalyst for the Chemoselective Hydrogenation of Substituted Aldehydes: a Remarkable Ligand Effect. *J. Am. Chem. Soc.* **2015**, *137*, 7718−7727.
(304) Karim, W.; Spreafico, C.; Kleibert, A.; Gobrecht, J.; VandeVondele, J.; Ekinci, Y.; van Bokhoven, J. A. Catalyst support effects on hydrogen spillover. *Nature* **2017**, *541*, 68−71.
(305) Tamaura, Y.; Tahata, M. Complete reduction of carbon dioxide to carbon using cation-excess magnetite. *Nature* **1990**, *346*, 255−256.
(306) Prasomsri, T.; Nimmanwudipong, T.; Román-Leshkov, Y. Effective hydrodeoxygenation of biomass-derived oxygenates into unsaturated hydrocarbons by MoO_3 using low H_2 pressures. *Energy Environ. Sci.* **2013**, *6*, 1732−1738.
(307) Chen, G.; Xu, C.; Huang, X.; Ye, J.; Gu, L.; Li, G.; Tang, Z.; Wu, B.; Yang, H.; Zhao, Z.; et al. Interfacial electronic effects control the reaction selectivity of platinum catalysts. *Nat. Mater.* **2016**, *15*, 564−569.
(308) Liang, Y.; Li, Y.; Wang, H.; Zhou, J.; Wang, J.; Regier, T.; Dai, H. Co_3O_4 nanocrystals on graphene as a synergistic catalyst for oxygen reduction reaction. *Nat. Mater.* **2011**, *10*, 780−786.
(309) Wu, G.; More, K. L.; Johnston, C. M.; Zelenay, P. High-performance electrocatalysts for oxygen reduction derived from polyaniline, iron, and cobalt. *Science* **2011**, *332*, 443−447.
(310) Ramaswamy, N.; Tylus, U.; Jia, Q.; Mukerjee, S. Activity descriptor identification for oxygen reduction on nonprecious electrocatalysts: linking surface science to coordination chemistry. *J. Am. Chem. Soc.* **2013**, *135*, 15443−15449.
(311) Chung, H. T.; Won, J. H.; Zelenay, P. Active and stable carbon nanotube/nanoparticle composite electrocatalyst for oxygen reduction. *Nat. Commun.* **2013**, *4*, 1922.
(312) Banerjee, D.; Jagadeesh, R. V.; Junge, K.; Pohl, M. M.; Radnik, J.; Bruckner, A.; Beller, M. Convenient and mild epoxidation of alkenes using heterogeneous cobalt oxide catalysts. *Angew. Chem., Int. Ed.* **2014**, *53*, 4359−4363.
(313) Stemmler, T.; Westerhaus, F. A.; Surkus, A.-E.; Pohl, M.-M.; Junge, K.; Beller, M. General and selective reductive amination of carbonyl compounds using a core−shell structured Co_3O_4/NGr@C catalyst. *Green Chem.* **2014**, *16*, 4535−4540.
(314) Jagadeesh, R. V.; Junge, H.; Beller, M. Green synthesis of nitriles using non-noble metal oxides-based nanocatalysts. *Nat. Commun.* **2014**, *5*, 4123.
(315) Stemmler, T.; Surkus, A. E.; Pohl, M. M.; Junge, K.; Beller, M. Iron-catalyzed synthesis of secondary amines: on the way to green reductive aminations. *ChemSusChem* **2014**, *7*, 3012−3016.
(316) Jagadeesh, R. V.; Natte, K.; Junge, H.; Beller, M. Nitrogen-Doped Graphene-Activated Iron-Oxide-Based Nanocatalysts for Selective Transfer Hydrogenation of Nitroarenes. *ACS Catal.* **2015**, *5*, 1526−1529.
(317) Chen, F.; Surkus, A. E.; He, L.; Pohl, M. M.; Radnik, J.; Topf, C.; Junge, K.; Beller, M. Selective Catalytic Hydrogenation of Heteroarenes with N-Graphene-Modified Cobalt Nanoparticles (Co_3O_4-Co/NGr@α-Al_2O_3). *J. Am. Chem. Soc.* **2015**, *137*, 11718−11724.
(318) Chen, F.; Kreyenschulte, C.; Radnik, J.; Lund, H.; Surkus, A.-E.; Junge, K.; Beller, M. Selective Semihydrogenation of Alkynes with N-Graphitic-Modified Cobalt Nanoparticles Supported on Silica. *ACS Catal.* **2017**, *7*, 1526−1532.
(319) Chen, F.; Topf, C.; Radnik, J.; Kreyenschulte, C.; Lund, H.; Schneider, M.; Surkus, A. E.; He, L.; Junge, K.; Beller, M. Stable and Inert Cobalt Catalysts for Highly Selective and Practical Hydrogenation of C≡N and C = O Bonds. *J. Am. Chem. Soc.* **2016**, *138*, 8781−8788.
(320) He, L.; Weniger, F.; Neumann, H.; Beller, M. Synthesis, Characterization, and Application of Metal Nanoparticles Supported on Nitrogen-Doped Carbon: Catalysis beyond Electrochemistry. *Angew. Chem., Int. Ed.* **2016**, *55*, 12582−12594.
(321) Kramm, U. I.; Herranz, J.; Larouche, N.; Arruda, T. M.; Lefevre, M.; Jaouen, F.; Bogdanoff, P.; Fiechter, S.; Abs-Wurmbach, I.; Mukerjee, S.; et al. Structure of the catalytic sites in Fe/N/C-catalysts for O_2-reduction in PEM fuel cells. *Phys. Chem. Chem. Phys.* **2012**, *14*, 11673−11688.
(322) Wang, J.; Wang, G.; Miao, S.; Jiang, X.; Li, J.; Bao, X. Synthesis of Fe/Fe_3C nanoparticles encapsulated in nitrogen-doped carbon with single-source molecular precursor for the oxygen reduction reaction. *Carbon* **2014**, *75*, 381−389.
(323) Zitolo, A.; Goellner, V.; Armel, V.; Sougrati, M. T.; Mineva, T.; Stievano, L.; Fonda, E.; Jaouen, F. Identification of catalytic sites for oxygen reduction in iron- and nitrogen-doped graphene materials. *Nat. Mater.* **2015**, *14*, 937−942.
(324) Zhang, L.; Wang, A.; Wang, W.; Huang, Y.; Liu, X.; Miao, S.; Liu, J.; Zhang, T. Co−N−C Catalyst for C−C Coupling Reactions: On the Catalytic Performance and Active Sites. *ACS Catal.* **2015**, *5*, 6563−6572.
(325) Deng, D.; Yu, L.; Chen, X.; Wang, G.; Jin, L.; Pan, X.; Deng, J.; Sun, G.; Bao, X. Iron encapsulated within pod-like carbon nanotubes for oxygen reduction reaction. *Angew. Chem., Int. Ed.* **2013**, *52*, 371−375.
(326) Fu, T.; Wang, M.; Cai, W.; Cui, Y.; Gao, F.; Peng, L.; Chen, W.; Ding, W. Acid-Resistant Catalysis without Use of Noble Metals: Carbon Nitride with Underlying Nickel. *ACS Catal.* **2014**, *4*, 2536−2543.
(327) Liu, W.; Zhang, L.; Liu, X.; Liu, X.; Yang, X.; Miao, S.; Wang, W.; Wang, A.; Zhang, T. Discriminating Catalytically Active FeN_x Species of Atomically Dispersed Fe-N-C Catalyst for Selective Oxidation of the C-H Bond. *J. Am. Chem. Soc.* **2017**, *139*, 10790−10798.
(328) Proietti, E.; Jaouen, F.; Lefevre, M.; Larouche, N.; Tian, J.; Herranz, J.; Dodelet, J. P. Iron-based cathode catalyst with enhanced power density in polymer electrolyte membrane fuel cells. *Nat. Commun.* **2011**, *2*, 416.
(329) Nørskov, J. K.; Bligaard, T.; Logadottir, A.; Bahn, S.; Hansen, L. B.; Bollinger, M.; Bengaard, H.; Hammer, B.; Sljivancanin, Z.; Mavrikakis, M.; et al. Universality in Heterogeneous Catalysis. *J. Catal.* **2002**, *209*, 275−278.
(330) Darby, M. T.; Stamatakis, M.; Michaelides, A.; Sykes, E. C. H. Lonely Atoms with Special Gifts: Breaking Linear Scaling Relationships in Heterogeneous Catalysis with Single-Atom Alloys. *J. Phys. Chem. Lett.* **2018**, *9*, 5636−5646.
(331) Larsson, M.; Hultén, M.; Blekkan, E. A.; Andersson, B. The Effect of Reaction Conditions and Time on Stream on the Coke

DOI: 10.1021/acs.chemrev.9b00230
Chem. Rev. XXXX, XXX, XXX−XXX

Formed during Propane Dehydrogenation. *J. Catal.* **1996**, *164*, 44−53.
(332) Sun, G.; Zhao, Z.-J.; Mu, R.; Zha, S.; Li, L.; Chen, S.; Zang, K.; Luo, J.; Li, Z.; Purdy, S. C.; Kropf, A. J.; Miller, J. T.; Zeng, L.; Gong, J. Breaking the scaling relationship via thermally stable Pt/Cu single atom alloys for catalytic dehydrogenation. *Nat. Commun.* **2018**, *9*, 4454.
(333) Schweitzer, N. M.; Hu, B.; Das, U.; Kim, H.; Greeley, J.; Curtiss, L. A.; Stair, P. C.; Miller, J. T.; Hock, A. S. Propylene Hydrogenation and Propane Dehydrogenation by a Single-Site Zn^{2+} on Silica Catalyst. *ACS Catal.* **2014**, *4*, 1091−1098.
(334) Zhang, G.; Yang, C.; Miller, J. T. Tetrahedral Nickel(II) Phosphosilicate Single-Site Selective Propane Dehydrogenation Catalyst. *ChemCatChem* **2018**, *10*, 961−964.

DOI: 10.1021/acs.chemrev.9b00230
Chem. Rev. XXXX, XXX, XXX−XXX